LARGE-SCALE STRUCTURE NON-GAUSSIANITIES WITH MODAL METHODS

Marcel Schmittfull

BCCP Fellow (UCB/LBNL)

arXiv:1108.3813 (PRD 86 123524)
arXiv:1207.5678 (PRD 88 063512)

Collaborators
Paul Shellard (DAMTP Cambridge)
Donough Regan (Sussex)
James Fergusson (DAMTP Cambridge)

Berkeley 22 Oct 2013

OVERVIEW

- Deviations from Gaussianity: Motivation
- Theoretical expectations
- Non-Gaussian initial conditions
- Estimating non-Gaussianity
- Simulation results

Part II: CMB lensing

NON-GAUSSIANITY FROM INFLATION

- Vacuum expectation value of a quantum field perturbation $\delta\varphi$ with inflationary Lagrangian $\mathcal{L}$

$$\langle\Omega|\delta\varphi_{\mathbf{k}_1}\cdots\delta\varphi_{\mathbf{k}_n}|\Omega\rangle = \frac{\int \mathcal{D}[\delta\varphi]\delta\varphi_{\mathbf{k}_1}\cdots\delta\varphi_{\mathbf{k}_n}\exp(i\int_C \mathcal{L}(\delta\varphi_{\mathbf{k}}))}{\int \mathcal{D}[\delta\varphi]\exp(i\int_C \mathcal{L}(\delta\varphi_{\mathbf{k}}))}$$

- ***Free*** theory $\mathcal{L}\sim\delta\varphi^2 \quad \Rightarrow \quad e^{i\int_C \mathcal{L}}$ is ***Gaussian***

$$\langle\Omega|\delta\varphi_{\mathbf{k}_1}\cdots\delta\varphi_{\mathbf{k}_n}|\Omega\rangle = \begin{cases} \text{determined by 2-point function,} & n \text{ even,} \\ 0, & n \text{ odd.} \end{cases}$$

- ***Interacting*** theory $\mathcal{L}\sim\delta\varphi^3,\delta\varphi^4,\dots \quad \Rightarrow \quad e^{i\int_C \mathcal{L}}$ is ***non-Gaussian***

$\langle\Omega|\delta\varphi_{\mathbf{k}_1}\cdots\delta\varphi_{\mathbf{k}_n}|\Omega\rangle \neq 0$ possible for all n, $\mathbf{k}$-dependence characterises interactions

➟ Inflationary interactions are mapped to specific types of non-Gaussianity

NON-GAUSSIANITY FROM INFLATION

As the universe expands, quantum fluctuations become classical perturbations Φ, whose probability density $\mathrm{Pr}[\Phi]$ is determined by the inflationary Lagrangian $\mathcal{L}$

Bardeen potential in MDU, $\Phi = -3\mathcal{R}/5$

$$\langle \Phi_{\mathbf{k}_1} \cdots \Phi_{\mathbf{k}_n} \rangle = \int \mathcal{D}[\Phi] \Phi_{\mathbf{k}_1} \cdots \Phi_{\mathbf{k}_n} \mathrm{Pr}[\Phi]$$

Constrain inflation by measuring these correlation functions in observations

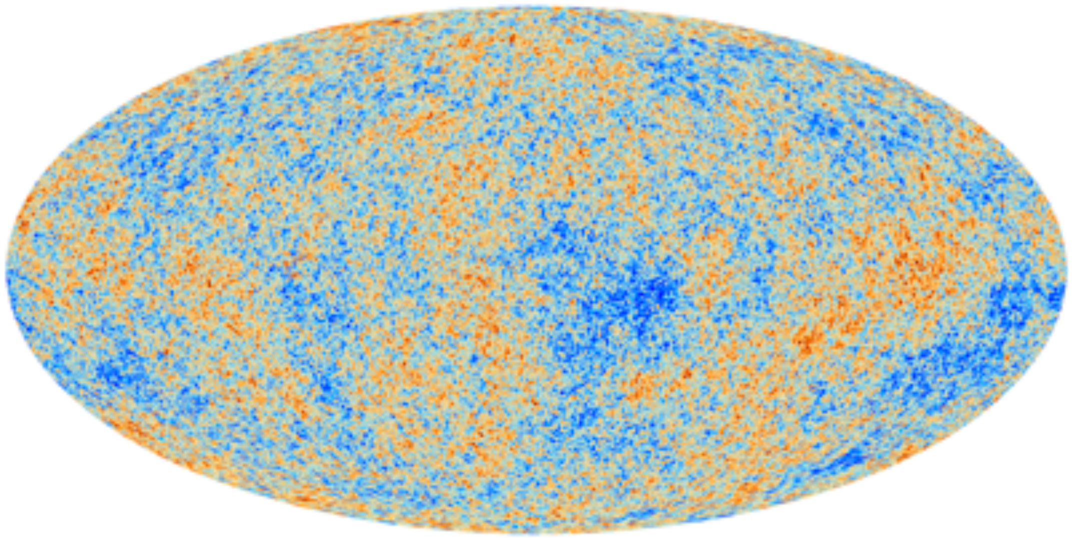

Planck

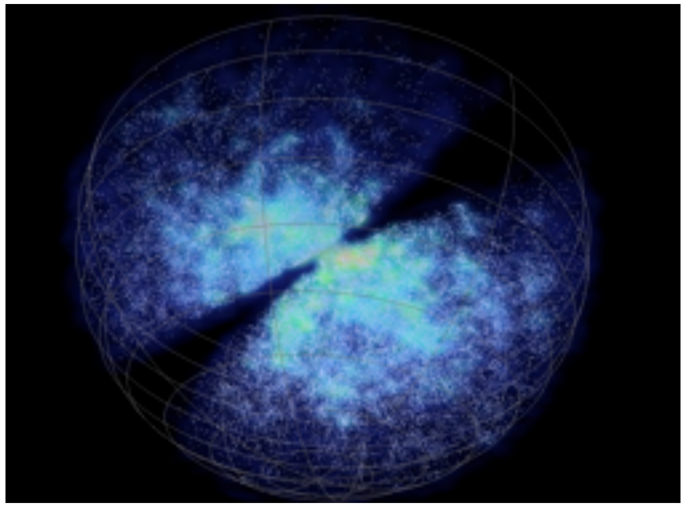

6df galaxy survey

NON-GAUSSIANITY FROM INFLATION

As the universe expands, quantum fluctuations become classical perturbations Φ, whose probability density $\Pr[\Phi]$ is determined by the inflationary Lagrangian $\mathcal{L}$

Bardeen potential in MDU, $\Phi = -3\mathcal{R}/5$

$$\langle \Phi_{\mathbf{k}_1} \cdots \Phi_{\mathbf{k}_n} \rangle = \int \mathcal{D}[\Phi] \Phi_{\mathbf{k}_1} \cdots \Phi_{\mathbf{k}_n} \Pr[\Phi]$$

Constrain inflation by measuring these correlation functions in observations

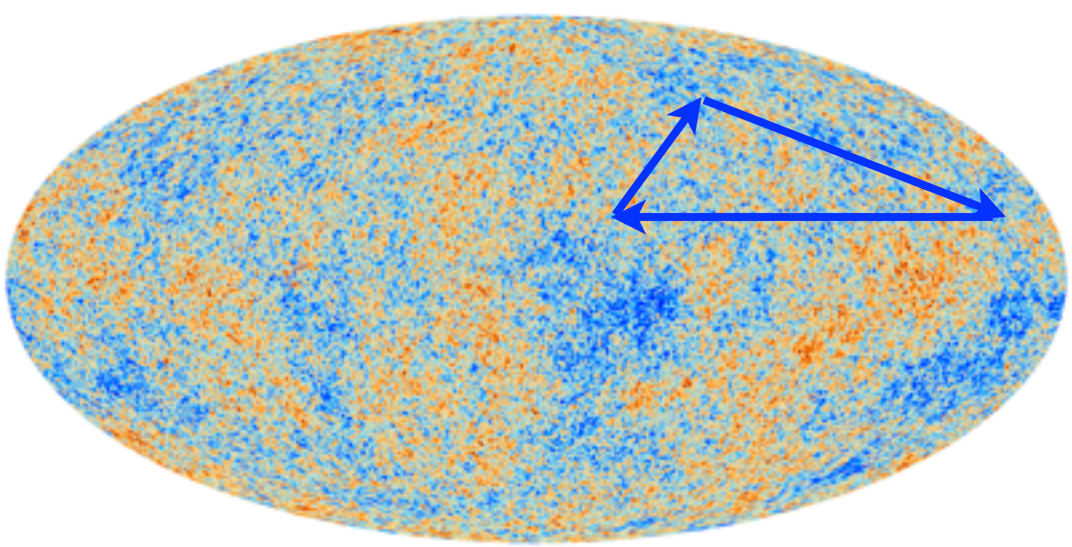

Planck

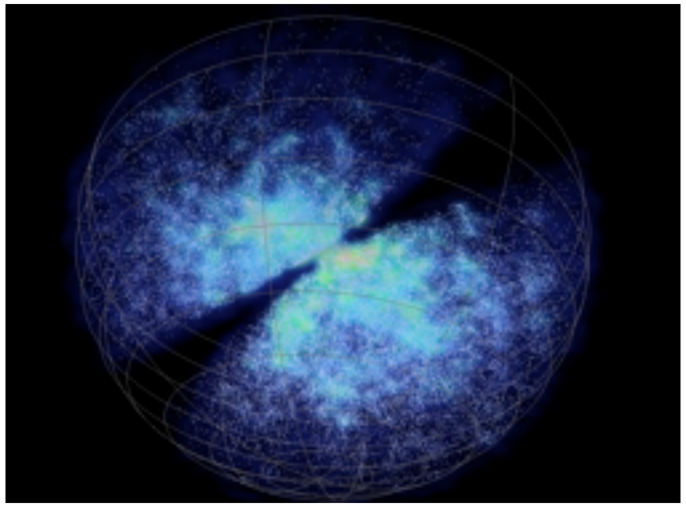

6df galaxy survey

NON-GAUSSIANITY FROM INFLATION

As the universe expands, quantum fluctuations become classical perturbations Φ, whose probability density $\Pr[\Phi]$ is determined by the inflationary Lagrangian $\mathcal{L}$

Bardeen potential in MDU, $\Phi = -3\mathcal{R}/5$

$$\langle \Phi_{\mathbf{k}_1} \cdots \Phi_{\mathbf{k}_n} \rangle = \int \mathcal{D}[\Phi] \Phi_{\mathbf{k}_1} \cdots \Phi_{\mathbf{k}_n} \Pr[\Phi]$$

Constrain inflation by measuring these correlation functions in observations

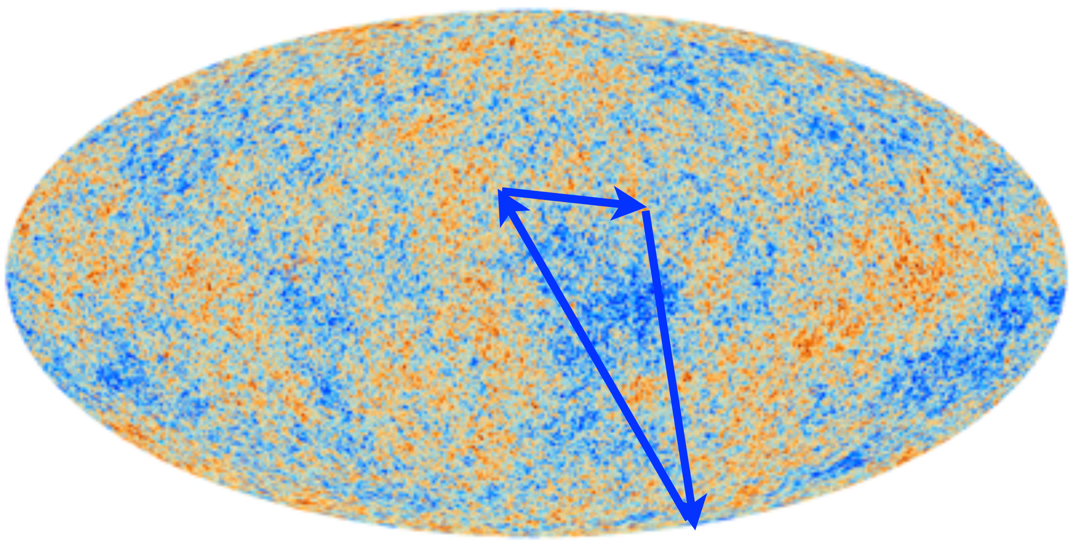

Planck

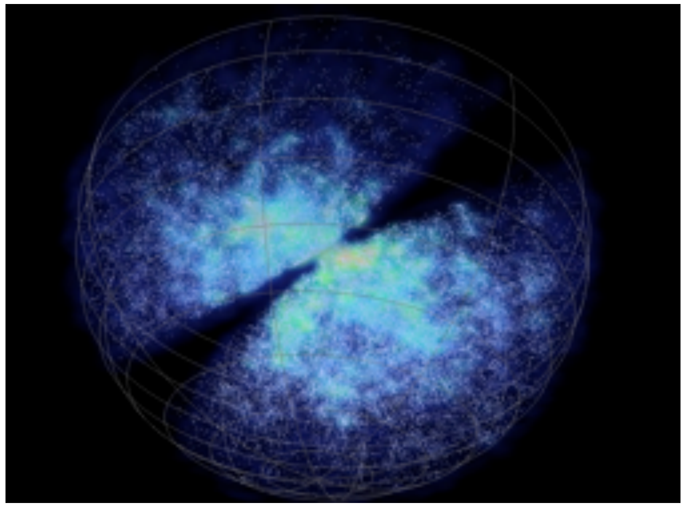

6df galaxy survey

NON-GAUSSIANITY FROM INFLATION

As the universe expands, quantum fluctuations become classical perturbations Φ, whose probability density $\Pr[\Phi]$ is determined by the inflationary Lagrangian $\mathcal{L}$

Bardeen potential in MDU, $\Phi = -3\mathcal{R}/5$

$$\langle \Phi_{\mathbf{k}_1} \cdots \Phi_{\mathbf{k}_n} \rangle = \int \mathcal{D}[\Phi] \Phi_{\mathbf{k}_1} \cdots \Phi_{\mathbf{k}_n} \Pr[\Phi]$$

Constrain inflation by measuring these correlation functions in observations

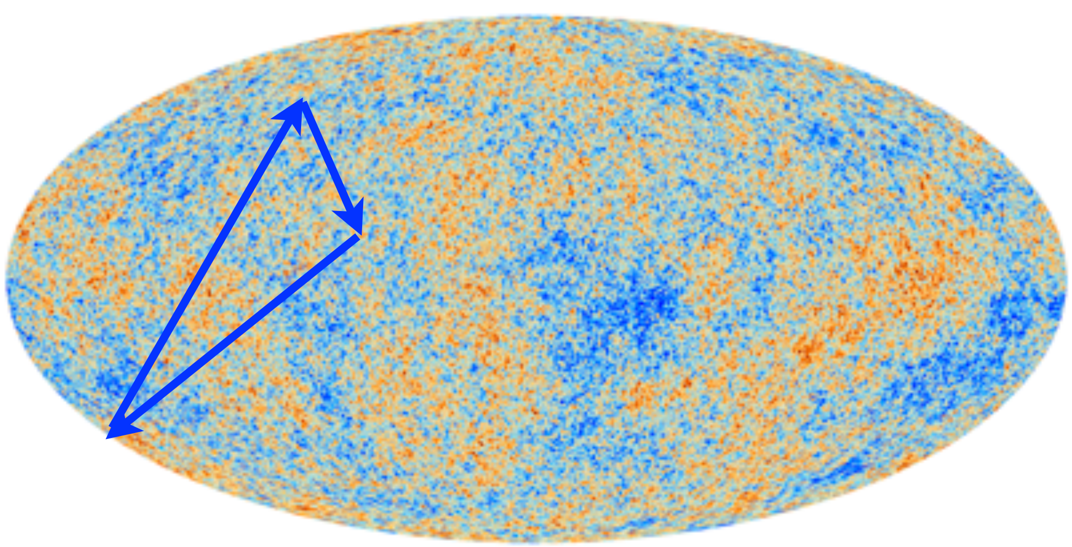

Planck

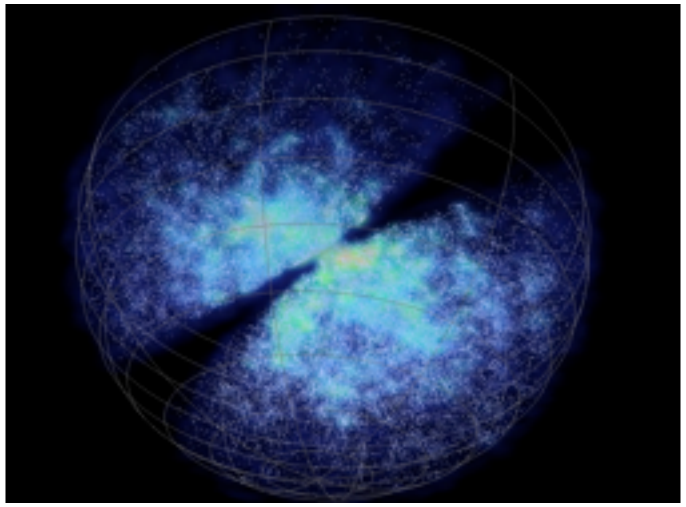

6df galaxy survey

NON-GAUSSIANITY FROM INFLATION

As the universe expands, quantum fluctuations become classical perturbations Φ, whose probability density $\mathrm{Pr}[\Phi]$ is determined by the inflationary Lagrangian $\mathcal{L}$

Bardeen potential in MDU, $\Phi = -3\mathcal{R}/5$

$$\langle \Phi_{\mathbf{k}_1} \cdots \Phi_{\mathbf{k}_n} \rangle = \int \mathcal{D}[\Phi] \Phi_{\mathbf{k}_1} \cdots \Phi_{\mathbf{k}_n} \mathrm{Pr}[\Phi]$$

Constrain inflation by measuring these correlation functions in observations

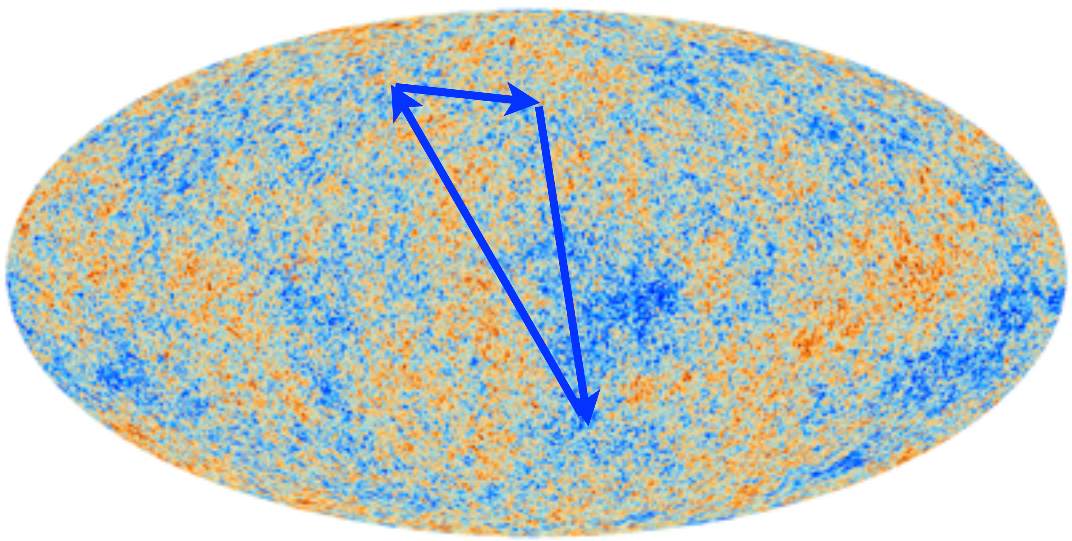

Planck

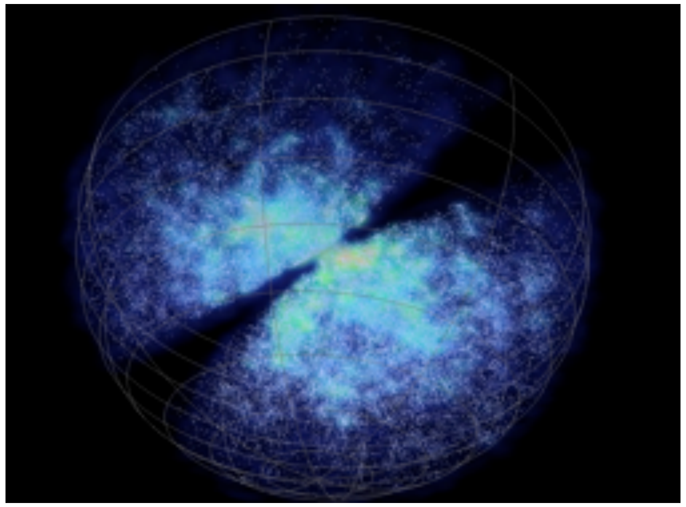

6df galaxy survey

NON-GAUSSIANITY FROM INFLATION

As the universe expands, quantum fluctuations become classical
perturbations Φ, whose prob ity $\Pr[\Phi]$ is determined
by the i

ardeen potential in
DU, $\Phi = -3\mathcal{R}/5$

Constra n
observa

Primordial non-Gaussianity =

Accelerator in the sky

(reaching energy scale of inflation)

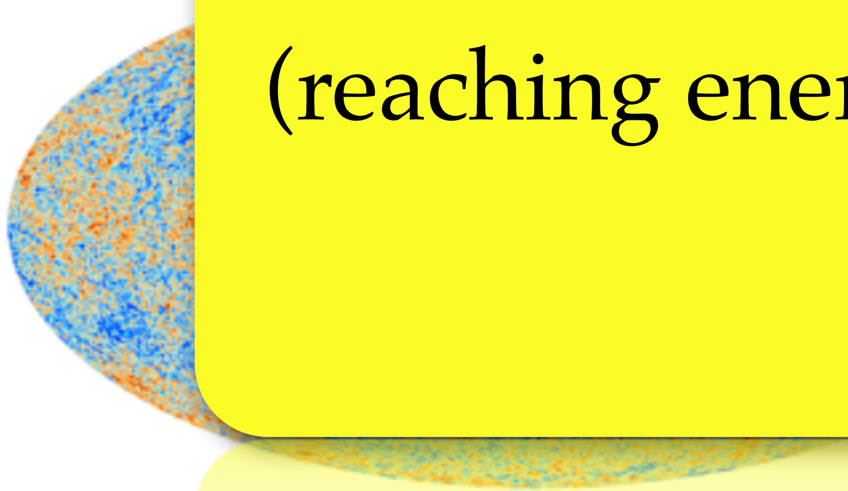

Planck

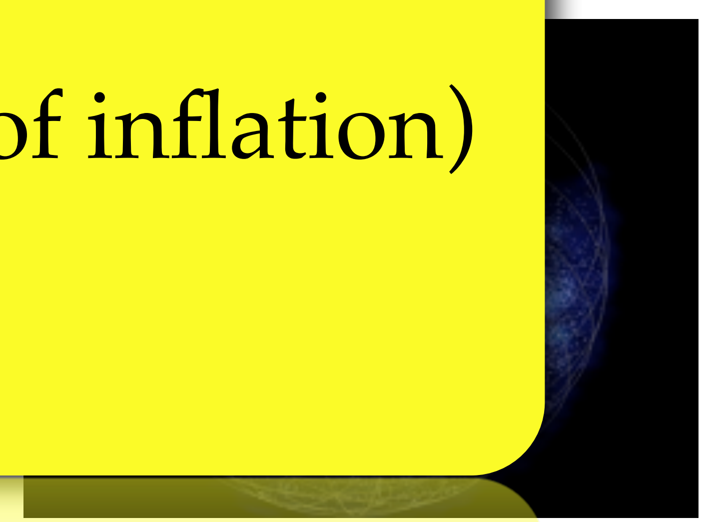

6df galaxy survey

NON-GAUSSIANITY FROM INFLATION

- *Why measure in large-scale structures?*

Advantages:

- LSS = most promising window for non-Gaussianity after Planck
- In principle more information than CMB because 3D
- Lots of data available or coming up (e.g. BOSS, DES, Euclid, LSST, WFIRST, SKA, ...)
- Single field inflation can be ruled out with halo bias (high sensitivity to squeezed limit of the bispectrum)

Complications:

- Non-linear gravity produces late time non-Gaussianity
- Non-linear evolution of primordial input non-Gaussianity
- Difficult modeling and data analysis
- Observational issues: Halo bias, redshifts space distortions, survey geometry, ...

NON-GAUSSIANITY FROM GRAVITY

- Even in a (boring) Gaussian universe, non-Gaussianity from gravity is interesting
    - Distribution of dark matter is different from that of galaxies ➟ "Galaxy bias"

NON-GAUSSIANITY FROM GRAVITY

- Even in a (boring) Gaussian universe, non-Gaussianity from gravity is interesting
  - Distribution of *human population density* is different from that of *night light* ➟ "Galaxy bias"

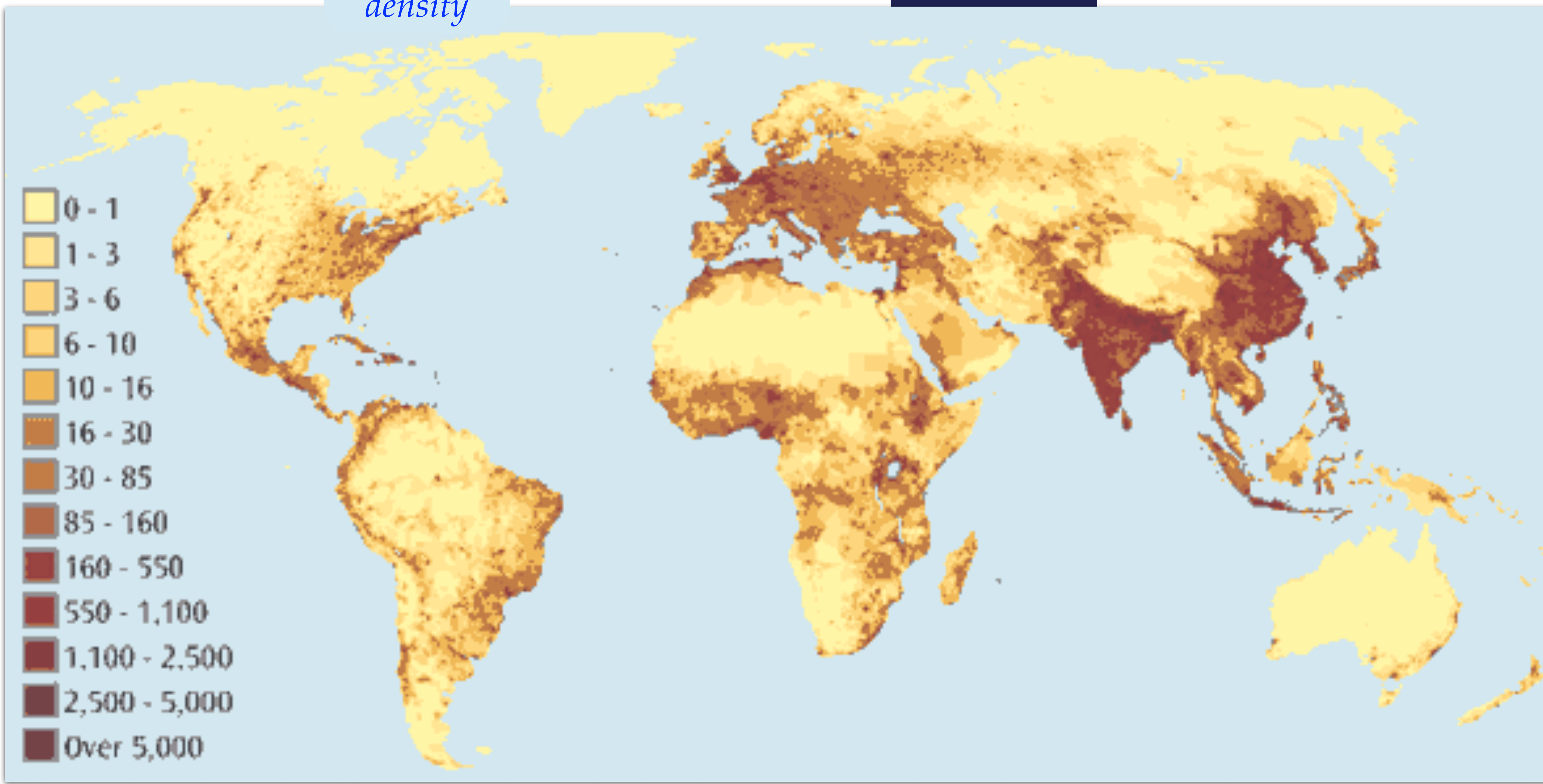

Adopted from Tobias Baldauf

NON-GAUSSIANITY FROM GRAVITY

- Even in a (boring) Gaussian universe, non-Gaussianity from gravity is interesting
  - Distribution of *human population density* is different from that of *night light* ➟ "Galaxy bias"

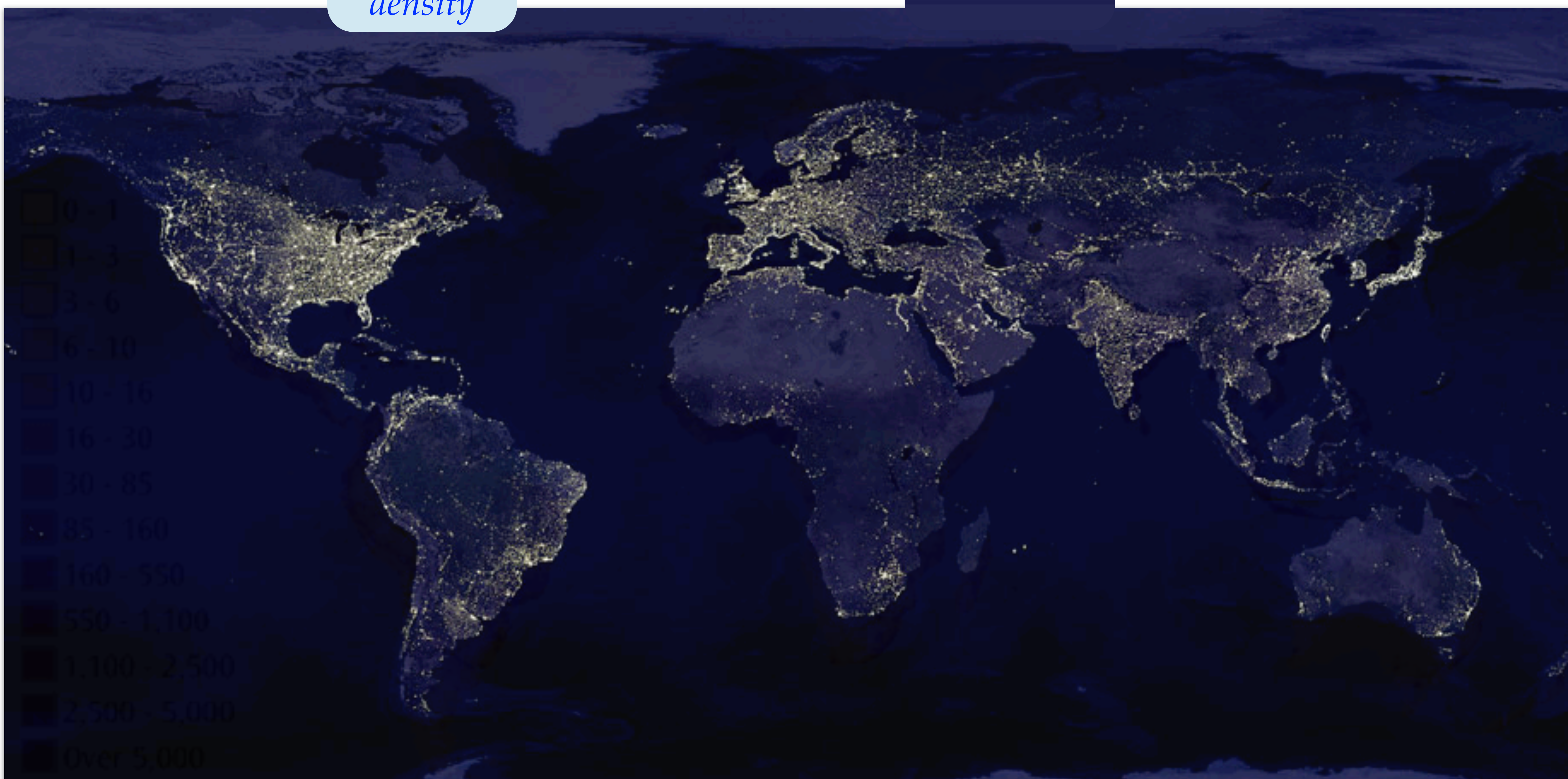

Adopted from Tobias Baldauf

NON-GAUSSIANITY FROM GRAVITY

- Even in a (boring) Gaussian universe, non-Gaussianity from gravity is interesting

  - Distribution of dark matter is different from that of galaxies ➟ "Galaxy bias"

    Simplest ansatz:

    $$\delta_g(\mathbf{x}) \sim b_1 \delta(\mathbf{x}) + \frac{1}{2} b_2 \delta(\mathbf{x})^2 + \cdots$$

    3-point function pins down bias model & parameters (b_1, b_2, ...), which is required to do cosmology with LSS data

  - Break degeneracies of systematic effects or cosmological parameters that are present at the power spectrum (2-point) level

    ➟ Improve cosmological parameter constraints

NON-GAUSSIANITY FROM GRAVITY

- *Late-time* motivation for LSS non-Gaussianity:

δ: DM density
δ_g: galaxy density
b_1: linear bias
b_2: quadratic bias

From (naive) $\delta_g(\mathbf{x}) \sim b_1\delta(\mathbf{x}) + \frac{1}{2}b_2\delta(\mathbf{x})^2 + \cdots$ we get

Galaxy power spectrum (2-point)	*Galaxy bispectrum (3-point)*
$P_g(k) \approx b_1^2 P_\delta(k)$	$B_g(k_1,k_2,k_3) \approx b_1^3 B_\delta(k_1,k_2,k_3) + b_1^2 b_2 (P_\delta(k_1)P_\delta(k_2) + \text{perms})$
• Cannot distinguish rescaling of P_δ from b_1 ➟ b_1-Ω_m degeneracy	• Break b_1-Ω_m degeneracy, i.e. can **measure Ω_m from LSS alone** • Measure b_2

Fry 1994
Verde *et al*. 1997-2002
Scoccimarro *et al*. 1998
Sefusatti *et al*. 2006

<u>But:</u> No large-scale structure non-Gaussianity (bispectrum) pipeline

Complicated modeling (non-linear DM, bias, RSD, correlations, survey geometry, ...)

3-POINT CORRELATIONS (BISPECTRUM)

POWER SPECTRUM + BISPECTRUM

- 2-point function:

power spectrum $\mathbf{P_\Phi}$

statistical isotropy

$$\langle \Phi(\mathbf{k}_1)\Phi(\mathbf{k}_2)\rangle = (2\pi)^3\delta_D(\mathbf{k}_1+\mathbf{k}_2)P_\Phi(k_1)$$

statistical homogeneity

POWER SPECTRUM + BISPECTRUM

- 2-point function:

power spectrum $\mathbf{P}_\Phi$

statistical isotropy

$$\langle\Phi(\mathbf{k}_1)\Phi(\mathbf{k}_2)\rangle = (2\pi)^3\delta_D(\mathbf{k}_1+\mathbf{k}_2)P_\Phi(k_1)$$

statistical homogeneity

- 3-point function:

statistical isotropy

$$\langle\Phi(\mathbf{k}_1)\Phi(\mathbf{k}_2)\Phi(\mathbf{k}_3)\rangle = (2\pi)^3\delta_D(\mathbf{k}_1+\mathbf{k}_2+\mathbf{k}_3)f_{\rm NL}B_\Phi(k_1,k_2,k_3)$$

non-linear amplitude $f_{\rm NL}$

bispectrum $\mathbf{B}_\Phi$

primary diagnostic for non-Gaussianity (vanishes for Gaussian Φ)

BISPECTRUM

- **Bispectrum (3-point correlation function in Fourier space)**
  - Defined for closed triangles (statistical homogeneity and isotropy)

non-linear amplitude

$$\langle \Phi(\mathbf{k}_1)\Phi(\mathbf{k}_2)\Phi(\mathbf{k}_3)\rangle = (2\pi)^3\delta_D(\mathbf{k}_1+\mathbf{k}_2+\mathbf{k}_3)\, f_{\rm NL} B_\Phi(k_1,k_2,k_3)$$

bispectrum

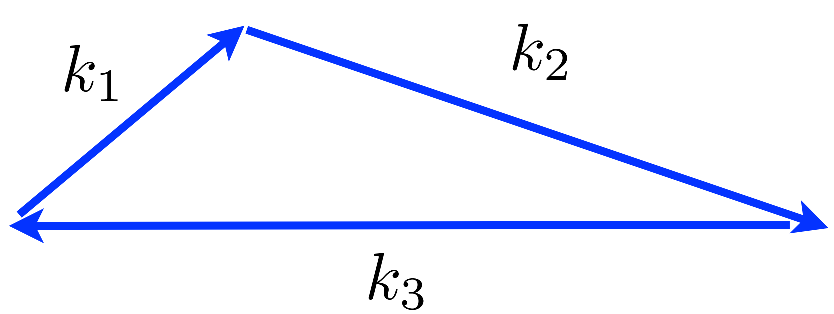

sum of the two smaller sides ≥ longest side

$\Rightarrow$

Bispectrum domain = 'tetrapyd'

(=space of triangle configurations)

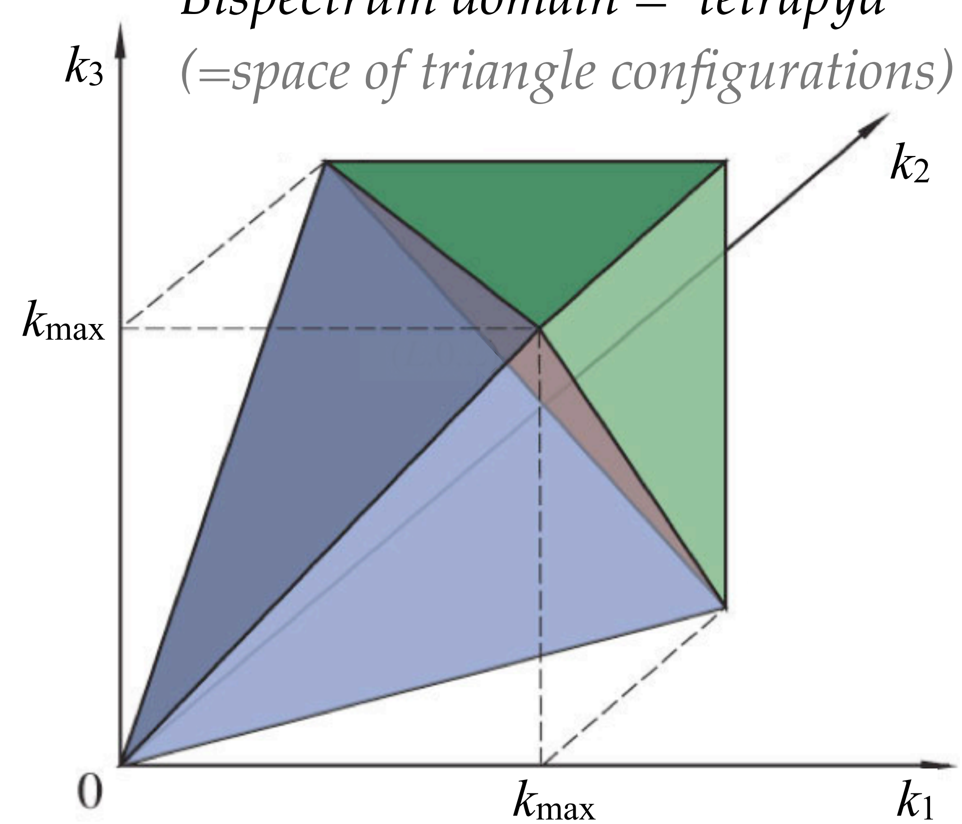

(every point corresponds to a triangle config.)

BISPECTRUM SHAPES

Different inflation models induce different momentum dependencies (shapes) of $B_\Phi(k_1, k_2, k_3)$

Squeezed triangles (local shape)

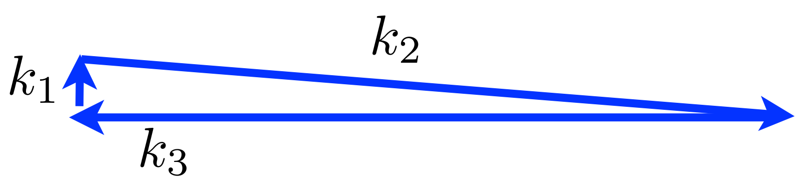

$k_2 \approx k_3 \gg k_1$

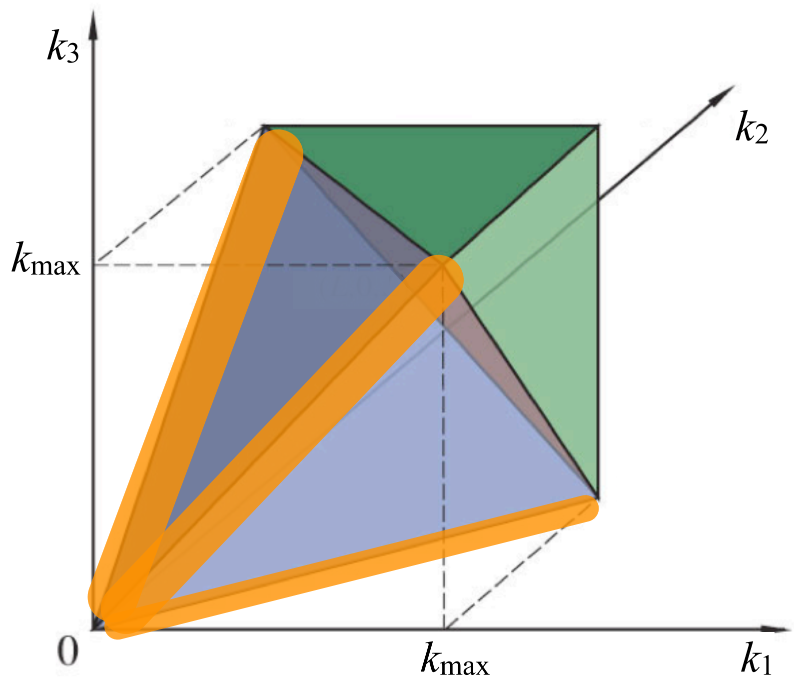

Arises in multifield inflation; detection would rule out all single field models!

Equilateral triangles

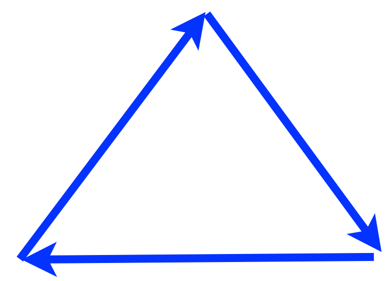

$k_1 \approx k_2 \approx k_3$

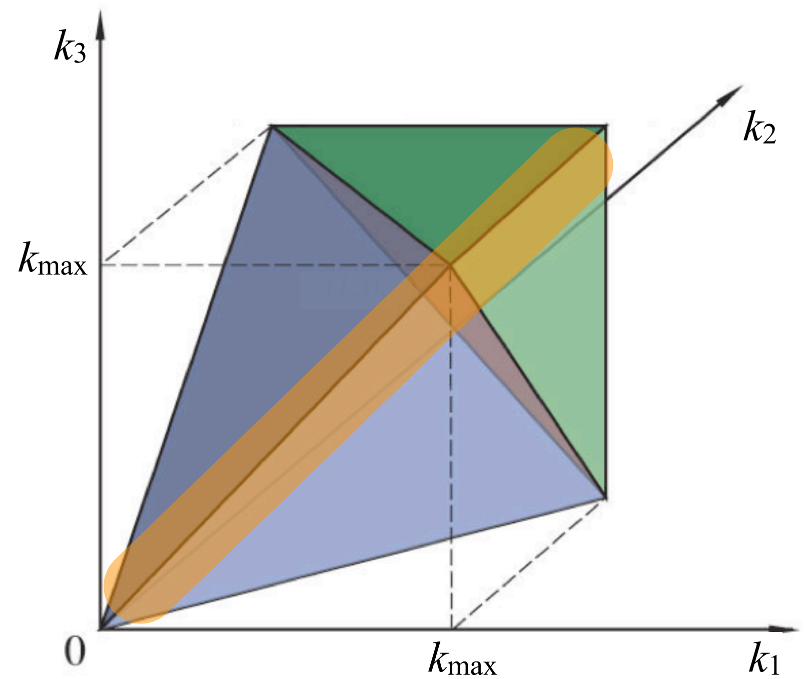

Typically higher derivative kinetic terms, e.g. DBI inflation

Folded triangles

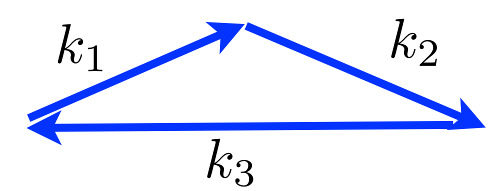

$k_3 = 2k_1 = 2k_2$

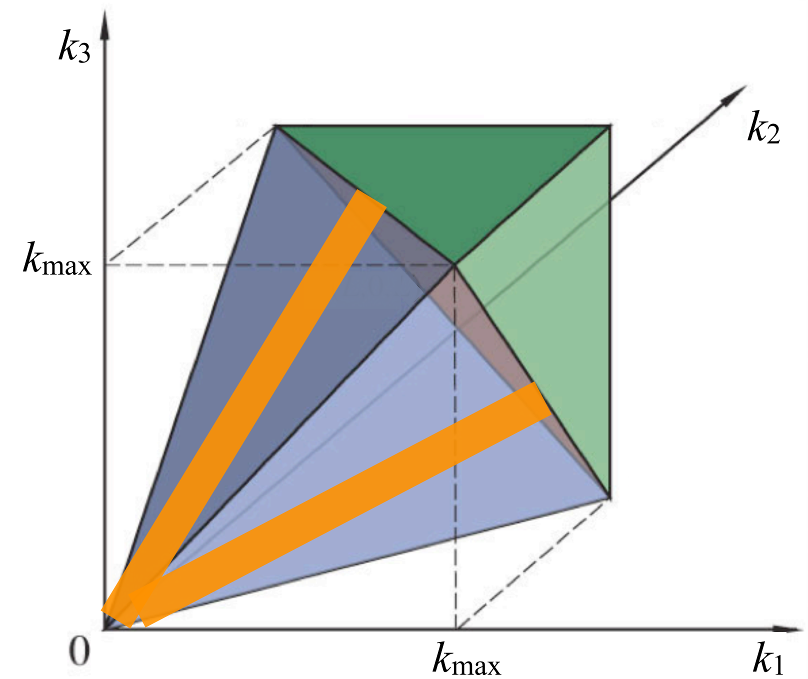

E.g. non-Bunch-Davies vacuum

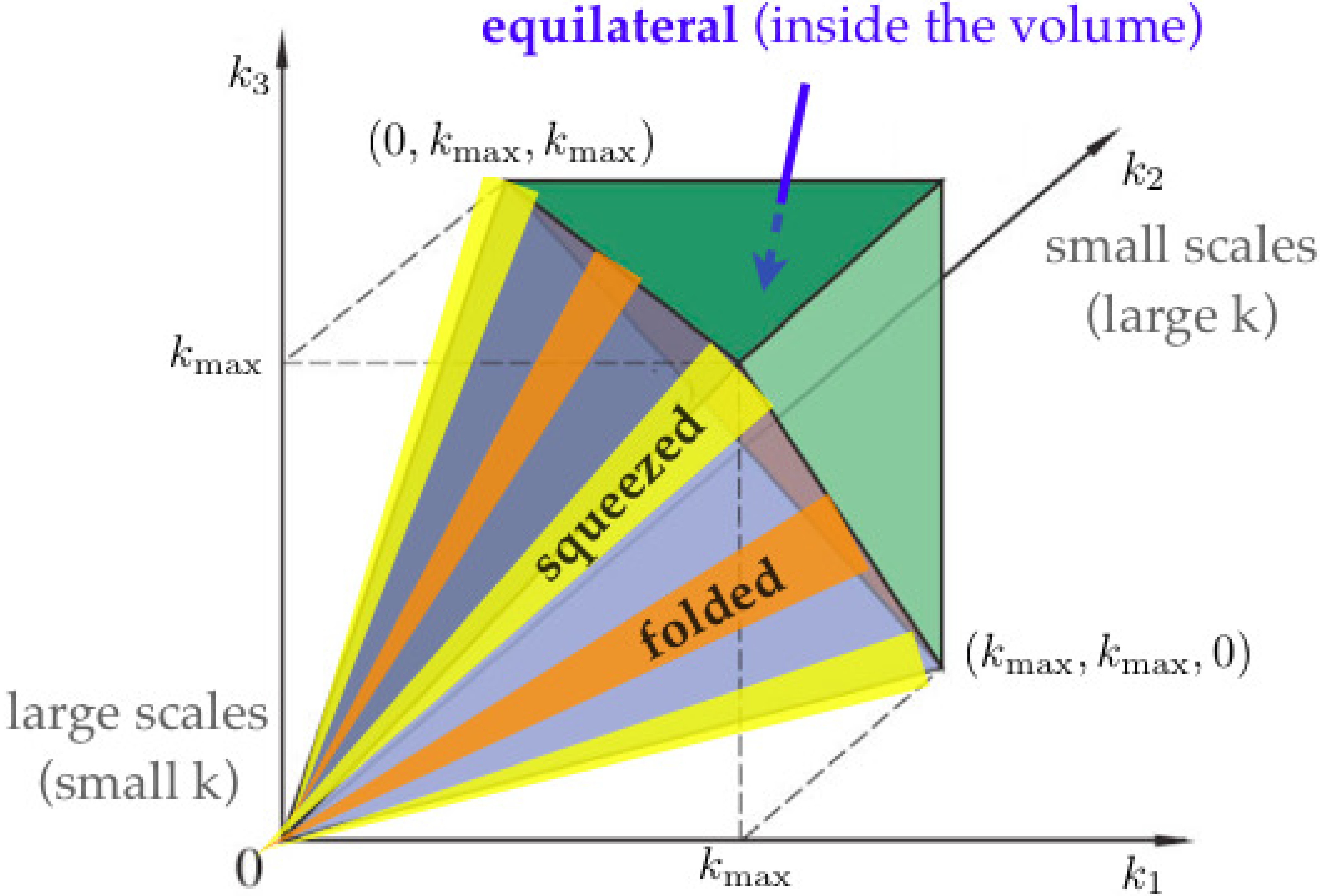

bispectrum drawn on space of triangle configurations

NON-GAUSSIANITY
IN
LARGE SCALE STRUCTURES

NG IN LSS

$$B_\delta \quad = \quad B_\delta^{\rm grav} \quad + \quad B_\delta^{\rm prim}$$

full matter bispectrum

gravitational

primordial

NG IN LSS

$$B_\delta \quad = \quad \boxed{B_\delta^{\mathrm{grav}}} \quad + \quad B_\delta^{\mathrm{prim}}$$

full matter bispectrum

gravitational

primordial

GRAVITATIONAL NG

e.g. Bernardeau, Colombi, Gaztanaga, Scoccimarro 2002

Use perturbation theory on large scales:

$$\delta(\mathbf{k},t) = \sum_{n=1}^{\infty} D(t)^n \delta_n(\mathbf{k})$$

$$\delta_n(\mathbf{k}) = \int d^3\mathbf{q}_1 \cdots \int d^3\mathbf{q}_n \delta_D(\mathbf{k} - \mathbf{q}_1 - \cdots - \mathbf{q}_n) F_n^{(s)}(\mathbf{q}_1, \ldots, \mathbf{q}_n) \delta_1(\mathbf{q}_1) \cdots \delta_1(\mathbf{q}_n)$$

where

$D(t) =$ linear growth factor $\quad (= a(t)$ during matter domination)

$F_n^{(s)} =$ kernels determined by Newtonian equations of motion

GRAVITATIONAL NG

For Gaussian initial conditions (Gaussian δ_1) the leading order bispectrum from gravity is

$$\langle \delta(\mathbf{k}_1,t)\delta(\mathbf{k}_2,t)\delta(\mathbf{k}_3,t)\rangle = D^4(t)\langle \delta_1(\mathbf{k}_1)\delta_1(\mathbf{k}_2)\delta_2(\mathbf{k}_3)\rangle + \text{ 2 perms}$$

$$\Rightarrow B_\delta^{\text{grav}}(k_1,k_2,k_3) = 2P_\delta(k_1;t)P_\delta(k_2;t)F_2^{(s)}(\mathbf{k}_1,\mathbf{k}_2) + \text{ 2 perms}$$

$$F_2^{(s)}(\mathbf{k}_1,\mathbf{k}_2) = \frac{10}{14} + \frac{1}{2}\frac{\mathbf{k}_1\cdot\mathbf{k}_2}{k_1k_2}\left(\frac{k_1}{k_2}+\frac{k_2}{k_1}\right) + \frac{2}{7}\left(\frac{\mathbf{k}_1\cdot\mathbf{k}_2}{k_1k_2}\right)^2$$

from $\nabla\delta\cdot\mathbf{v}$ in continuity eqn. from $(\mathbf{v}\cdot\nabla)\mathbf{v}$ in Euler eqn.

maximum for $\mathbf{k_1} = \mathbf{k_2}$ (folded), 0 for $\mathbf{k_1} = -\mathbf{k_2}$ (squeezed)

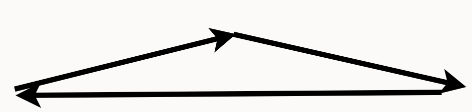

$P_\delta(k_1;t) \equiv (2\pi)^3\delta_D(\mathbf{k}_1+\mathbf{k_2})D^2(t)\langle\delta_1(\mathbf{k}_1)\delta_1(\mathbf{k}_2)\rangle$

$\mathbf{k_1}\cdot\mathbf{k_2} = \frac{1}{2}(k_3^2 - k_1^2 - k_2^2)$

NG IN LSS

$$B_\delta = B_\delta^{\mathrm{grav}} + \boxed{B_\delta^{\mathrm{prim}}}$$

full matter bispectrum

gravitational

primordial

PRIMORDIAL NG

Relation to density perturbation with Poisson equation (in linear theory):

linear matter transfer function (=1 on very large scales)

linear growth function (= a(t) during matter domination)

$$\delta(\mathbf{k},t) = \frac{2}{3}\frac{c^2k^2T(k)D(t)}{\Omega_m H_0^2}\Phi(\mathbf{k}) \equiv M(k,t)\Phi(\mathbf{k})$$

$$\Rightarrow \quad \underbrace{B_\delta^{\rm prim}(k_1,k_2,k_3;t)}_{\text{late time}} = \underbrace{M(k_1,t)M(k_2,t)M(k_3,t)}_{\text{linear transfer}}\underbrace{F_{\rm NL}B_\Phi(k_1,k_2,k_3)}_{\text{primordial}}$$

time dependence: $B_\delta^{\rm prim} \propto D^3(t), \quad B_\delta^{\rm grav} \propto D^4(t)$

- easier to see primordial contribution at earlier times (high z)

SIMULATION SETUP

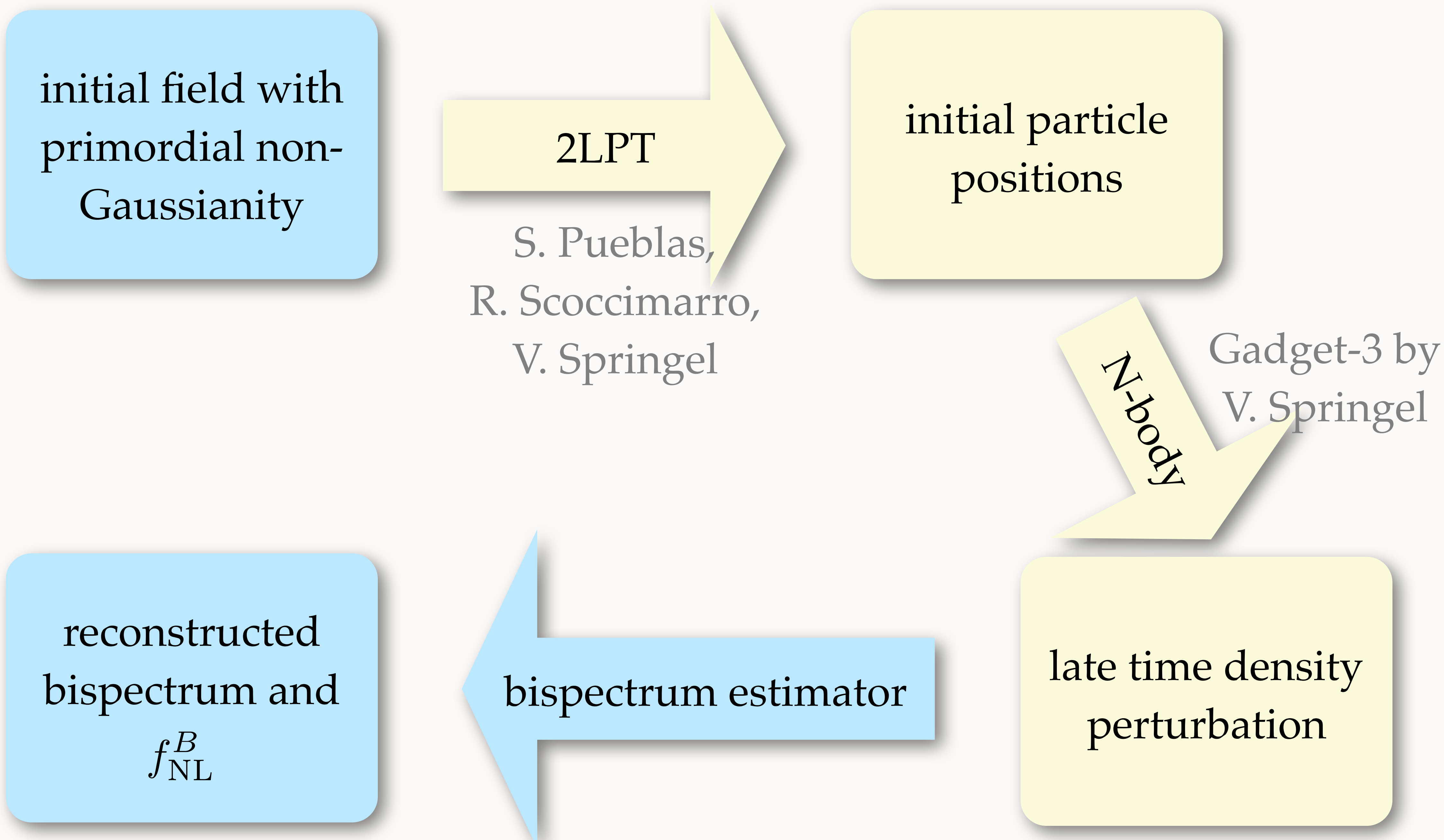

INITIAL CONDITIONS

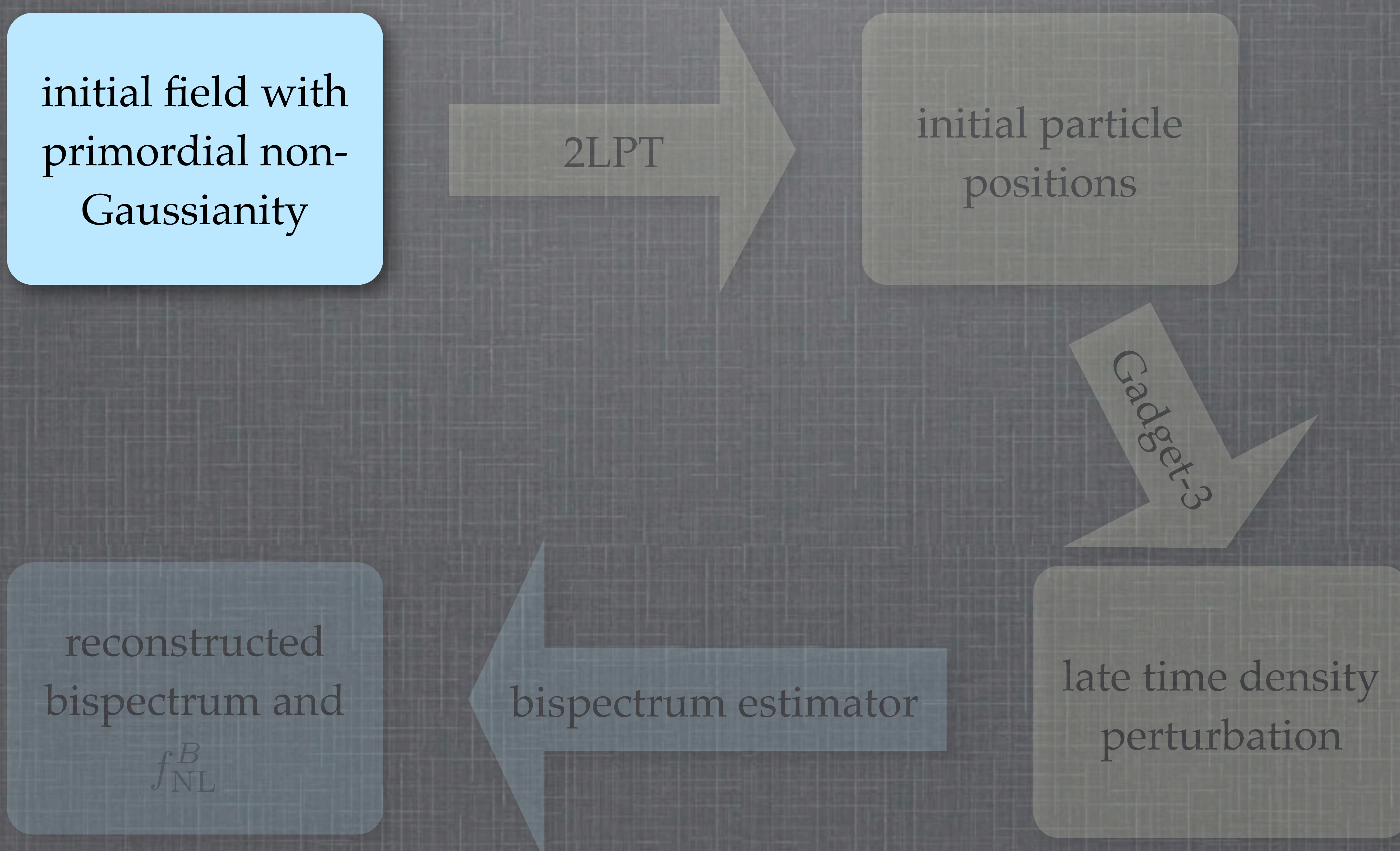

INITIAL CONDITIONS: MATHS

Aim: Create non-Gaussian field

$$\underbrace{\Phi(\mathbf{x})}_{\text{full field}} = \underbrace{\Phi_G(\mathbf{x})}_{\text{Gaussian}} + \underbrace{\Phi_{NG}(\mathbf{x})}_{\text{non-Gaussian part}}$$

INITIAL CONDITIONS: MATHS

Aim: Create non-Gaussian field

$$\underset{\text{full field}}{\Phi(\mathbf{x})} = \underset{\text{Gaussian}}{\Phi_G(\mathbf{x})} + \underset{\text{non-Gaussian part}}{\Phi_{NG}(\mathbf{x})}$$

Simplest case: local non-Gaussianity

$$\Phi(\mathbf{x}) = \Phi_G(\mathbf{x}) + f_{\mathrm{NL}}(\Phi_G^2(\mathbf{x}) - \langle\Phi_G^2\rangle)$$

INITIAL CONDITIONS: MATHS

Aim: Create non-Gaussian field

$$\underset{\text{full field}}{\Phi(\mathbf{x})} = \underset{\text{Gaussian}}{\Phi_G(\mathbf{x})} + \underset{\text{non-Gaussian part}}{\Phi_{NG}(\mathbf{x})}$$

Simplest case: local non-Gaussianity

$$\Phi(\mathbf{x}) = \Phi_G(\mathbf{x}) + f_{\rm NL}(\Phi_G^2(\mathbf{x}) - \langle\Phi_G^2\rangle)$$

General case: arbitrary bispectrum B_Φ

$$\Phi_{NG}(\mathbf{k}) = \frac{f_{\rm NL}}{2}\int\frac{d^3\mathbf{k}'d^3\mathbf{k}''}{(2\pi)^3}\delta_D(\mathbf{k}-\mathbf{k}'-\mathbf{k}'')W_B(k,k',k'')\Phi_G(\mathbf{k}')\Phi_G(\mathbf{k}'')$$

Wagner et al 2010

$$W_B(k,k',k'') \equiv \frac{B_\Phi(k,k',k'')}{P_\Phi(k)P_\Phi(k')+P_\Phi(k)P_\Phi(k'')+P_\Phi(k')P_\Phi(k'')}$$

(=2 in local case)

Symmetrisation required to preserve power spectrum

SPEED?

- **Non-separable** bispectrum kernel: $W_B(k, k', k'') = \frac{1}{k + k' + k''}$

$$\Rightarrow \quad \Phi_{NG}(\mathbf{k}) \sim \int d^3\mathbf{k}' d^3\mathbf{k}'' \frac{1}{k + k' + k''} \Phi_G(\mathbf{k}') \Phi_G(\mathbf{k}'')$$

(k″ = -k-k′)

➟ **SLOW:** different integral over **k′** for every **k**, i.e. ~N^2 operations

$N =$ total # ptcles $\sim 10^9$

SPEED?

- **Non-separable** bispectrum kernel: $W_B(k,k',k'') = \dfrac{1}{k+k'+k''}$

$$\Rightarrow \quad \Phi_{NG}(\mathbf{k}) \sim \int d^3\mathbf{k}' d^3\mathbf{k}'' \frac{1}{k+k'+k''} \Phi_G(\mathbf{k}')\Phi_G(\mathbf{k}'')$$

($\mathbf{k}'' = -\mathbf{k}-\mathbf{k}'$)

➟ **SLOW:** different integral over **k′** for every **k**, i.e. ~N^2 operations

$N =$ total # ptcles $\sim 10^9$

- **Separable** bispectrum kernel: $W_B(k,k',k'') = kk'k''$

$$\Rightarrow \quad \Phi_{NG}(\mathbf{k}) \sim \int d^3\mathbf{k}' d^3\mathbf{k}'' kk'k'' \Phi_G(\mathbf{k}')\Phi_G(\mathbf{k}'')$$

$$= k \left[\int d^3\mathbf{k}' k' \Phi_G(\mathbf{k}') \right] \times \left[\int d^3\mathbf{k}'' k'' \Phi_G(\mathbf{k}'') \right]$$

➟ **FAST:** two 3D integrals, i.e. ~N operations

SPEED?

- **Non-separable** bispectrum kernel: $W_B(k,k',k'') = \dfrac{1}{k+k'+k''}$

(**k″ = -k-k′**)

perations

al $\#$ ptcles $\sim 10^9$

- **Separable** b

Separability = Efficiency

➟ **FAST:** two 3D integrals, i.e. ~N operations

FAST INITIAL CONDITIONS

$N = \text{total } \# \text{ ptcles} \approx 10^9$

Fergusson, Regan, Shellard PRD 86, 063511 (2012), arXiv: 1008.1730
Regan, MS, Shellard, Fergusson PRD 86, 123524 (2012), arXiv:1108.3813

Need ~N^2 operations in general, but only ~N operations if W_B was **separable**:

$$W_B(k, k', k'') = f_1(k) f_2(k') f_3(k'') + \text{ perms}$$

Expand W_B in separable basis functions to get ~N scaling for *any** bispectrum:

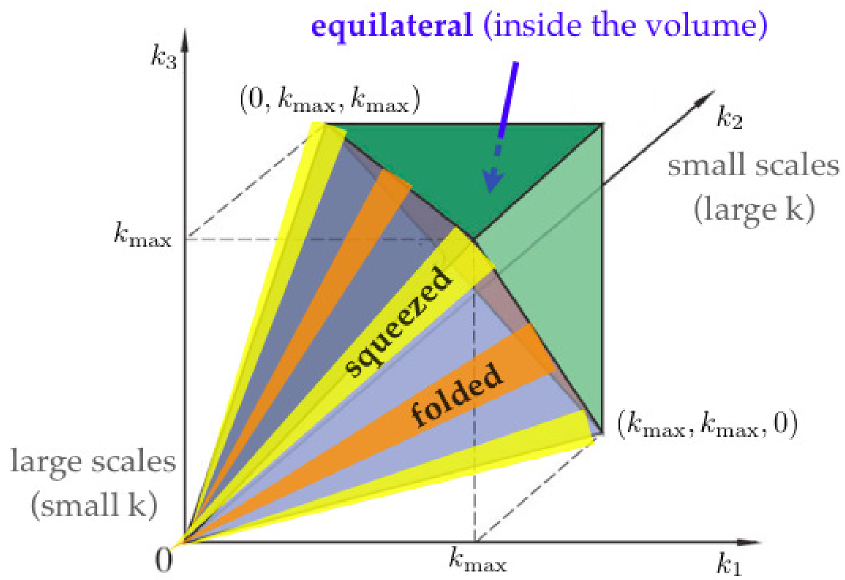

$W_B(k,k',k'')$ on space of triangle configurations

$= \alpha_0 + \alpha_1$ 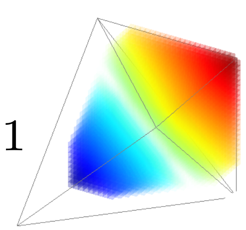 $+\alpha_2$ 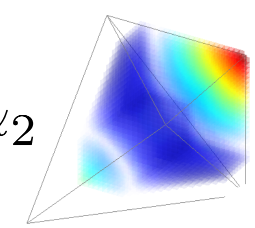 $+ \cdots + \alpha_{n_{\max}}$ 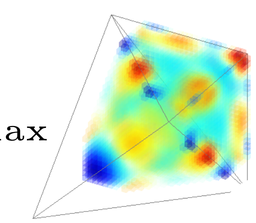

$$= \alpha_0 + \alpha_1 k k' k'' \quad + \alpha_2 (k k' k'')^2 + \cdots$$

expansion in separable basis functions
(decorrelate for convenience; around 100 basis functions represent all investigated bispectra with high accuracy)

*Scoccimarro and Verde groups try to rewrite W_B analytically in separable form; this works sometimes, but not in general

INITIAL CONDITIONS

Regan, MS, Shellard, Fergusson PRD 86, 123524 (2012), arXiv:1108.3813

- Fast and general non-Gaussian **initial conditions** for N-body simulations
  - Arbitrary (including non-separable) bispectra, diagonal-independent trispectra
  - This is the only method to simulate structure formation for general inflation models to date
  - Idea:

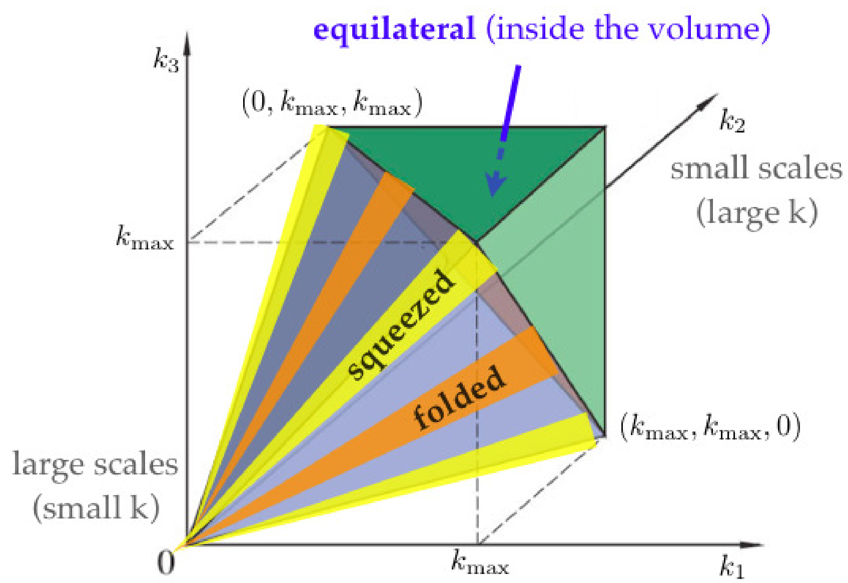

bispectrum drawn on space of triangle configurations

$= \alpha_0 + \alpha_1$ 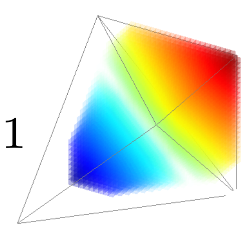 $+ \alpha_2$ 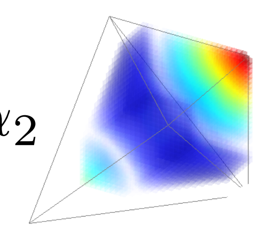 $+ \cdots + \alpha_{n_{\max}}$ 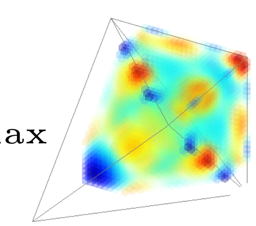

expansion in separable, uncorrelated basis functions (around 100 basis functions represent all investigated bispectra with high accuracy)

NON-GAUSSIAN *N*-BODY SIMS

MS, Regan, Shellard 1207.5678

- Application:
  - Generate non-Gaussian density
  - Convert to initial particle positions and velocities by applying 2LPT to glass configuration or regular grid (spurious bispectrum at high z decays at low z)
  - Feed into Gadget3

Name	NG shape	$f_{\rm NL}$	$L[\frac{\rm Mpc}{h}]$	N_p	z_i	$L_s[\frac{\rm kpc}{h}]$	N_r	glass
G512g	–	–	1600	512	49	156	3	yes
G512	–	–	1600	512	49	156	3	no
G_L^{512}	–	–	$\{400, 100\}$	512	49	$\{39, 9.8\}$	3	no
G768	–	–	2400	768	19	90	3	no
G1024	–	–	1875	1024	19	40	2	no
Loc10g	local	10	1600	512	49	156	3	yes
Loc10	local	10	1600	512	49	156	3	no
$\mathrm{Loc10}_L^{512}$	local	10	$\{400, 100\}$	512	49	$\{39, 9.8\}$	3	no
$\mathrm{Loc10}^-$	local	-10	1600	512	49	156	3	no
Loc20	local	20	1600	512	49	156	3	no
Loc50	local	50	1600	512	49	156	3	no
Eq100g	equil	100	1600	512	49	156	3	yes
Eq100	equil	100	1600	512	49	156	3	no
$\mathrm{Eq100}_L^{512}$	equil	100	$\{400, 100\}$	512	49	$\{39, 9.8\}$	3	no
$\mathrm{Eq100}^-$	equil	-100	1600	512	49	156	3	no
Orth100g	orth	100	1600	512	49	156	3	yes
Orth100	orth	100	1600	512	49	156	3	no
$\mathrm{Orth100}_{400}^{512}$	orth	100	400	512	49	39	3	no
$\mathrm{Orth100}^-$	orth	-100	1600	512	49	156	3	no
Flat10	flat	10	1600	512	49	156	3	no
$\mathrm{Flat10}_{400}^{512}$	flat	100	400	512	49	39	3	no

BISPECTRUM ESTIMATION

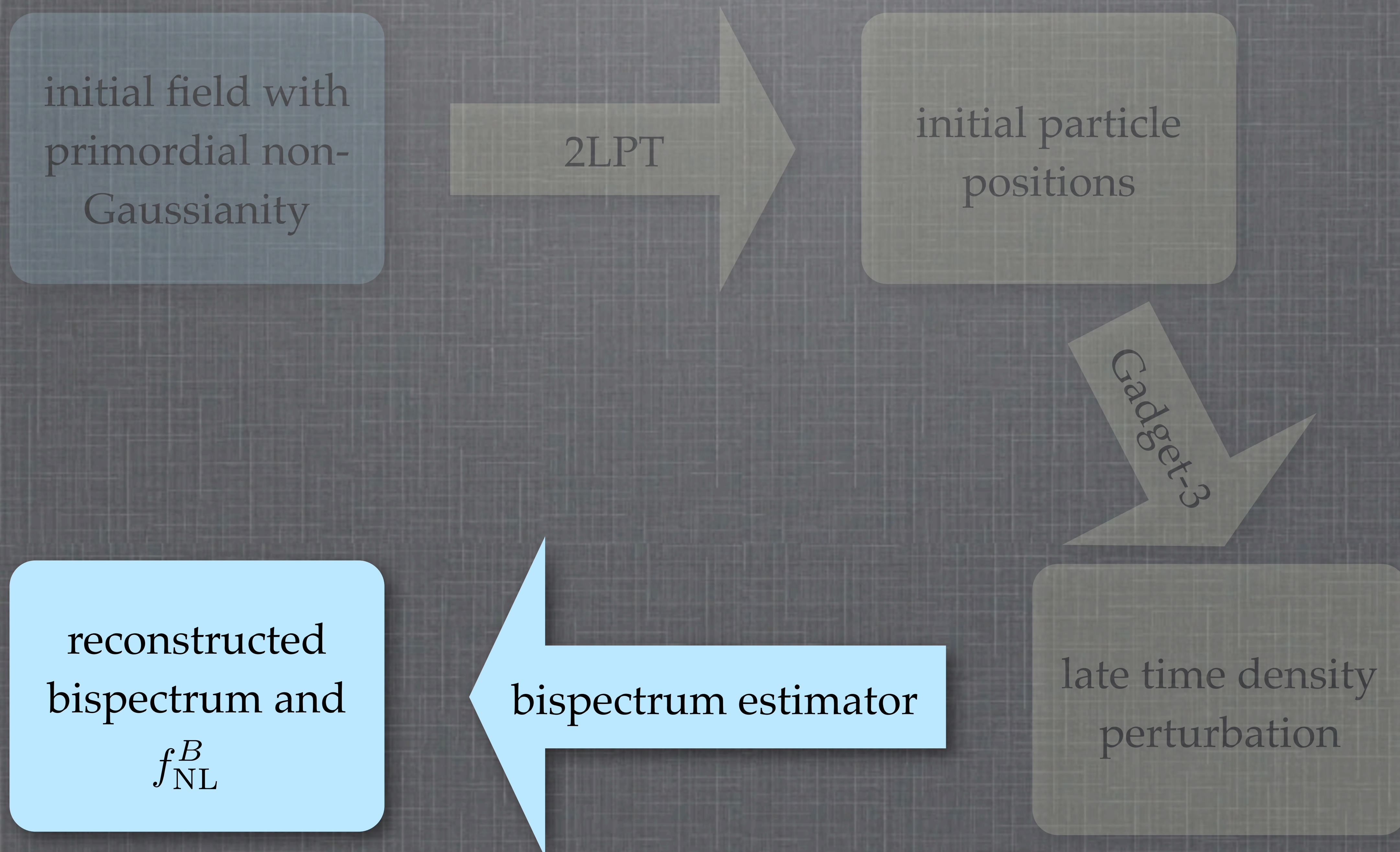

BISPECTRUM ESTIMATION: MATHS

Fergusson, Shellard et al. 2009-2012
MS, Regan, Shellard 1207.5678

Likelihood for $f_{\rm NL}$ given a density perturbation $\delta_{\mathbf{k}}$

$$\mathcal{L} \propto \int \frac{d^3\mathbf{k}_1}{(2\pi)^3}\frac{d^3\mathbf{k}_2}{(2\pi)^3}\frac{d^3\mathbf{k}_3}{(2\pi)^3}\left[1 - \frac{1}{6}\underbrace{\langle\delta_{\mathbf{k}_1}\delta_{\mathbf{k}_2}\delta_{\mathbf{k}_3}\rangle}_{\propto f_{\rm NL}B_\delta}\frac{\partial}{\partial\delta_{\mathbf{k}_1}}\frac{\partial}{\partial\delta_{\mathbf{k}_2}}\frac{\partial}{\partial\delta_{\mathbf{k}_3}} + \cdots\right]\frac{1}{\sqrt{\det C}}\prod_{ij} e^{-\frac{1}{2}\delta^*_{\mathbf{k}_i}(C^{-1})_{ij}\delta_{\mathbf{k}_j}}$$

$\propto P_\delta$

Maximise w.r.t. $f_{\rm NL}$ (given a theoretical bispectrum $B_\delta^{\rm theo}$)

$$\hat{f}_{NL}^{B_\delta^{\rm theo}} = \frac{1}{N_{f_{NL}}}\int \frac{d^3\mathbf{k}_1}{(2\pi)^3}\frac{d^3\mathbf{k}_2}{(2\pi)^3}\frac{d^3\mathbf{k}_3}{(2\pi)^3}\frac{(2\pi)^3\delta_D(\mathbf{k}_1+\mathbf{k}_2+\mathbf{k}_3)B_\delta^{\rm theo}(k_1,k_2,k_3)\delta_{\mathbf{k}_1}\delta_{\mathbf{k}_2}\delta_{\mathbf{k}_3}}{P_\delta(k_1)P_\delta(k_2)P_\delta(k_3)}$$

Requires ~N^2 operations in general, but only ~N operations if $B_\delta^{\rm theo}$ was separable

➟ Measure amplitudes β_n^R of separable basis functions

➟ Combine them to reconstruct full bispectrum from the data:

$$\hat{B}(k_1,k_2,k_3) = \sum_n \beta_n^R \sqrt{\frac{P_\delta(k_1)P_\delta(k_2)P_\delta(k_3)}{k_1k_2k_3}}R_n(k_1,k_2,k_3)$$

depends on data

where $\beta_n^R \equiv \sum_m \lambda_{nm}\beta_m^Q$, $\quad \beta_m^Q \equiv \int d^3\mathbf{x} M_r(\mathbf{x})M_s(\mathbf{x})M_t(\mathbf{x})$, $\quad M_r(\mathbf{x}) \equiv \int \frac{d^3\mathbf{k}}{(2\pi)^3}e^{i\mathbf{k}\mathbf{x}}\frac{q_r(k)\delta_{\mathbf{k}}^{\rm obs}}{\sqrt{kP_\delta(k)}}$

BISPECTRUM ESTIMATION

MS, Regan, Shellard 1207.5678

- Fast and general **bispectrum estimator** for *N*-body simulations
  - Measure ~100 $f_{\rm NL}$ amplitudes of separable basis shapes, combine them to reconstruct the full bispectrum
  - Scales like 100xN instead of N^2, where N~10^9 (speedup by factor ~10^7)
  - Can estimate bispectrum whenever power spectrum is typically measured

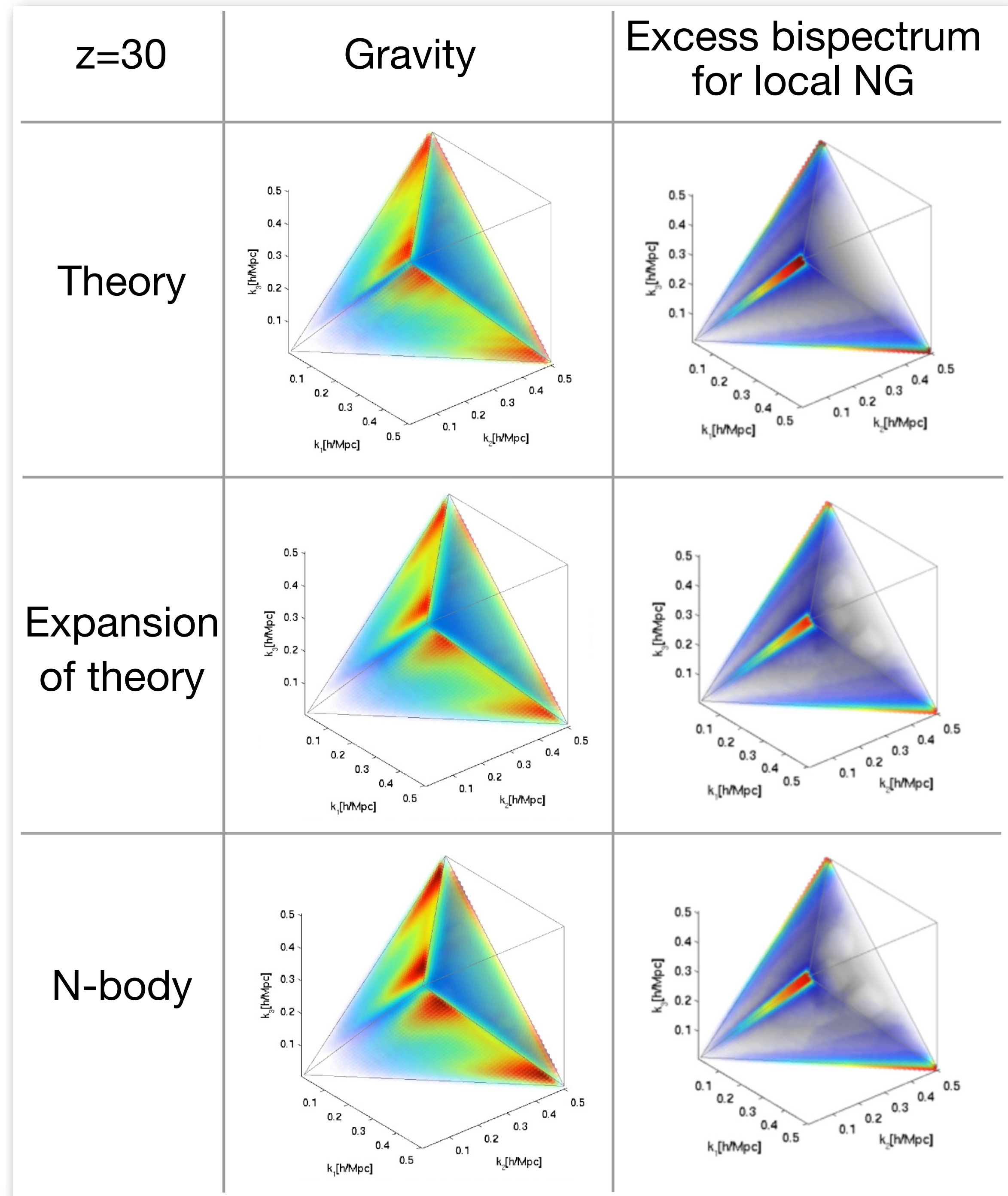

  - Validated against PT at high *z*
  - Useful compression to ~100 numbers
  - Automatically includes all triangles
  - Loss of total *S*/*N* due to truncation of basis is only a few percent (could be improved with larger basis; for ~*N* basis functions the estimator would be exact)

CONSISTENCY CHECK

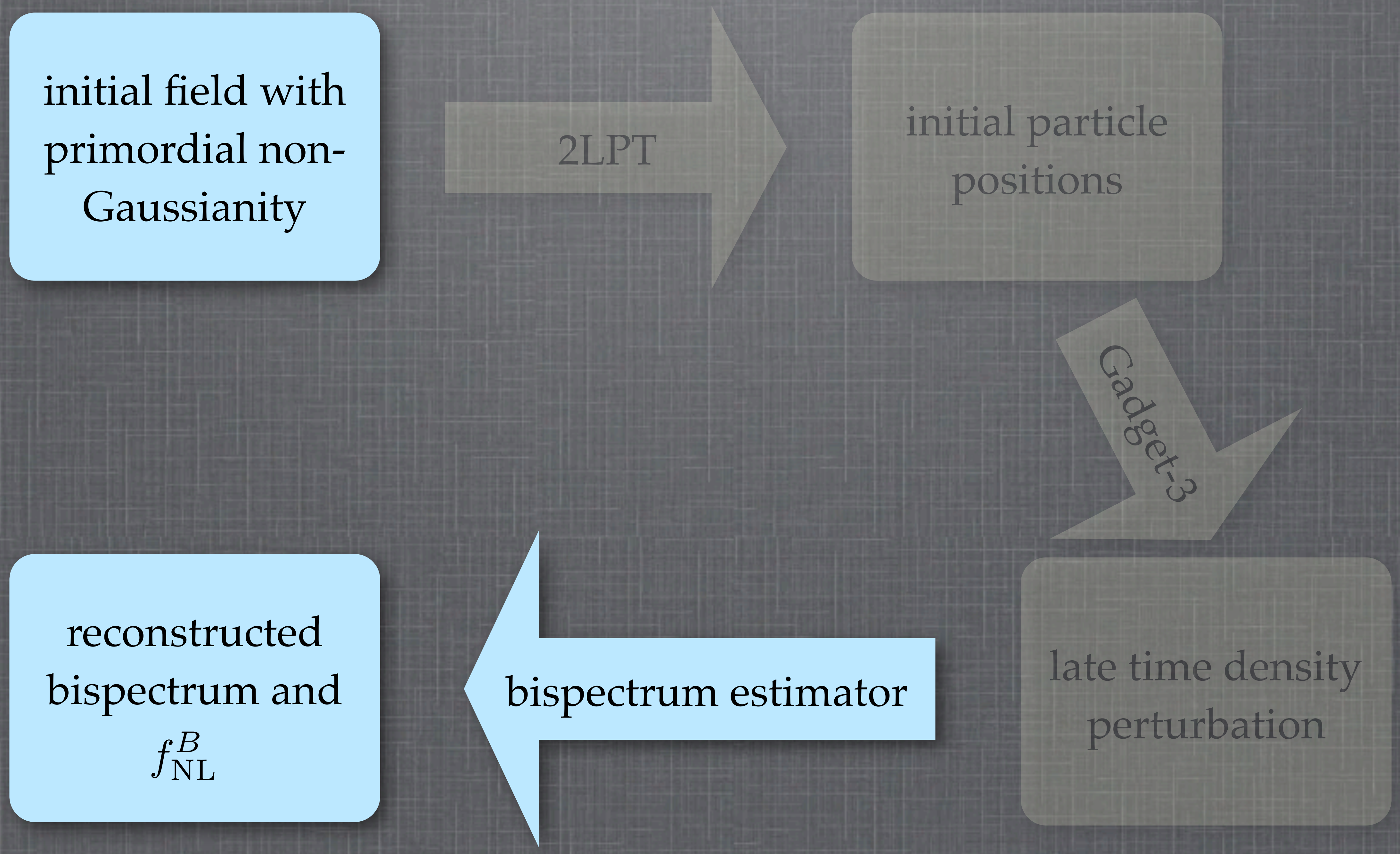

CONSISTENCY CHECK

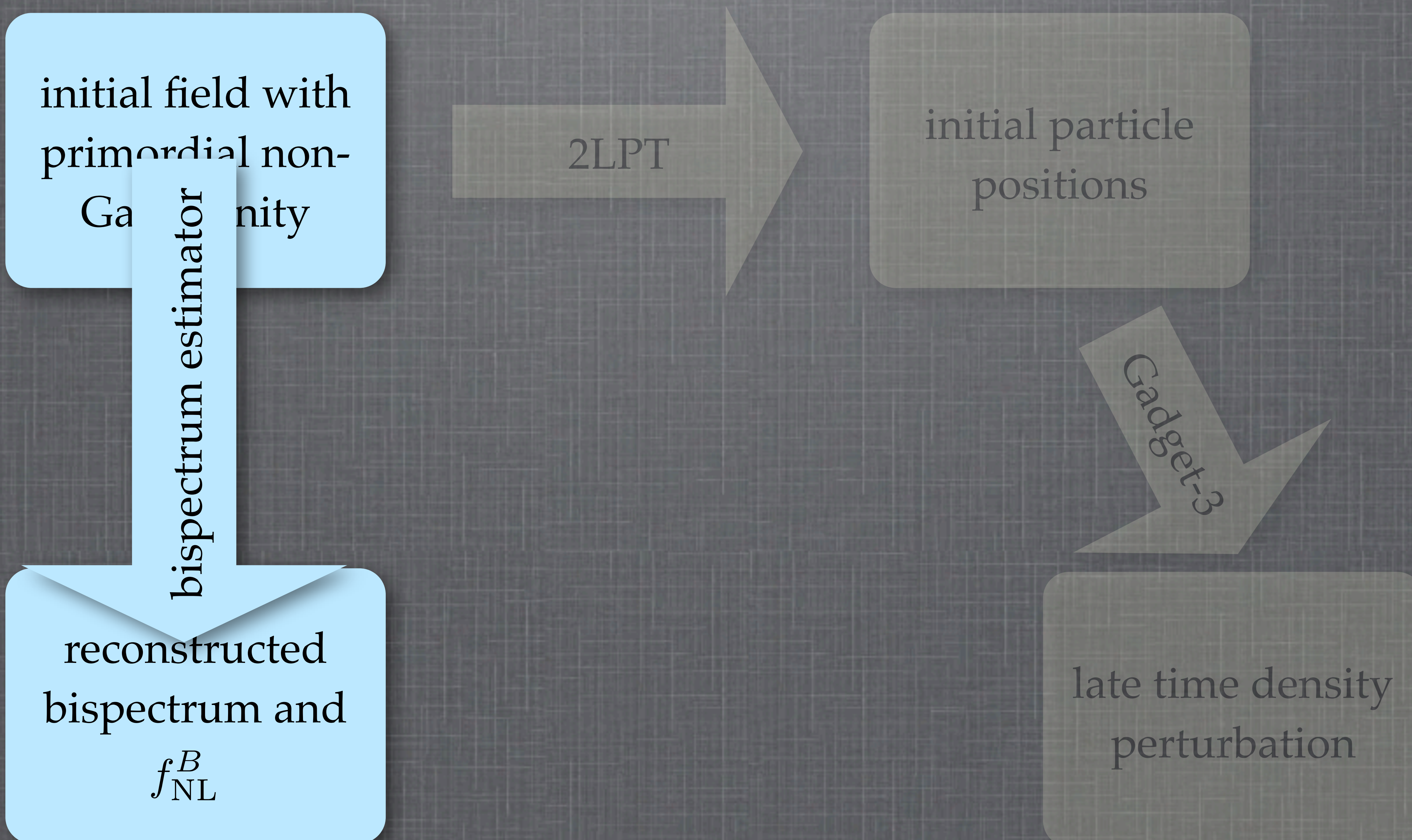

CONSISTENCY CHECK

Regan, MS, Shellard, Fergusson 1108.3813

Generate non-Gaussian field Φ and estimate its bispectrum, both with separable mode expansion (no time evolution)

(theory) (sims)

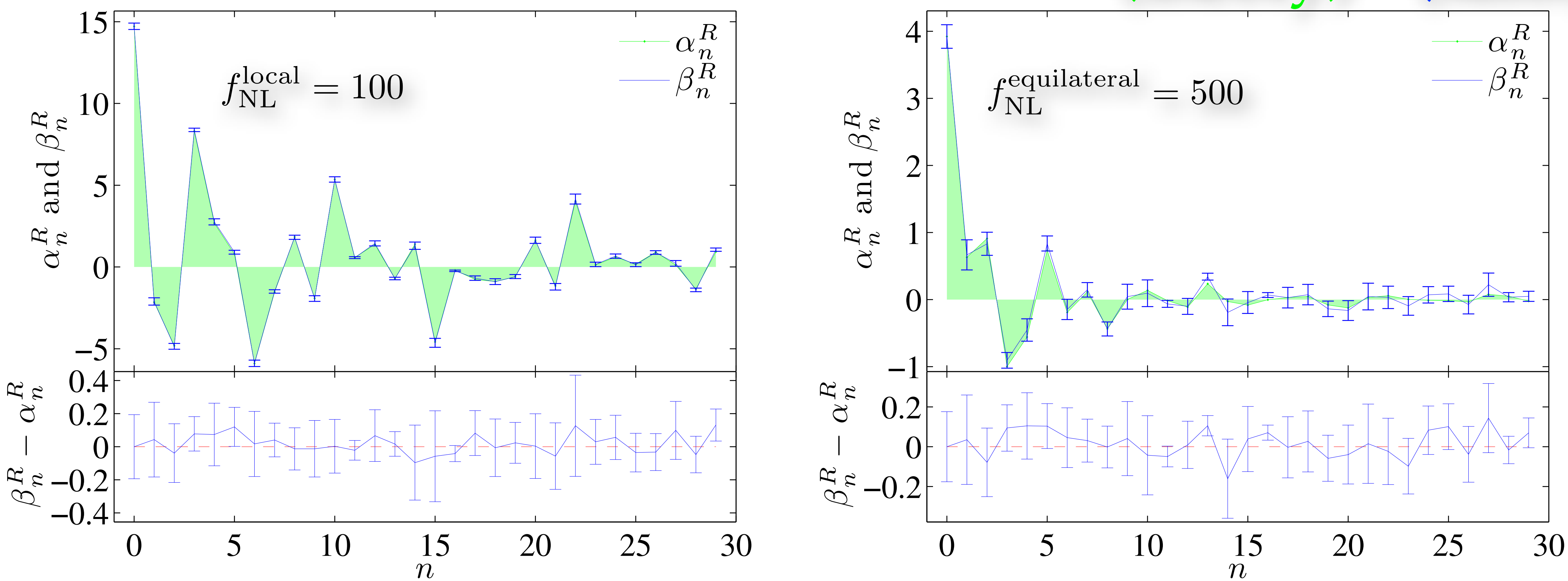

5 realisations with $N = 512$ and $L = 100$ Mpc/h

more shapes and generalisation to trispectrum: 1108.3813

FULL RUN & RESULTS

initial field with primordial non-Gaussianity

2LPT

initial particle positions

Gadget-3

late time density perturbation

bispectrum estimator

reconstructed bispectrum and f_{NL}^{B}

GAUSSIAN

SIMULATIONS

GAUSSIAN SIMULATIONS
COMPARISON WITH TREE LEVEL

MS, Regan, Shellard 1207.5678

z=30

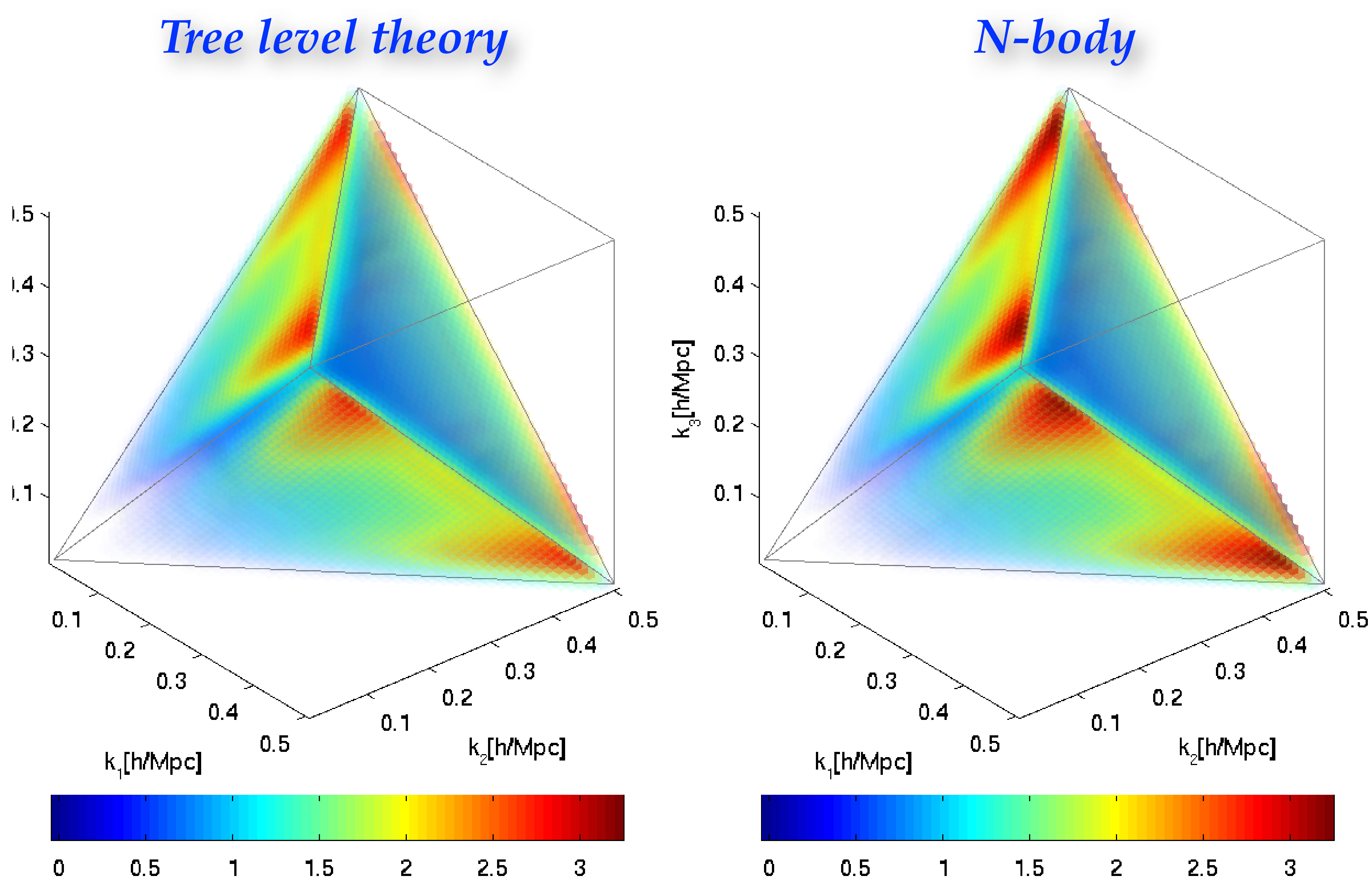

Plot S/N weighted bispectrum $\sqrt{k_1 k_2 k_3} B_\delta(k_1, k_2, k_3) / \sqrt{P_\delta(k_1) P_\delta(k_2) P_\delta(k_3)}$

3 realisations of 512^3 particles in a $L = 1600$ Mpc$/h$ box with $z_{\rm init} = 49$ and $k = 0.004$ - $0.5\ h/$Mpc

GAUSSIAN SIMULATIONS
COMPARISON WITH TREE LEVEL

MS, Regan, Shellard 1207.5678

z=2

Tree level theory

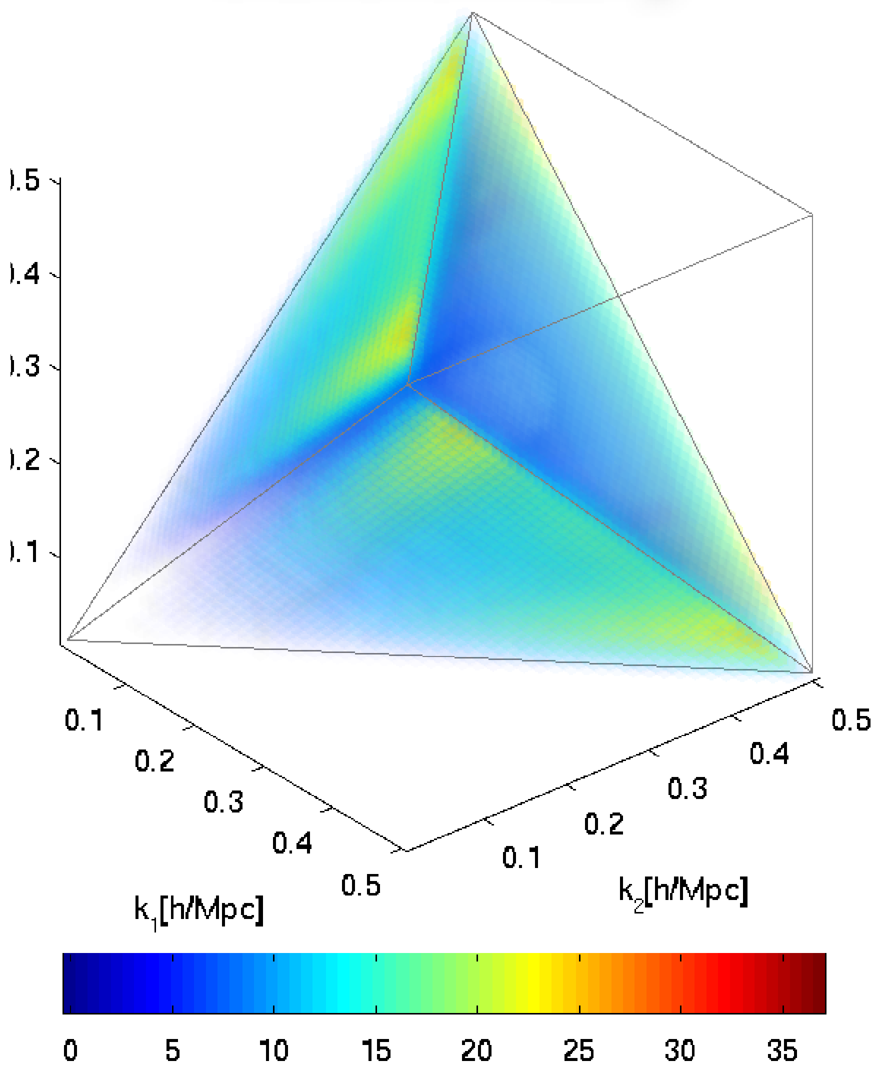

N-body

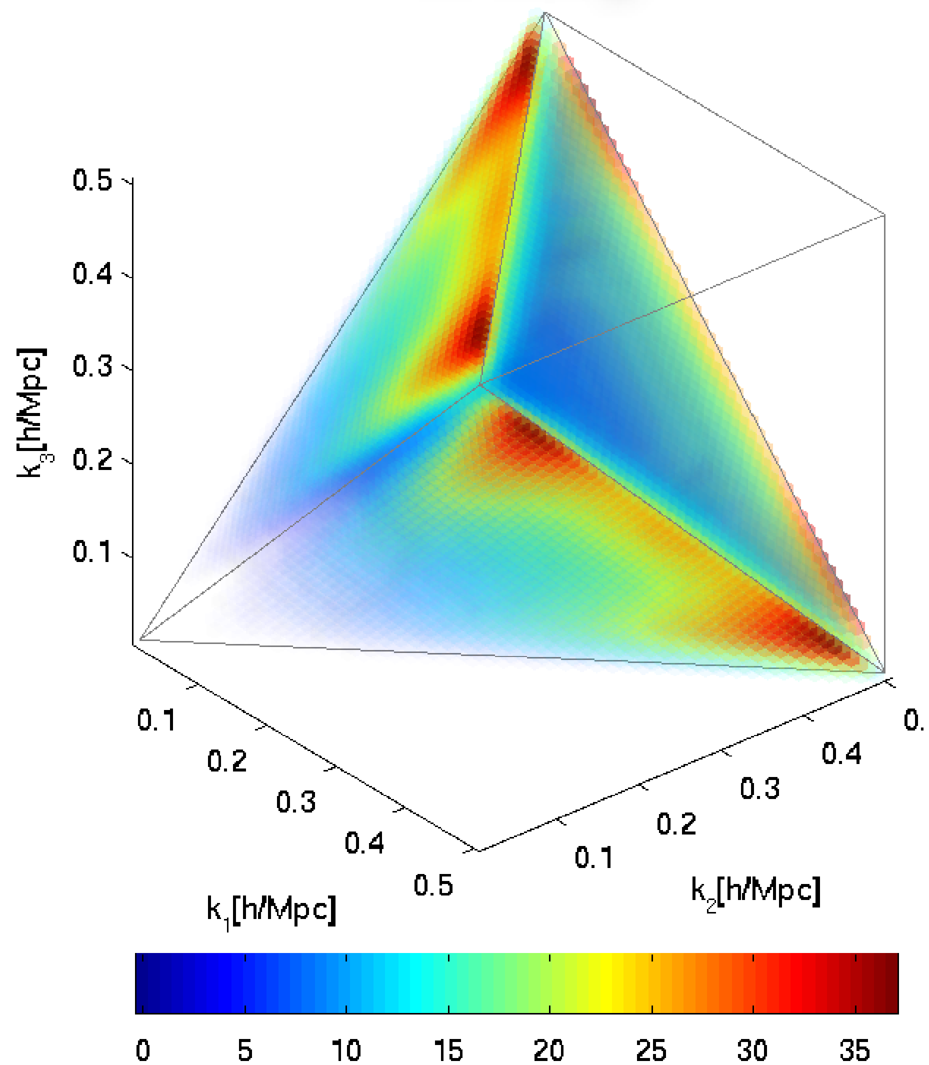

Plot S/N weighted bispectrum $\sqrt{k_1 k_2 k_3} B_\delta(k_1, k_2, k_3) / \sqrt{P_\delta(k_1) P_\delta(k_2) P_\delta(k_3)}$

3 realisations of 512^3 particles in a $L = 1600$ Mpc$/h$ box with $z_{\rm init} = 49$ and $k = 0.004$ - $0.5\ h/$Mpc

GAUSSIAN SIMULATIONS

COMPARISON WITH TREE LEVEL

MS, Regan, Shellard 1207.5678

z=0

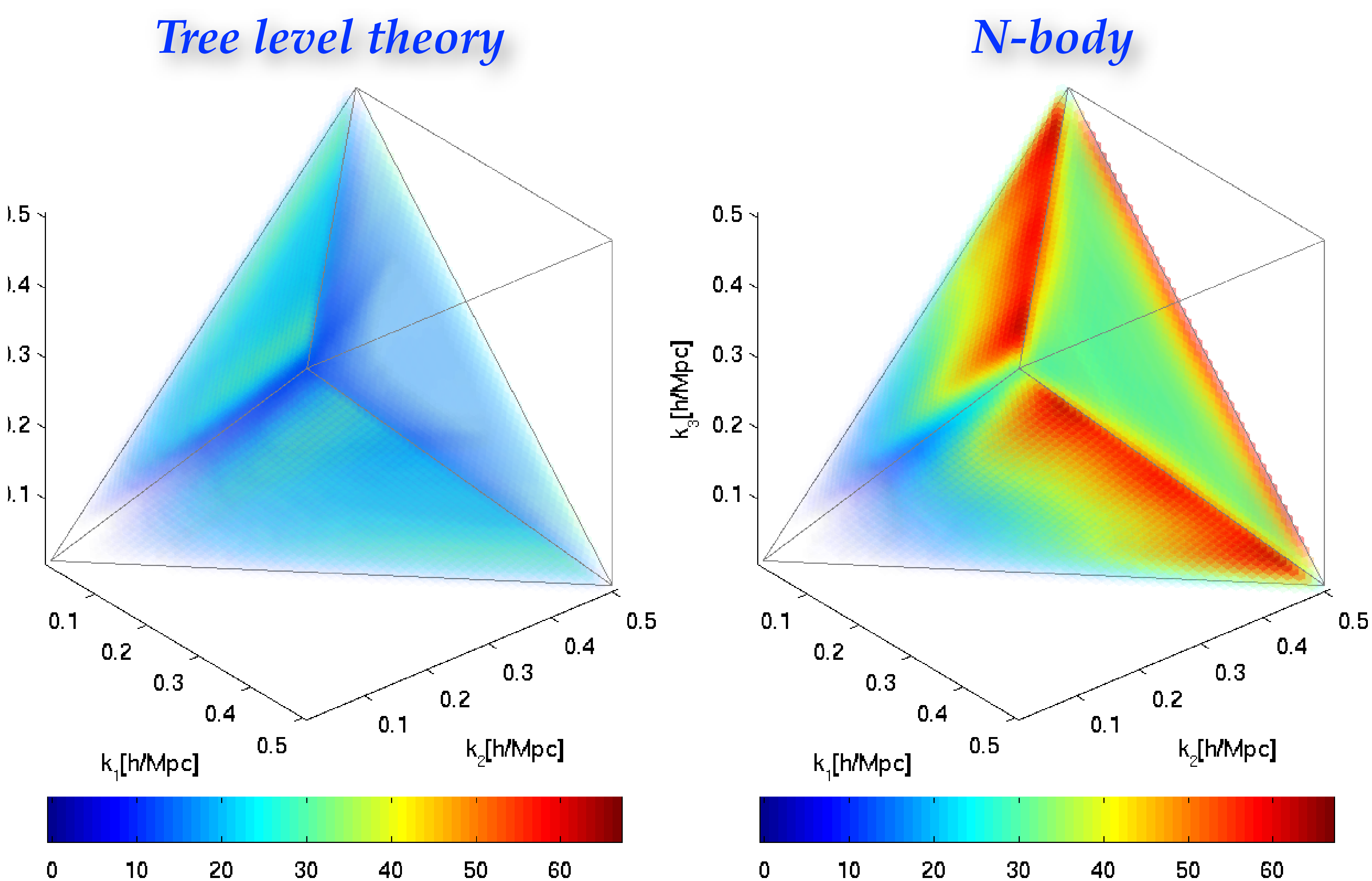

Plot S/N weighted bispectrum $\sqrt{k_1 k_2 k_3} B_\delta(k_1, k_2, k_3) / \sqrt{P_\delta(k_1) P_\delta(k_2) P_\delta(k_3)}$

3 realisations of 512^3 particles in a $L = 1600$ Mpc$/h$ box with $z_{\rm init} = 49$ and $k = 0.004$ - $0.5\ h/$Mpc

GAUSSIAN SIMULATIONS ON SMALL SCALES

MS, Regan, Shellard 1207.5678

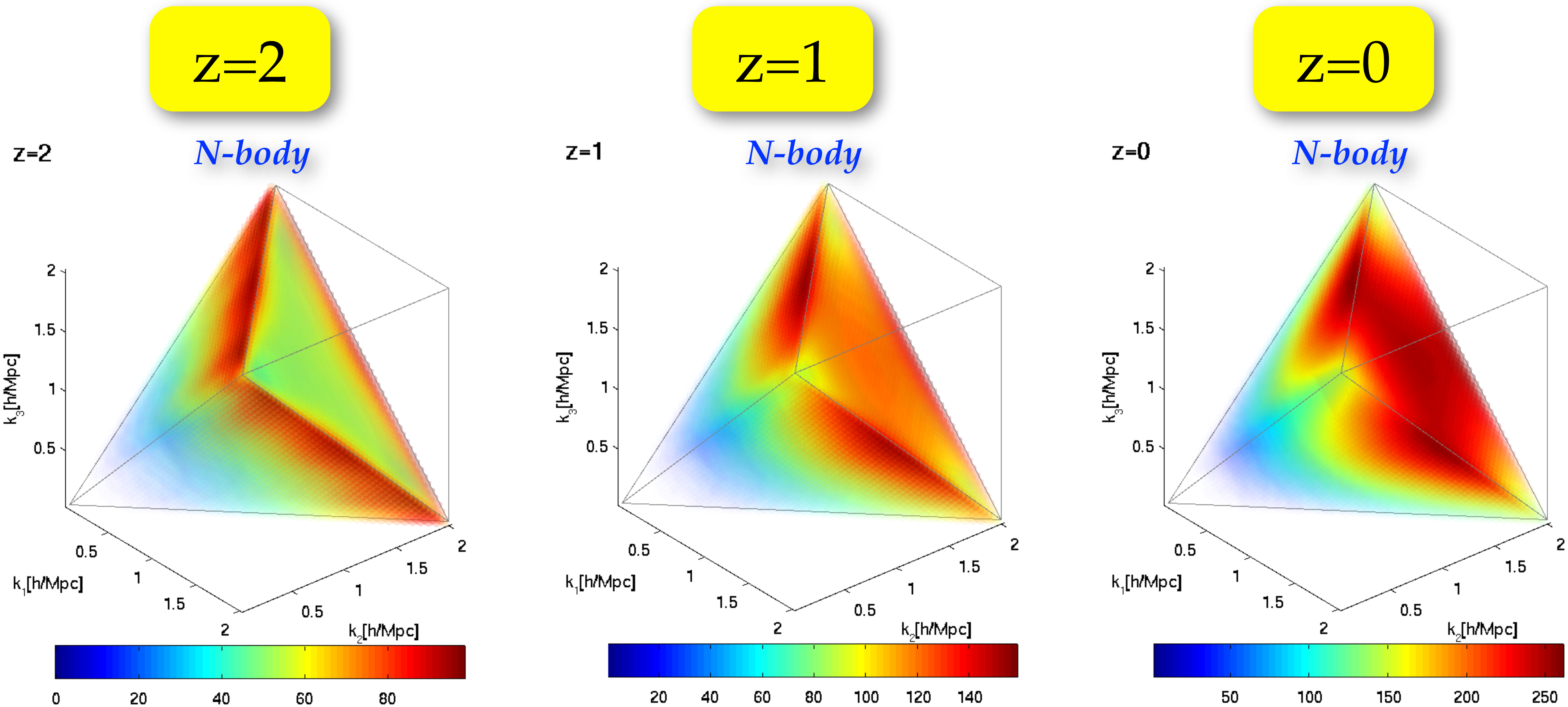

Plot S/N weighted bispectrum $\sqrt{k_1 k_2 k_3} B_\delta(k_1, k_2, k_3) / \sqrt{P_\delta(k_1) P_\delta(k_2) P_\delta(k_3)}$

3 realisations of 512^3 particles in a $L = 400$ Mpc$/h$ box with $z_{\rm init} = 49$ and $k = 0.016$ - $2.0\ h/$Mpc

GAUSSIAN SIMULATIONS

COMPARISON WITH DARK MATTER

z=4

MS, Regan, Shellard 1207.5678

DM density

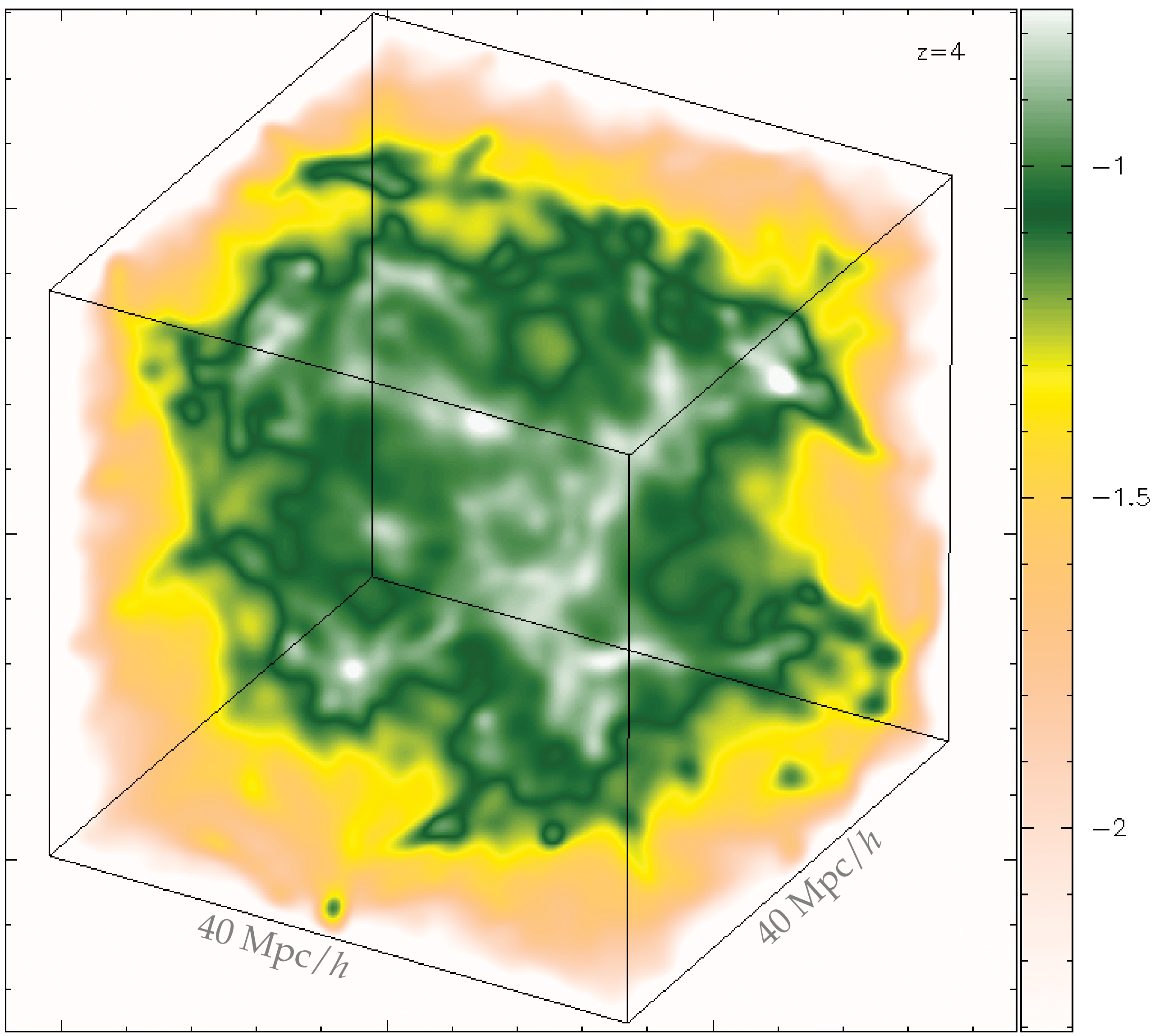

DM bispectrum

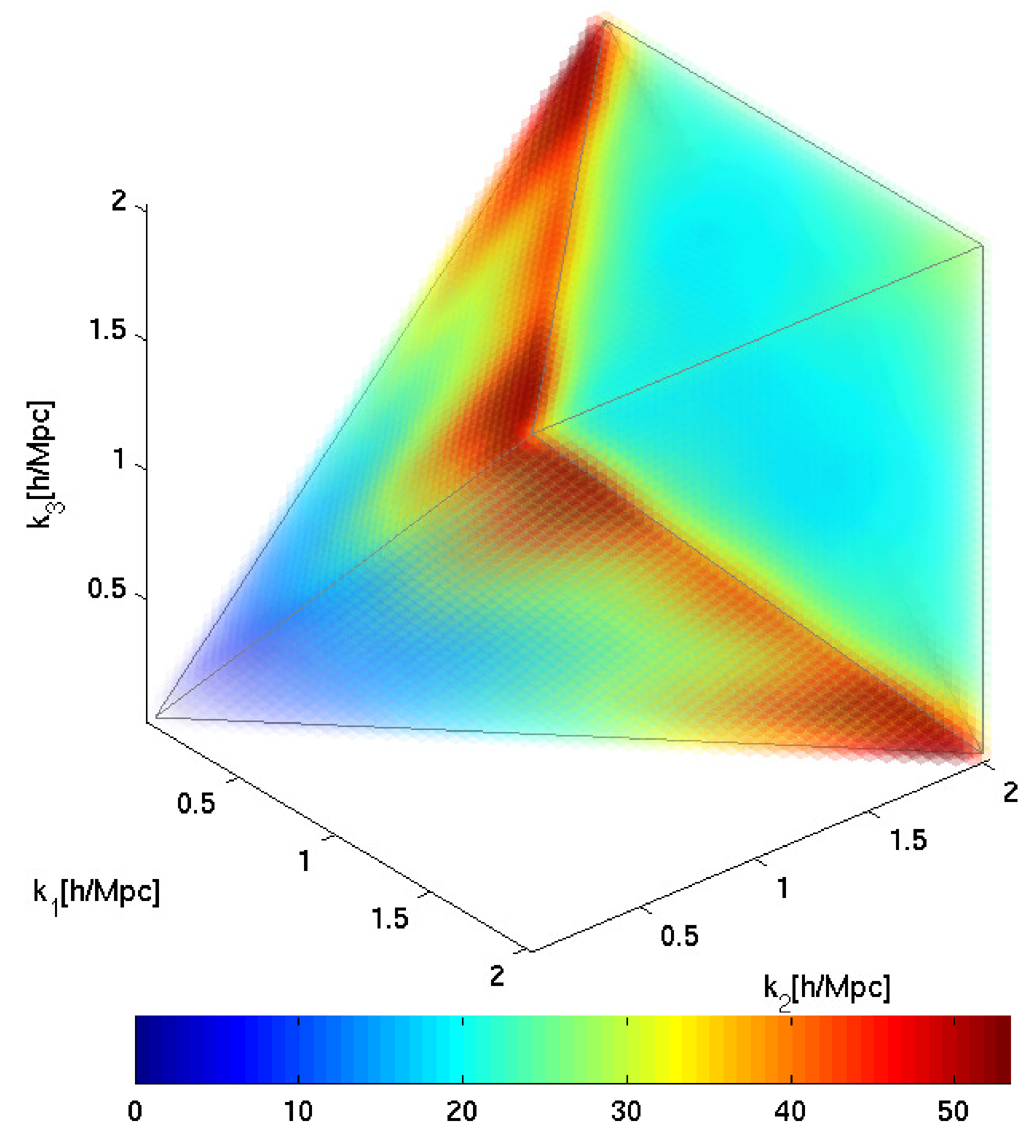

Plot DM density in $(40\ \mathrm{Mpc}/h)^3$ subbox and bispectrum signal $\sqrt{k_1 k_2 k_3} B_\delta(k_1, k_2, k_3) / \sqrt{P_\delta(k_1) P_\delta(k_2) P_\delta(k_3)}$

512^3 particles in a $L = 400\ \mathrm{Mpc}/h$ box with $z_{\mathrm{init}} = 49$ and $k = 0.016$ - $2\ h/\mathrm{Mpc}$

GAUSSIAN SIMULATIONS

COMPARISON WITH DARK MATTER

z=2

MS, Regan, Shellard 1207.5678

DM density

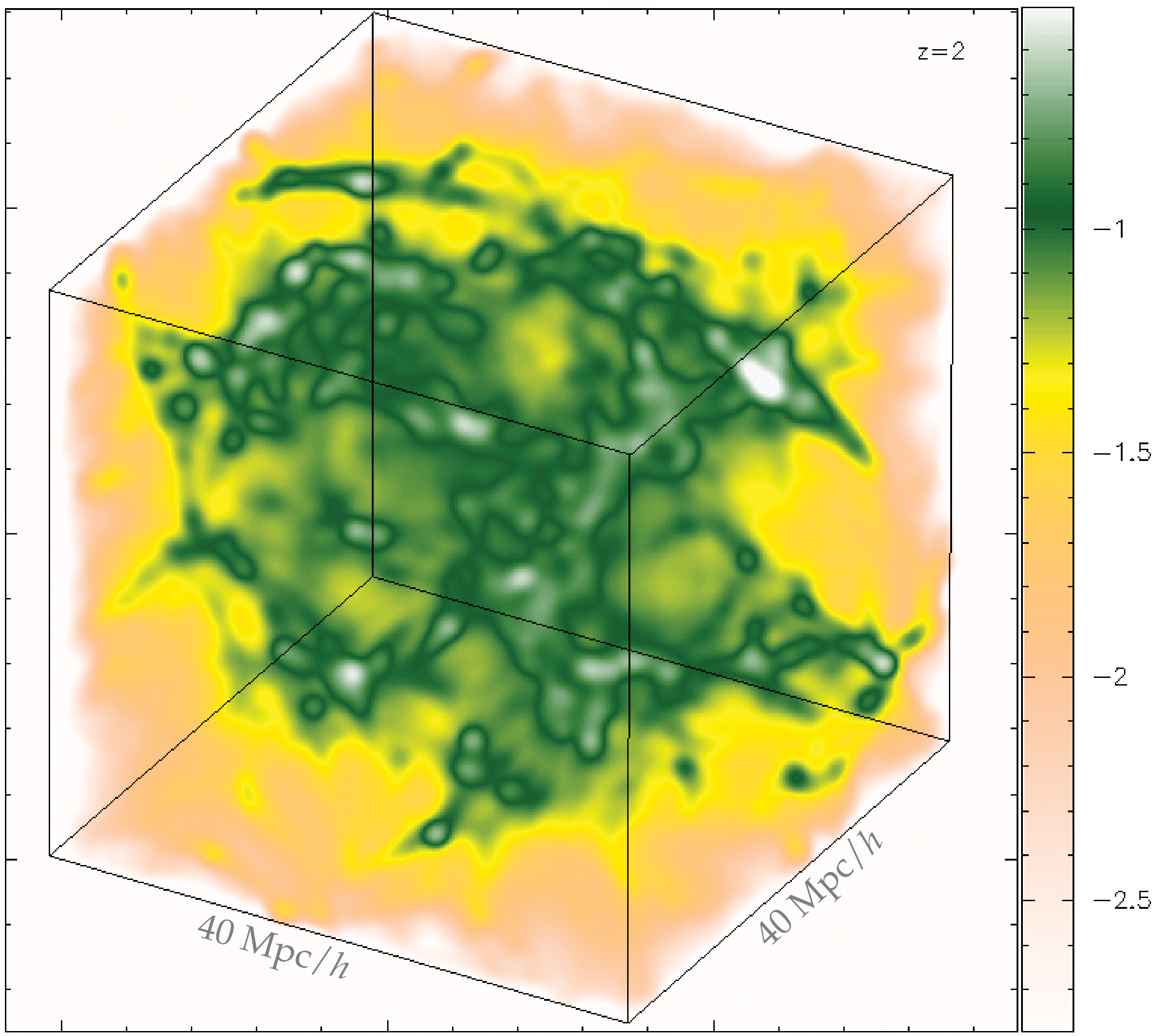

DM bispectrum

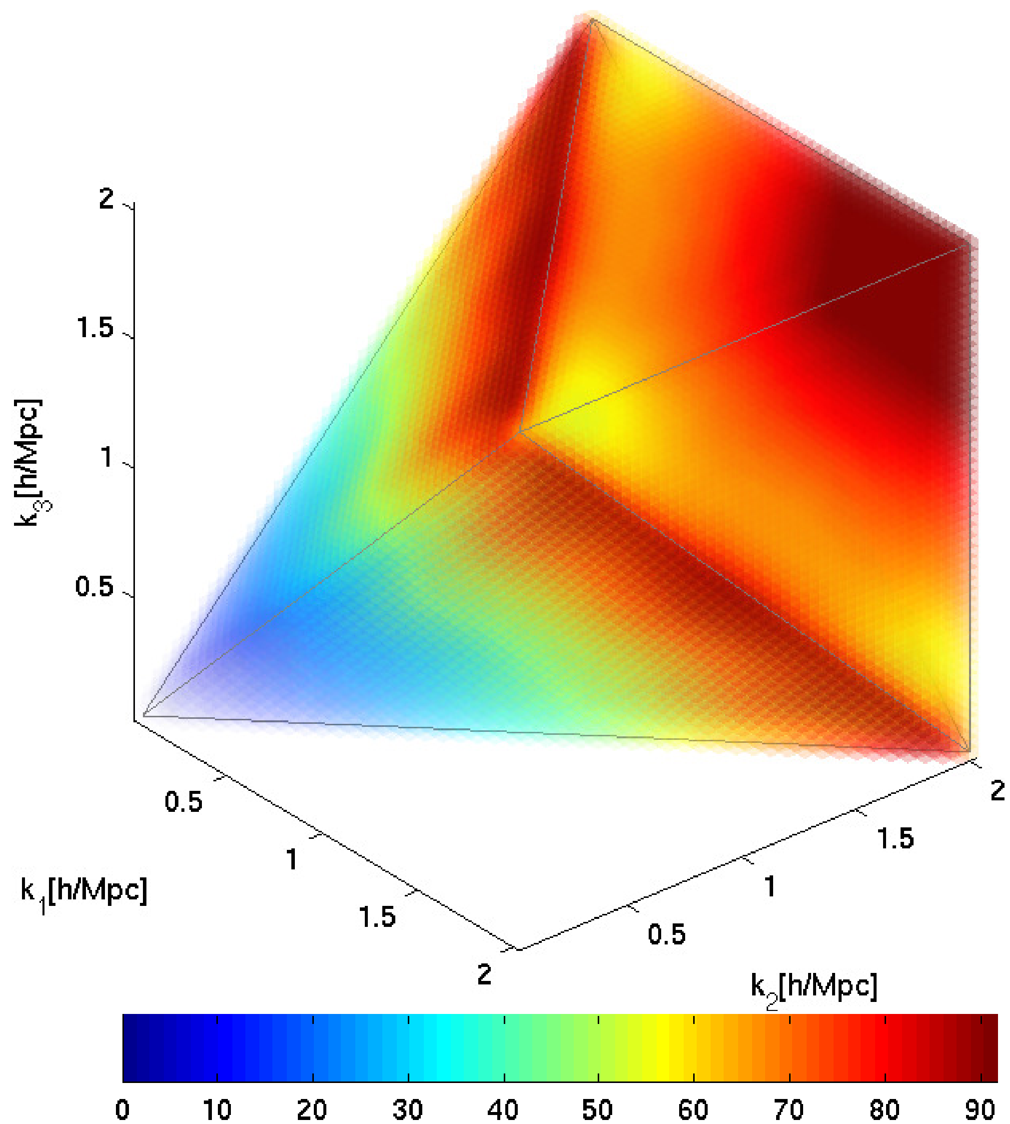

Plot DM density in (40 Mpc/h)^3 subbox and bispectrum signal $\sqrt{k_1 k_2 k_3} B_\delta(k_1, k_2, k_3) / \sqrt{P_\delta(k_1) P_\delta(k_2) P_\delta(k_3)}$

512^3 particles in a $L = 400$ Mpc/h box with $z_{\rm init} = 49$ and $k = 0.016$ - 2 h/Mpc

GAUSSIAN SIMULATIONS

COMPARISON WITH DARK MATTER

z=0

MS, Regan, Shellard 1207.5678

DM density

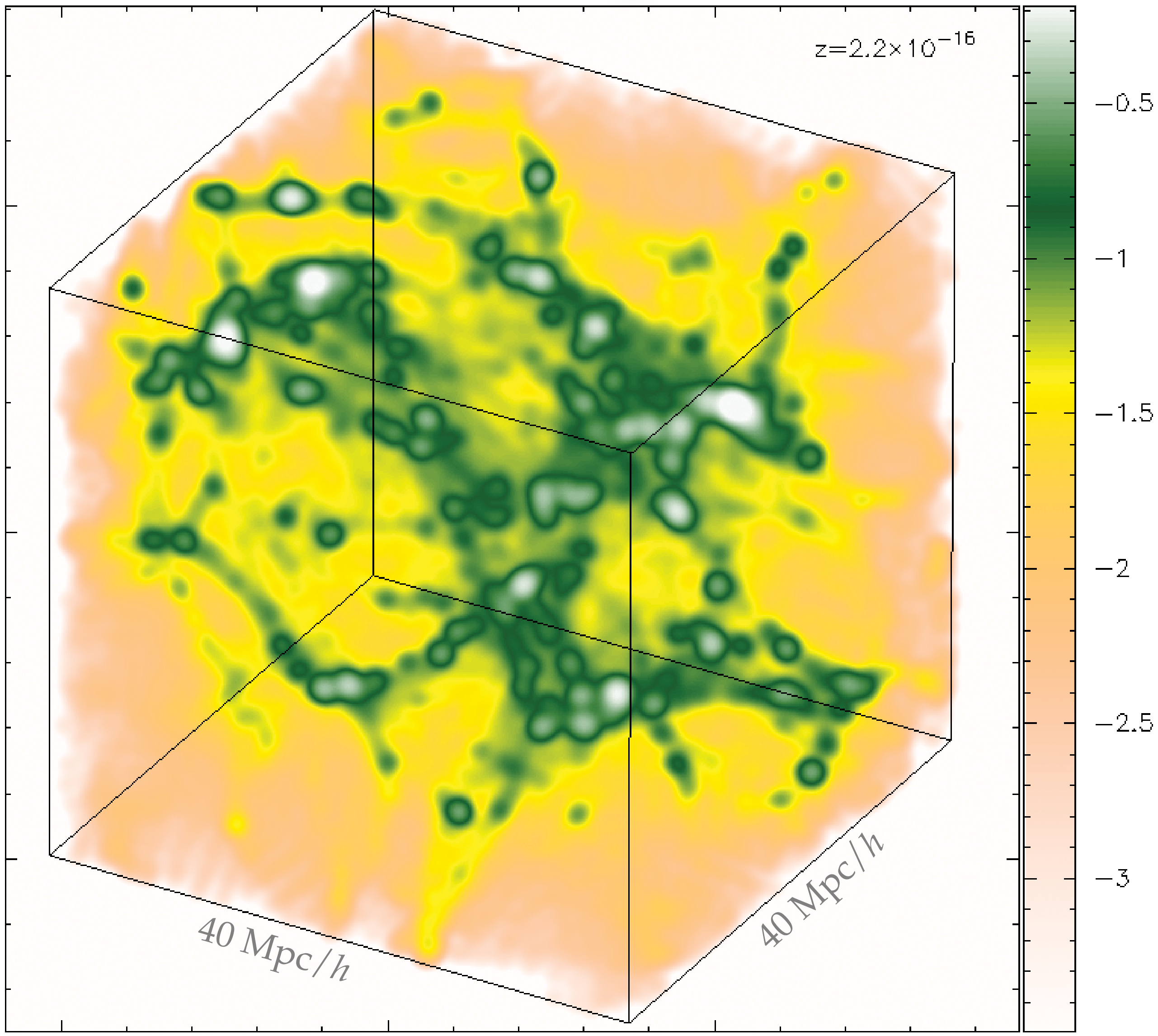

DM bispectrum

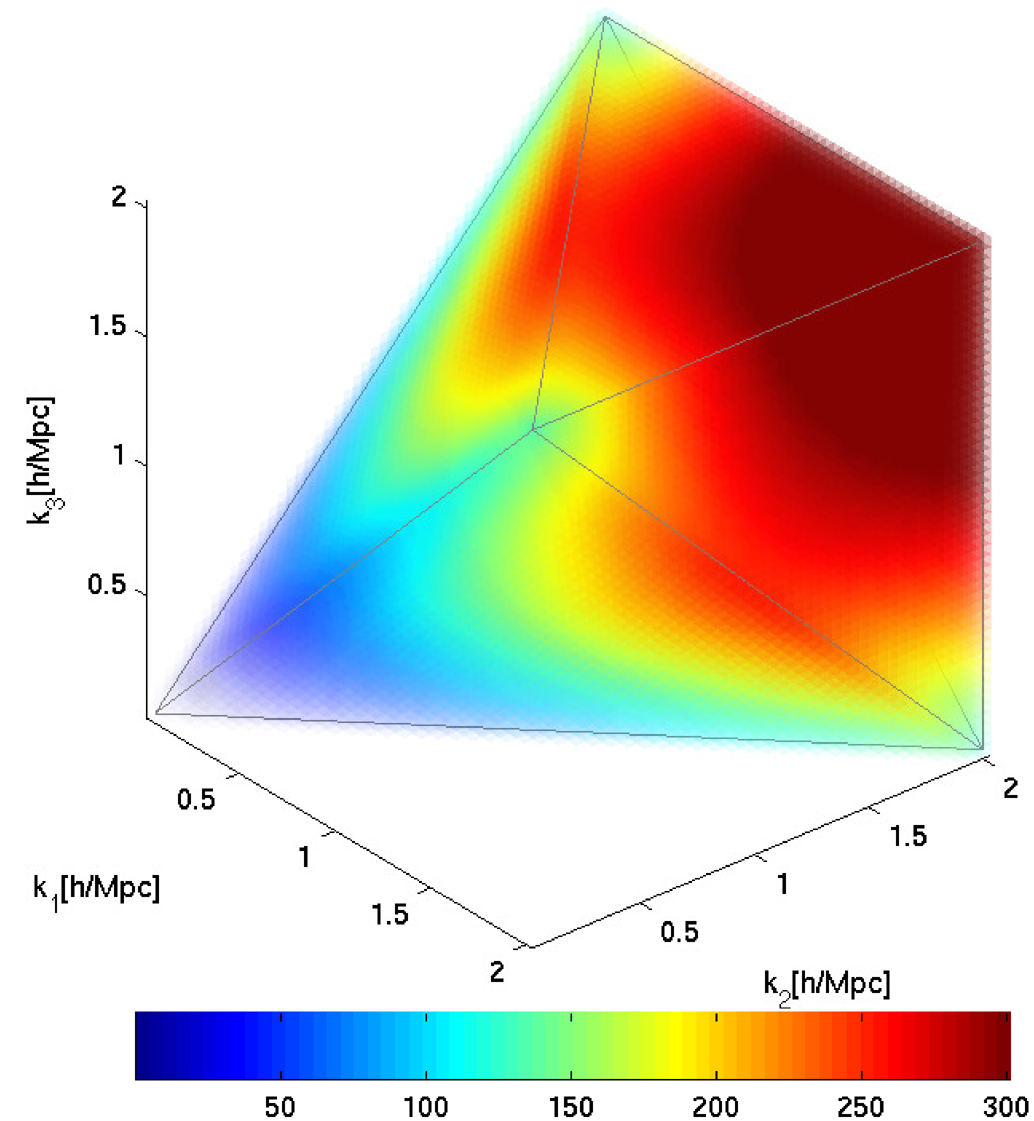

Plot DM density in (40 Mpc/h)^3 subbox and bispectrum signal $\sqrt{k_1k_2k_3}B_\delta(k_1,k_2,k_3)/\sqrt{P_\delta(k_1)P_\delta(k_2)P_\delta(k_3)}$

512^3 particles in a $L = 400$ Mpc/h box with $z_{\rm init} = 49$ and $k = 0.016$ - 2 h/Mpc

GAUSSIAN SIMULATIONS

SUMMARY

MS, Regan, Shellard 1207.5678

Summary Gaussian N-body simulations

- Measured gravitational DM bispectrum for all triangles down to k=2hMpc^{-1}
- Non-linearities mainly enhance 'constant' 1-halo bispectrum
- Bispectrum characterises 3d DM structures like pancakes, filaments, clusters
- Self-similarity
  (constant contribution appears towards late times at fixed length scale, and towards small scales at fixed time)

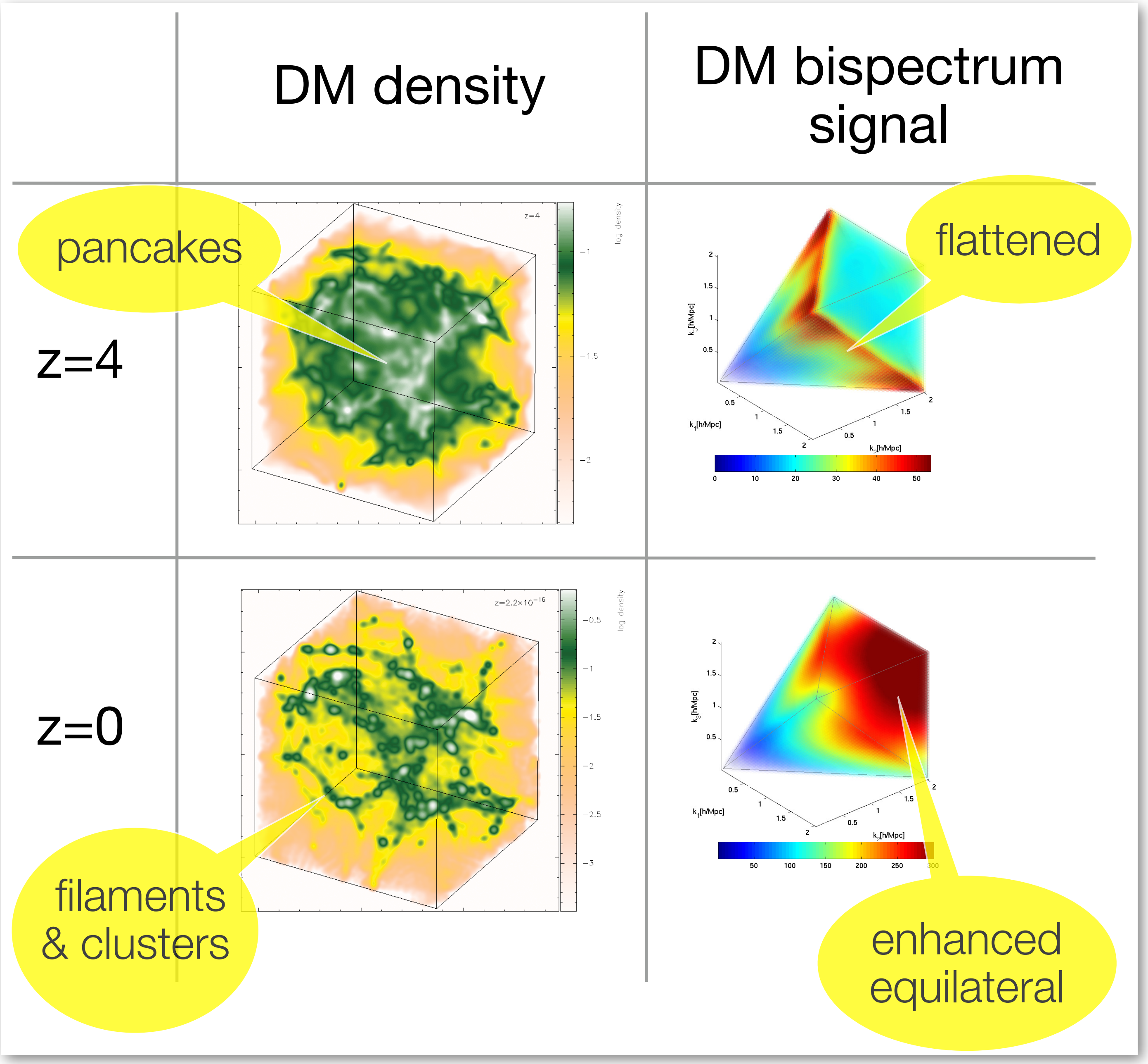

<u>NON</u>-GAUSSIAN

SIMULATIONS

LOCAL NON-GAUSSIAN SIMS

MS, Regan, Shellard 1207.5678

z=30

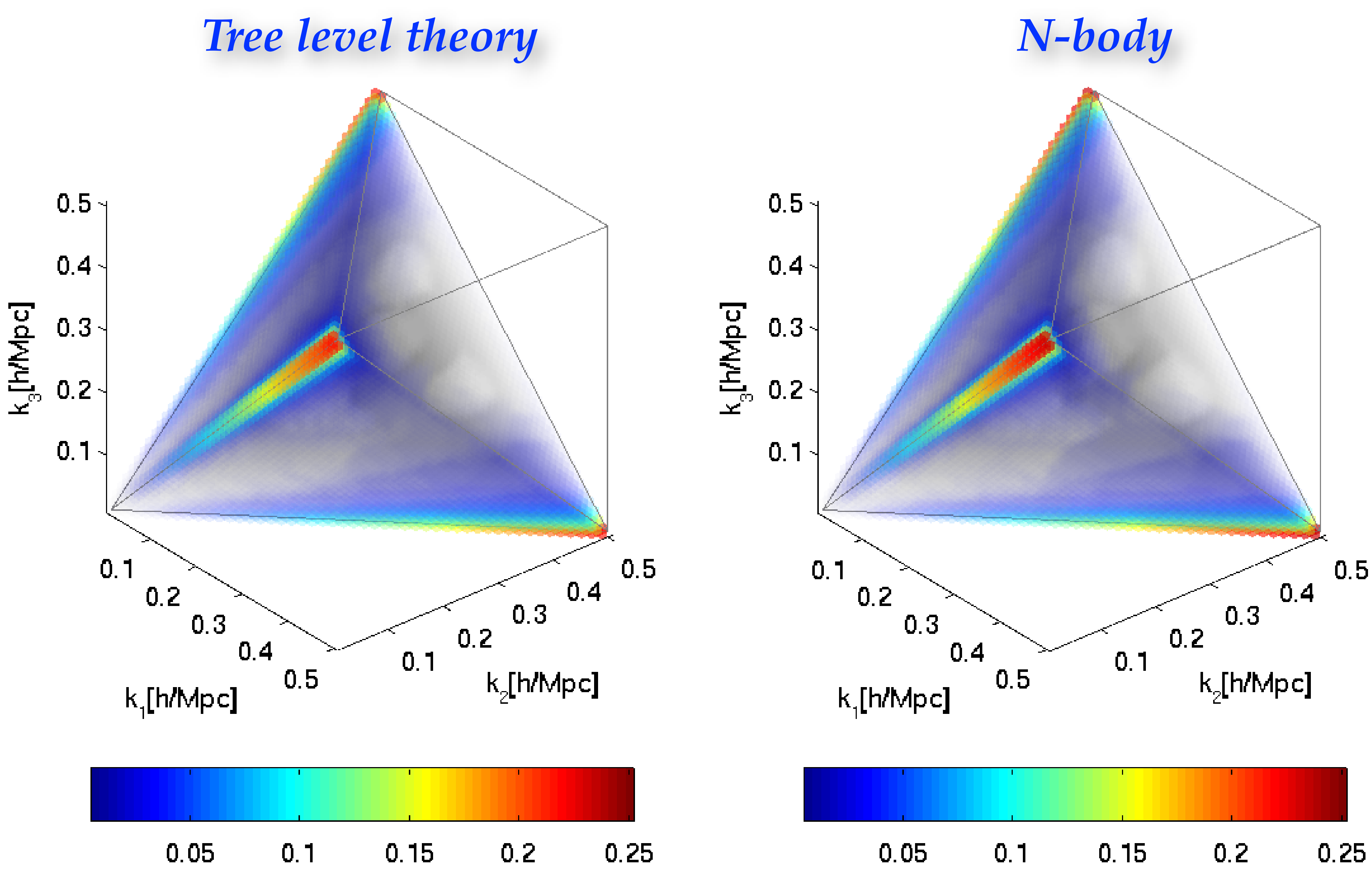

Plot S/N weighted **excess** bispectrum $\sqrt{k_1 k_2 k_3} B_\delta(k_1, k_2, k_3) / \sqrt{P_\delta(k_1) P_\delta(k_2) P_\delta(k_3)}$

3 realisations of 512^3 particles in a $L = 1600$ Mpc$/h$ box with $z_{\rm init} = 49$ and $k = 0.004$-$0.5\ h/$Mpc, f_{NL}=10

LOCAL NON-GAUSSIAN SIMS

MS, Regan, Shellard 1207.5678

z=2

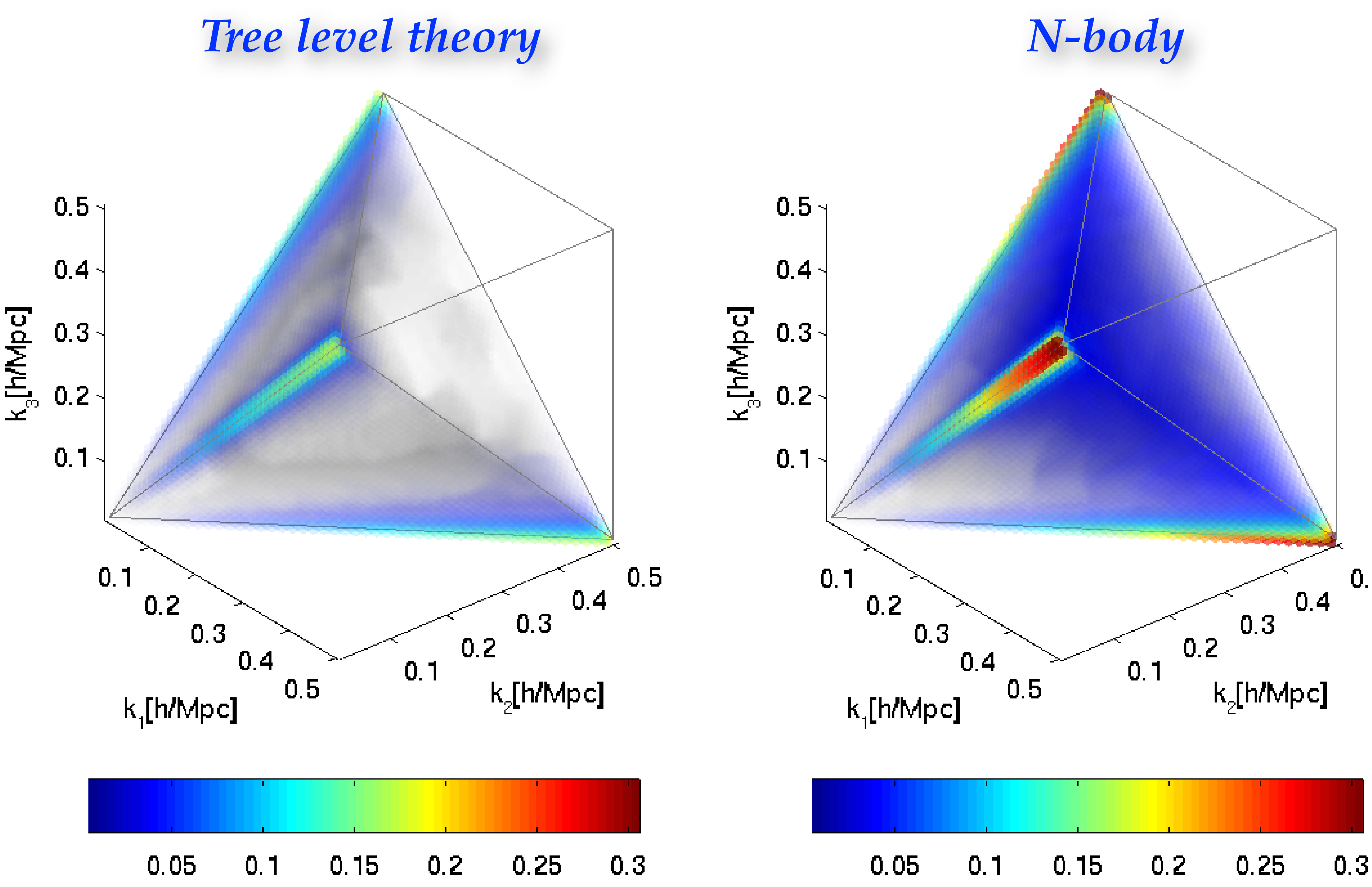

Plot S/N weighted **excess** bispectrum $\sqrt{k_1 k_2 k_3} B_\delta(k_1, k_2, k_3)/\sqrt{P_\delta(k_1)P_\delta(k_2)P_\delta(k_3)}$

3 realisations of 512^3 particles in a $L = 1600$ Mpc$/h$ box with $z_{\rm init} = 49$ and $k = 0.004$-$0.5\ h/$Mpc, f_{NL}=10

LOCAL NON-GAUSSIAN SIMS

MS, Regan, Shellard 1207.5678

z=0

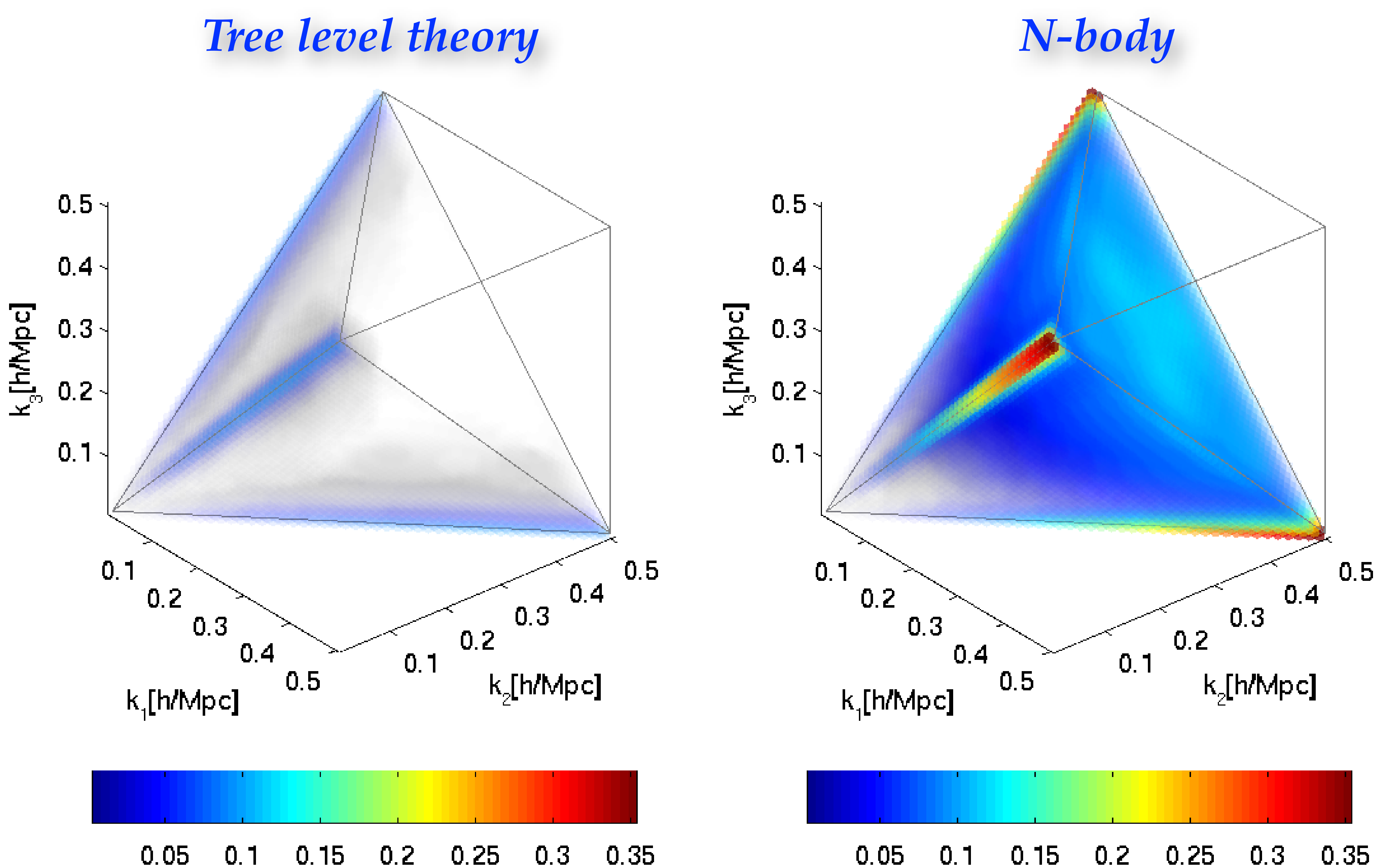

Plot S/N weighted **excess** bispectrum $\sqrt{k_1k_2k_3}B_\delta(k_1,k_2,k_3)/\sqrt{P_\delta(k_1)P_\delta(k_2)P_\delta(k_3)}$

3 realisations of 512^3 particles in a $L = 1600$ Mpc$/h$ box with $z_{\rm init} = 49$ and $k = 0.004$-$0.5\ h/$Mpc, f_{NL}=10

OTHER SHAPES

MS, Regan, Shellard 1207.5678

- **Excess DM bispectra** for other non-Gaussian initial conditions

multiple fields (local)

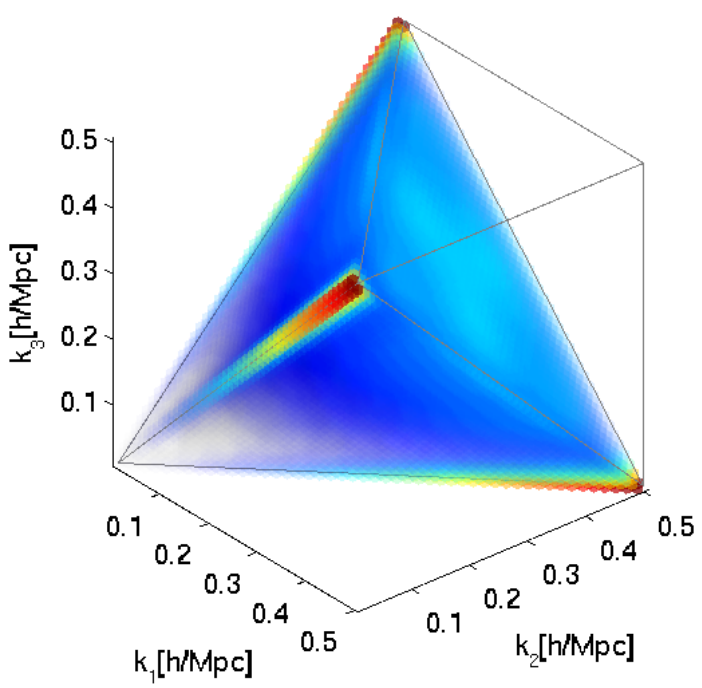

higher derivatives (equilateral)

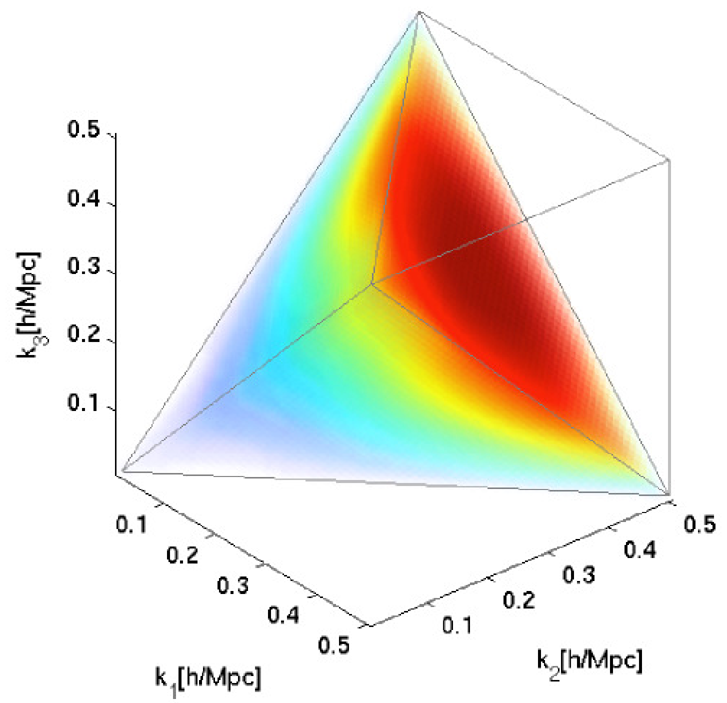

non-standard vacuum (flattened)

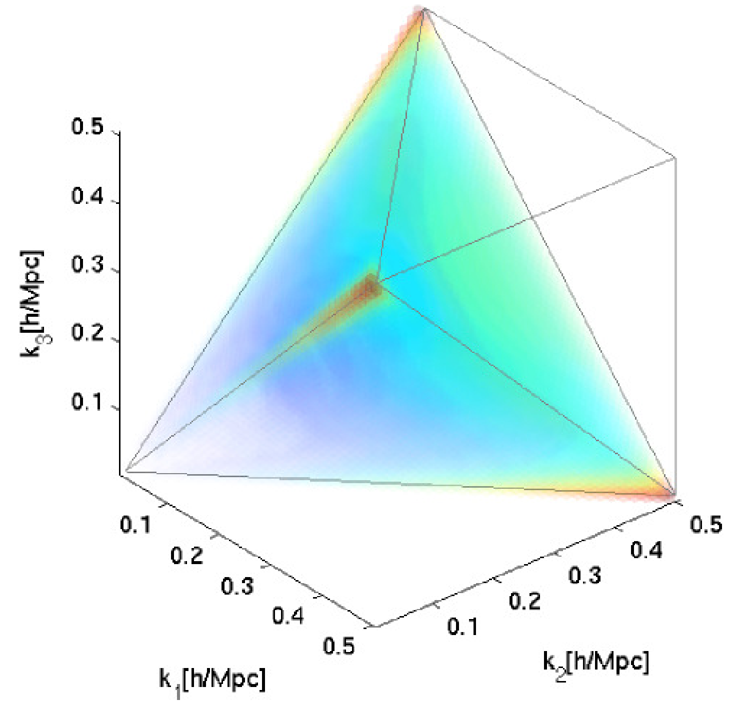

z=0, k_{max}=0.5hMpc^{-1}, 512^3 particles

Non-linear regime:

- Tree level shape is enhanced by non-linear power spectrum
- Additional ~constant contribution to bispectrum signal
- Quantitative characterisation with cumulative S/N and 3d shape correlations in 1207.5678

SIMILARITY OF SHAPES

Babich et al. 2004, Fergusson, Regan, Shellard 2010

Introduce scalar product $\langle \cdot, \cdot \rangle_{\rm est}$, shape correlation $\mathcal{C}$ and norm $||B||$

$$\langle B_i, B_j \rangle_{\rm est} \equiv \frac{V}{\pi} \int_{\mathcal{V}_B} dk_1 dk_2 dk_3 \frac{k_1 k_2 k_3 B_i(k_1, k_2, k_3) B_j(k_1, k_2, k_3)}{P_\delta(k_1) P_\delta(k_2) P_\delta(k_3)}$$

$$\mathcal{C}(B_i, B_j) \equiv \frac{\langle B_i, B_j \rangle_{\rm est}}{\sqrt{\langle B_i, B_i \rangle_{\rm est} \langle B_j, B_j \rangle_{\rm est}}} \in [-1, 1]$$

if $|\mathcal{C}(B_1, B_2)| \ll 1$ then estimator for B_1 cannot find any B_2 and vice versa

$$||B|| \equiv \sqrt{\langle B, B \rangle_{\rm est}}$$

total integrated S/N

$$\Rightarrow \quad \langle \hat{f}_{\rm NL}^{B^{\rm theo}} \rangle \; = \; \mathcal{C}(B_\delta^{\rm data}, B_\delta^{\rm theo}) \frac{||B_\delta^{\rm data}||}{||B_\delta^{\rm theo}||}$$

projection of data on theory

NG initial conditions with $f_{\rm NL}^{\rm local} = 10$

- □ $k \in [0.0039, 0.5]\,{\rm h/Mpc}$
- ○ $k \in [0.0039, 0.25]\,{\rm h/Mpc}$
- △ $k \in [0.0039, 0.13]\,{\rm h/Mpc}$

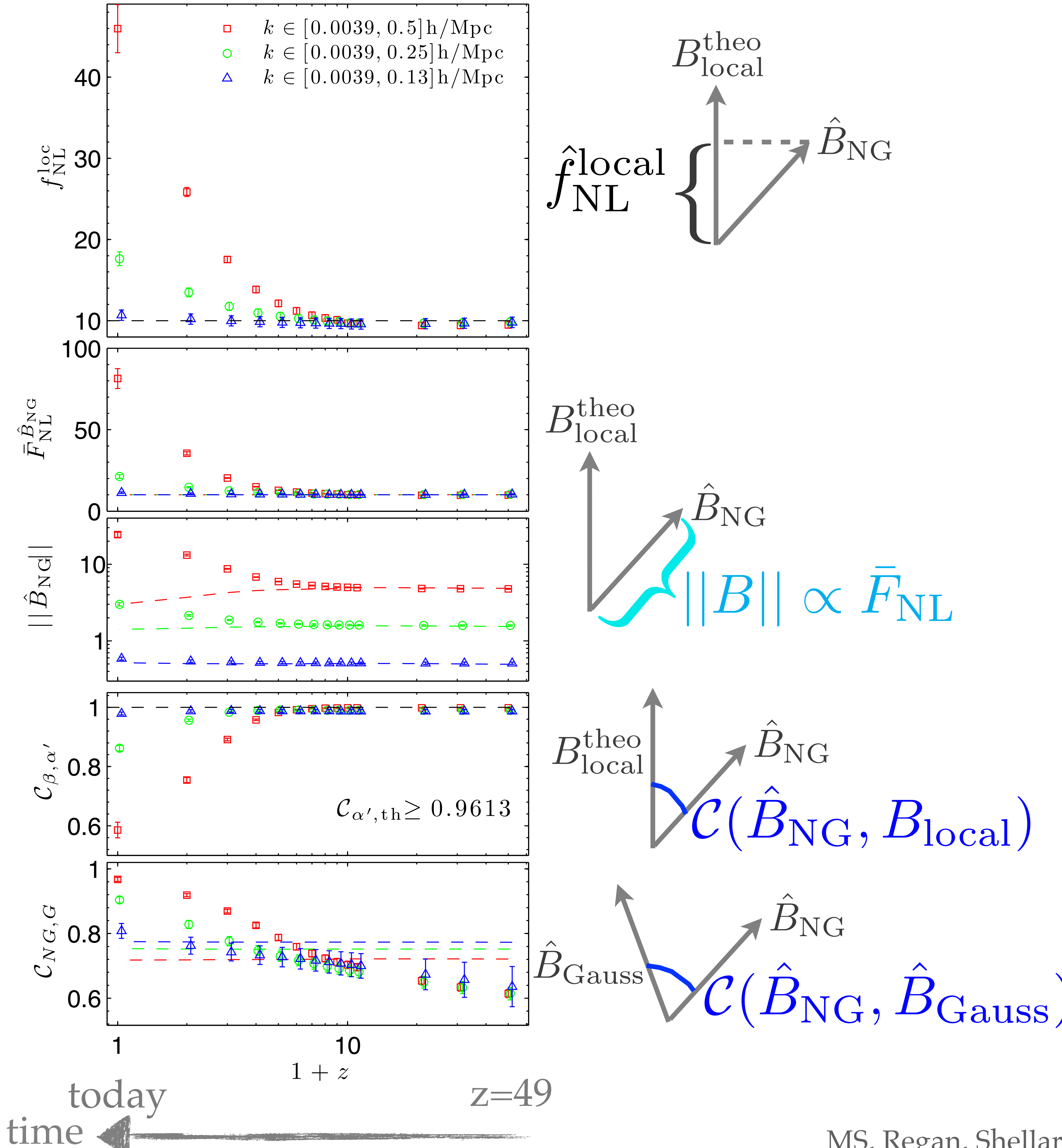

MS, Regan, Shellard 1207.5678

TIME SHIFT MODEL

MS, Regan, Shellard 1207.5678

Time shift model

- Non-Gaussian universe evolves slightly faster (or slower) than Gaussian universe
- Halos form earlier (later) in presence of primordial non-Gaussianity
- Primordial non-Gaussianity gives growth of the 1-halo bispectrum a 'headstart' (or delay)

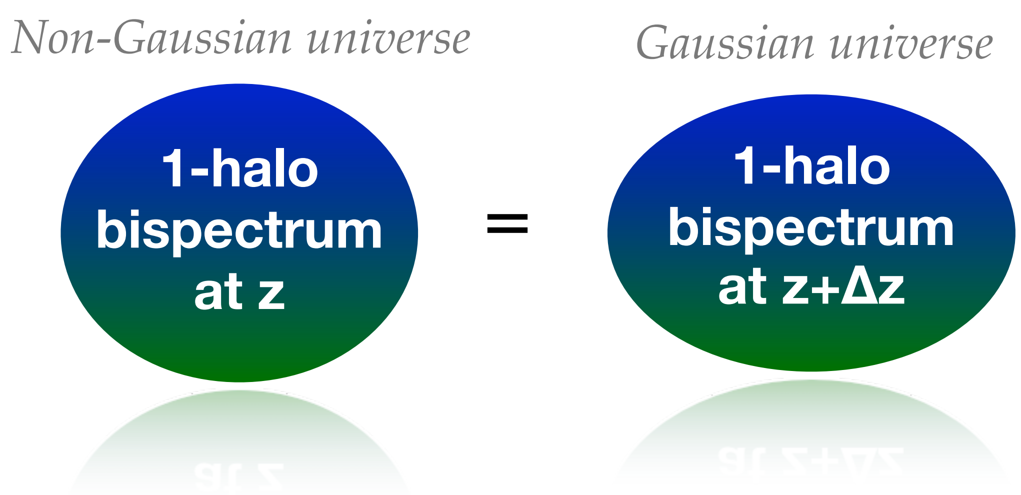

- Motivates simple form of non-Gaussian excess bispectrum:

$$B_\delta^{\rm NG} = \underbrace{\sqrt{\frac{P_\delta^{\rm NL}(k_1)P_\delta^{\rm NL}(k_2)P_\delta^{\rm NL}(k_3)}{P_\Phi(k_1)P_\Phi(k_2)P_\Phi(k_3)}}B_\Phi(k_1,k_2,k_3)}_{\text{perturbative with non-linear power}} + \underbrace{c\Delta z\partial_z[D^{n_h}(z)](k_1+k_2+k_3)^\nu}_{\text{time shifted 1-halo term}}$$

See Valageas for similar philosophy in Gaussian case (combing PT+halo model)

FITTING FORMULAE

MS, Regan, Shellard 1207.5678

- Simple **fitting formulae** for grav. and primordial DM bispectrum **shapes**
  - Valid at $0 \le z \le 20$, $k \le 2h\mathrm{Mpc}^{-1}$
    3d shape correlation with measured shapes is ≥ 94.4% at $0 \le z \le 20$ and ≥ 98 % at z=0 (≥ 99.8% for gravity at $0 \le z \le 20$)
  - Only ~3 free parameters per inflation model (local, equilateral, flattened, [orthogonal])

$$B_\delta^{\rm NG} = \underbrace{\sqrt{\frac{P_\delta^{\rm NL}(k_1)P_\delta^{\rm NL}(k_2)P_\delta^{\rm NL}(k_3)}{P_\Phi(k_1)P_\Phi(k_2)P_\Phi(k_3)}}B_\Phi(k_1,k_2,k_3)}_{\text{perturbative with non-linear power}} + \underbrace{c\Delta z\partial_z[D^{n_h}(z)](k_1+k_2+k_3)^\nu}_{\text{time shifted 1-halo term}}$$

$\nu \approx -1.7$

Simulation	$L[\frac{\rm Mpc}{\rm h}]$	$c_{1,2}$	$n_h^{\rm (prim)}$	*Quality of fit:* *all z*	*z=0*
G512g	1600	4.1×10^6	7	99.8%	99.8%
Loc10	1600	2×10^3	6	99.7%	99.8%
Eq100	1600	8.6×10^2	6	97.9%	99.4%
Flat10	1600	1.2×10^4	6	98.8%	98.9%
G_{400}^{512}	400	1.0×10^7	8	99.8%	99.8%
$\mathrm{Loc10}_{400}^{512}$	400	$2\times10^3 dD/da$	7	98.2%	99.0%
$\mathrm{Eq100}_{400}^{512}$	400	$8.6\times10^2 dD/da$	7	94.4%	97.9%
$\mathrm{Flat10}_{400}^{512}$	400	$1.2\times10^4 dD/da$	7	97.7%	99.1%
$\mathrm{Orth100}_{400}^{512}$	400	-2.6×10^2	6.5	97.3%	98.9%

Overall amplitude needs to be rescaled by (poorly understood) time-dependent prefactor; extends Gil-Marin *et al* formula to smaller scales and NG ICs

CONCLUSIONS

Conclusions

- Efficient and general non-Gaussian N-body initial conditions
- Fast estimation of full bispectrum
  - ☑ new standard diagnostic alongside power spectrum
- Tracked time evolution of the DM bispectrum in a large suite of non-Gaussian N-body simulations
- Time shift model for effect of primordial non-Gaussianity
- New fitting formulae for gravitational and primordial DM bispectra

See 1108.3813 (initial conditions)
1207.5678 (rest)

PART II: JOINT ANALYSIS OF CMB TEMPERATURE AND LENSING-RECONSTRUCTION POWER SPECTRA

arXiv:1308.0286 (PRD 88 063012)

Collaborators
Anthony Challinor (IoA/DAMTP Cambridge)
Duncan Hanson (McGill)
Antony Lewis (Sussex)

Berkeley 22 Oct 2013

THE COSMIC MICROWAVE BACKGROUND (CMB)

BASICS

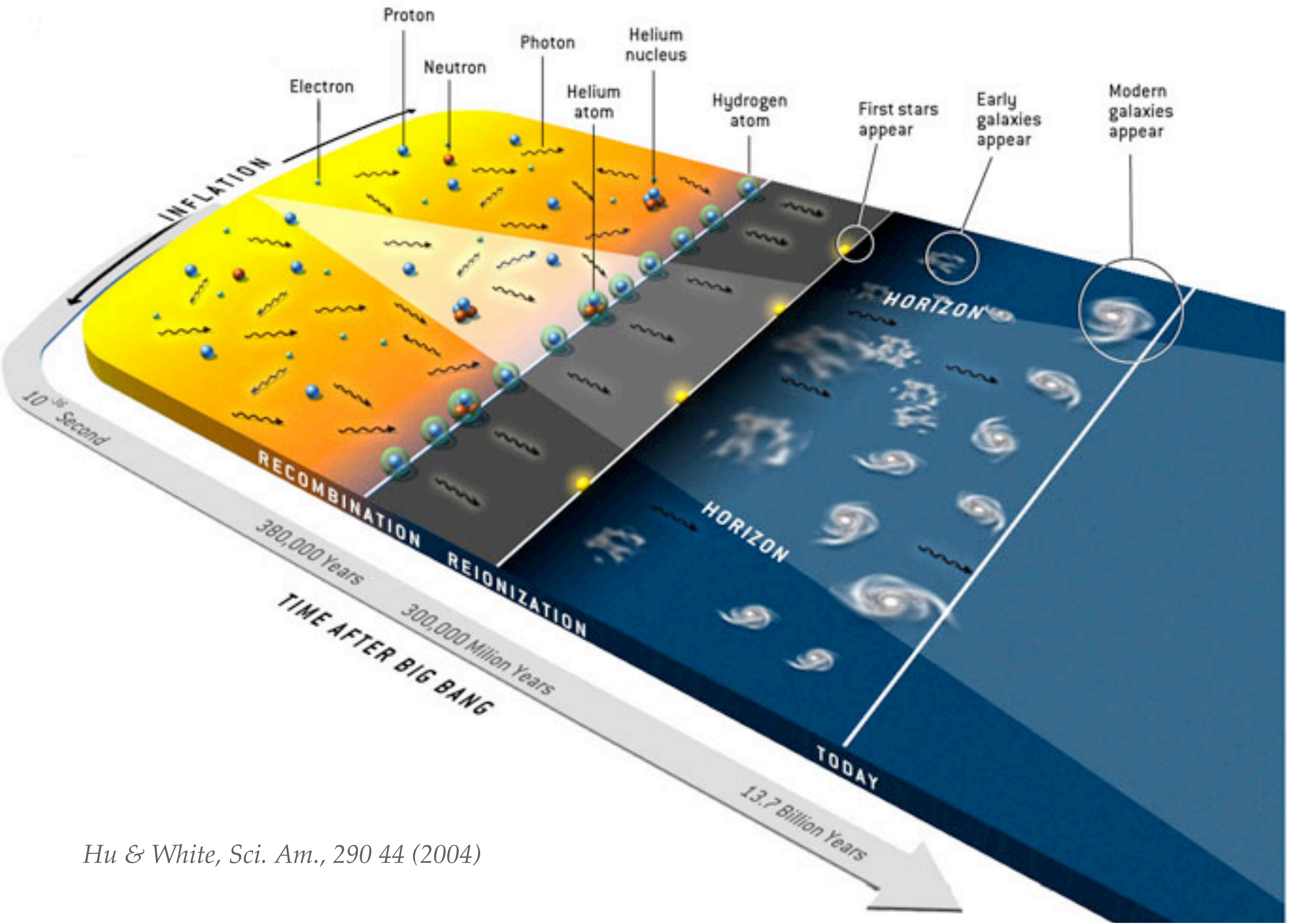

Hu & White, Sci. Am., 290 44 (2004)

The Cosmic Microwave Background as seen by Planck and WMAP

Credit:
ESA and Planck Collaboration;
NASA / WMAP Science Team

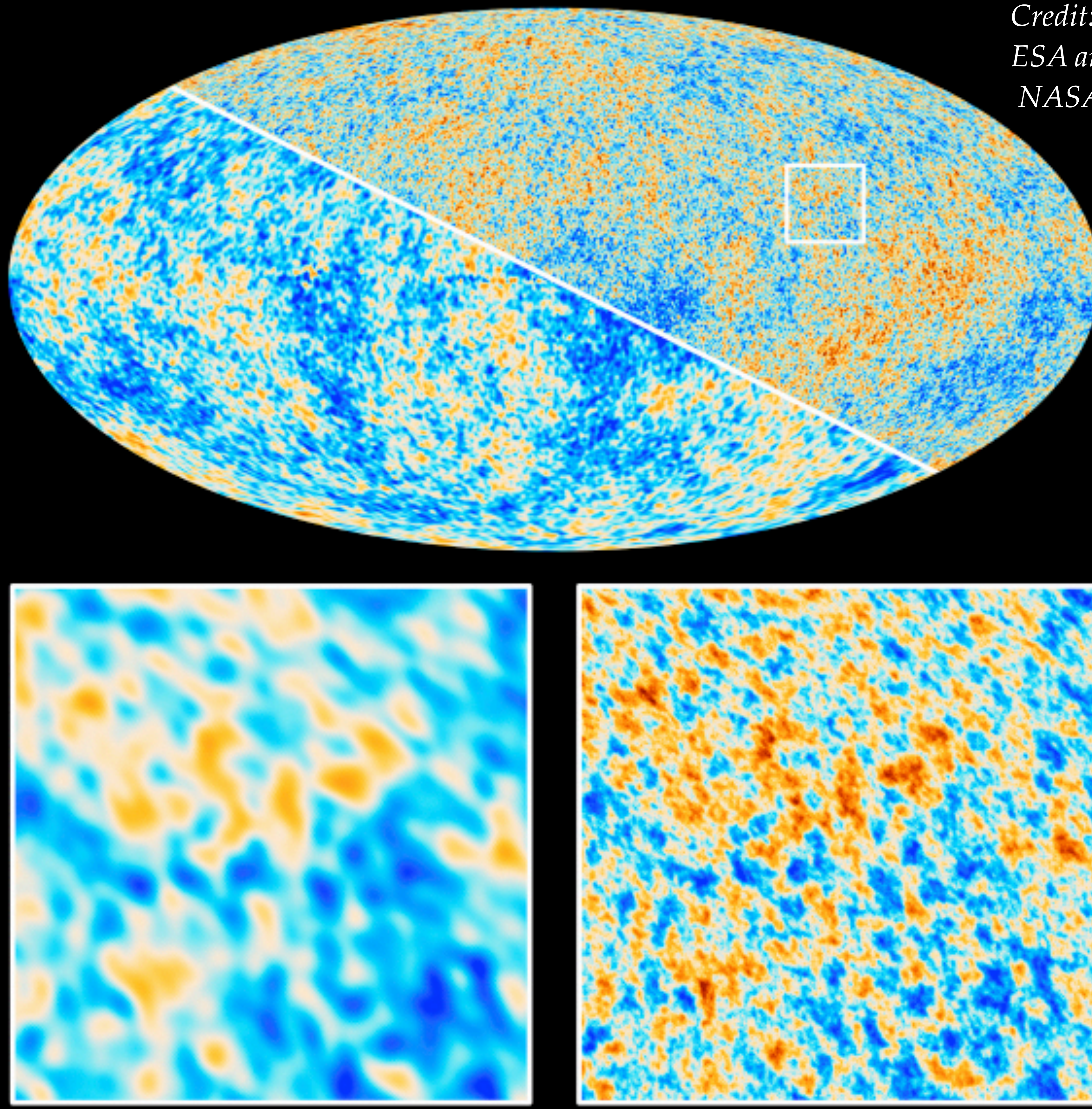

WMAP   Planck

Credit: Planck Chromoscope
http://astrog80.astro.cf.ac.uk/Planck/Chromoscope/
Chris North, Stuart Lowe
ESA/Planck Collaboration;
Paul Shellard

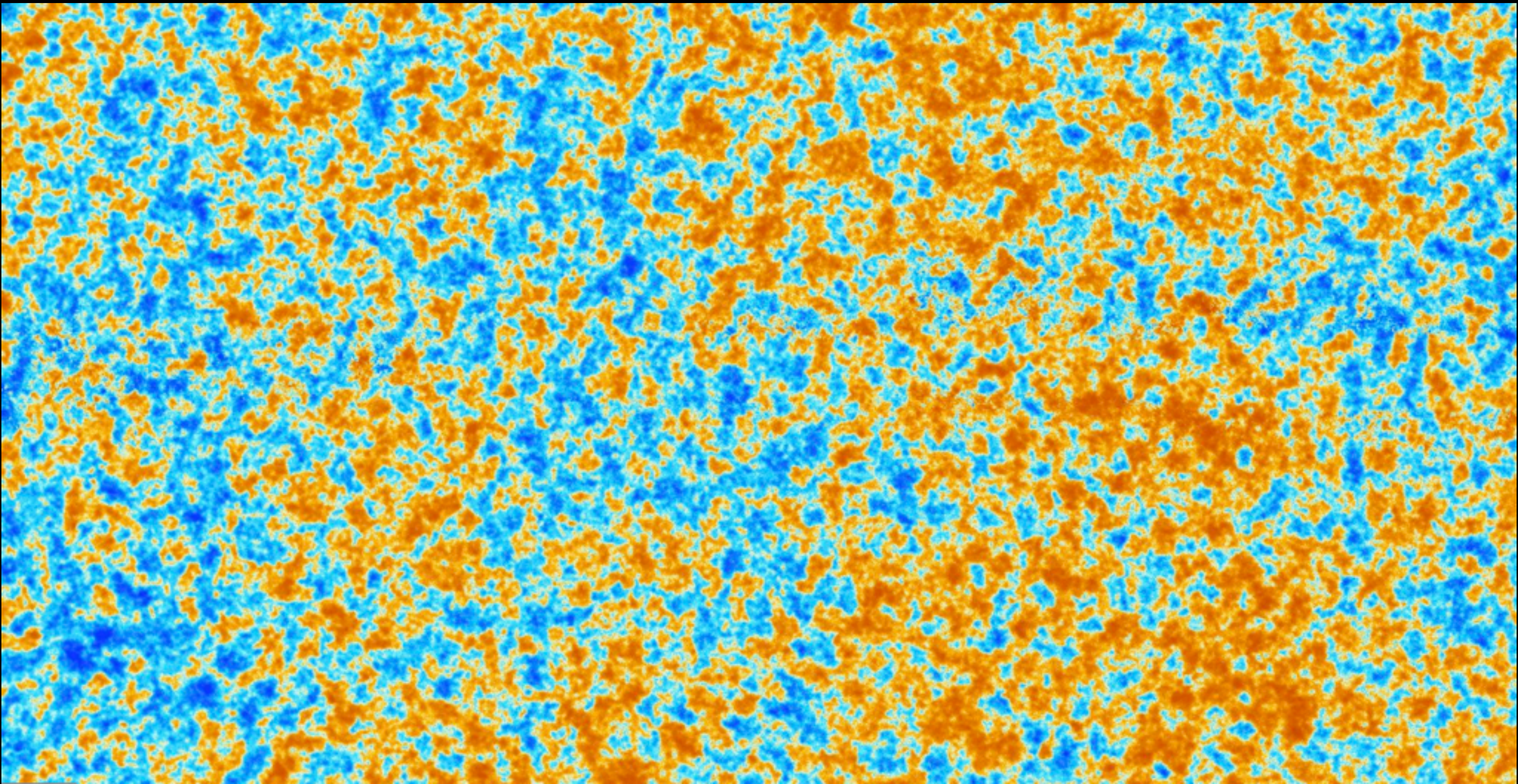

Credit: Planck Chromoscope
http://astrog80.astro.cf.ac.uk/Planck/Chromoscope/
Chris North, Stuart Lowe
ESA/Planck Collaboration;
Paul Shellard

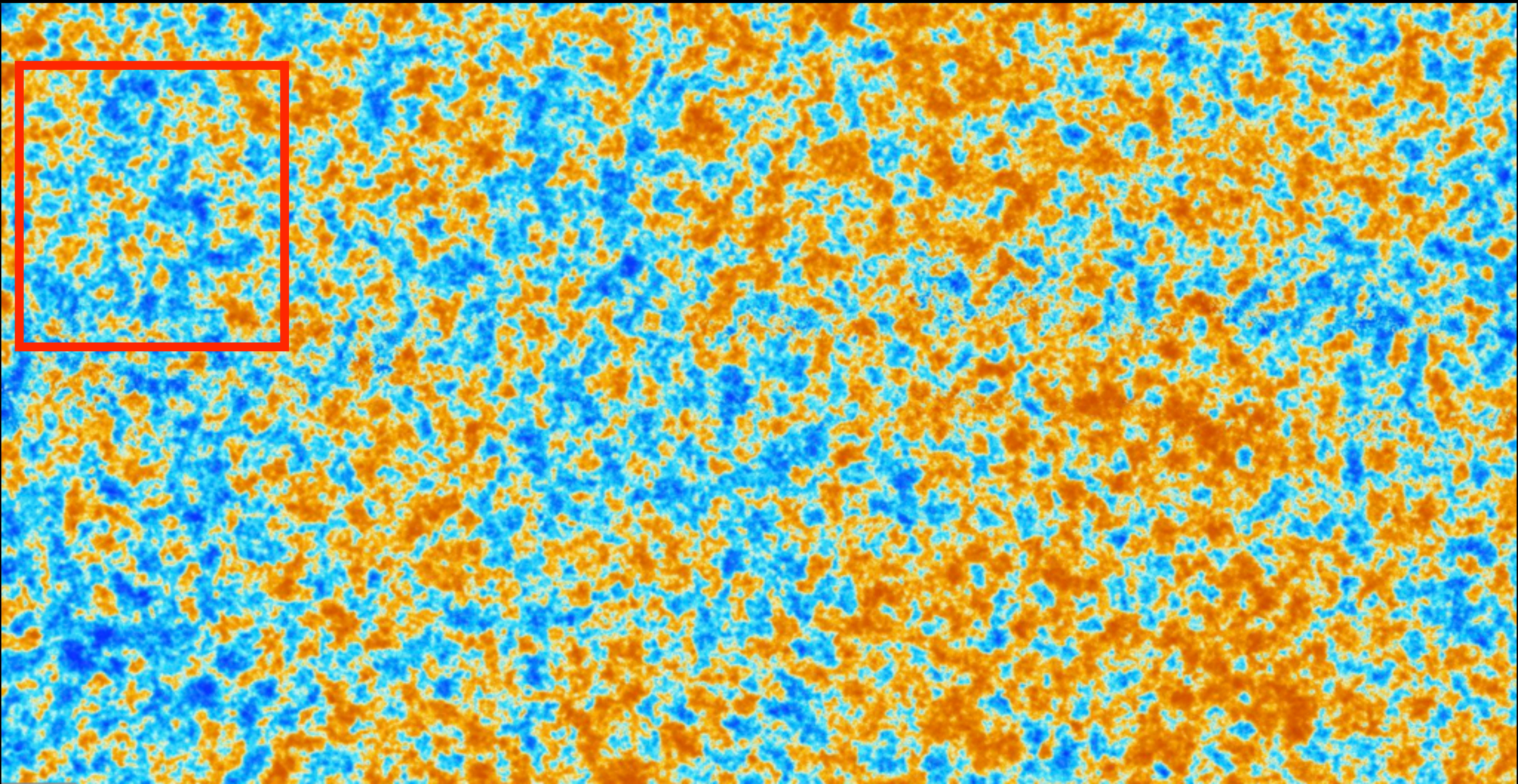

Credit: Planck Chromoscope
http://astrog80.astro.cf.ac.uk/Planck/Chromoscope/
Chris North, Stuart Lowe
ESA/Planck Collaboration;
Paul Shellard

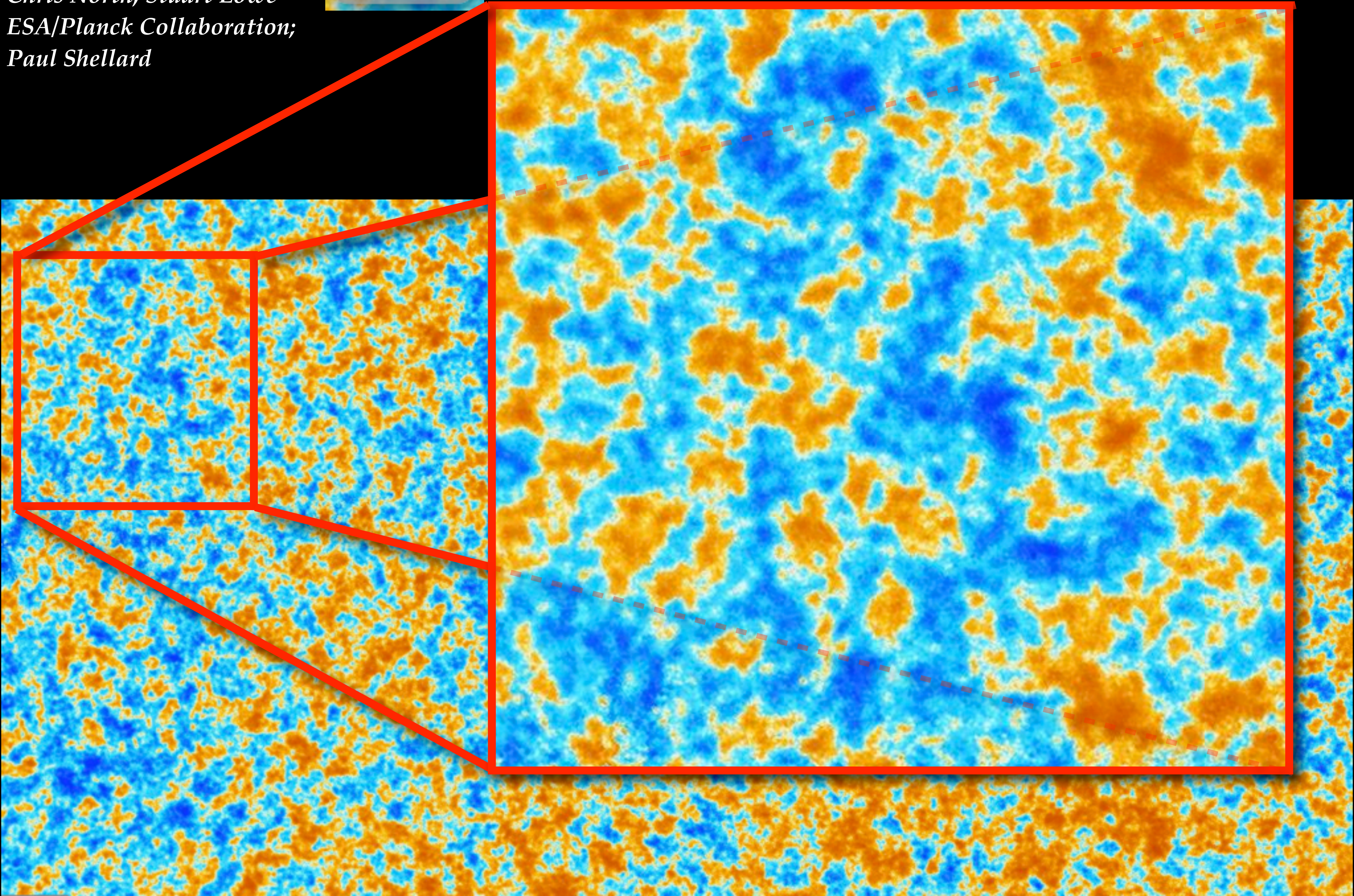

Credit: Planck Chromoscope
http://astrog80.astro.cf.ac.uk/Planck/Chromoscope/
Chris North, Stuart Lowe
ESA/Planck Collaboration;
Paul Shellard

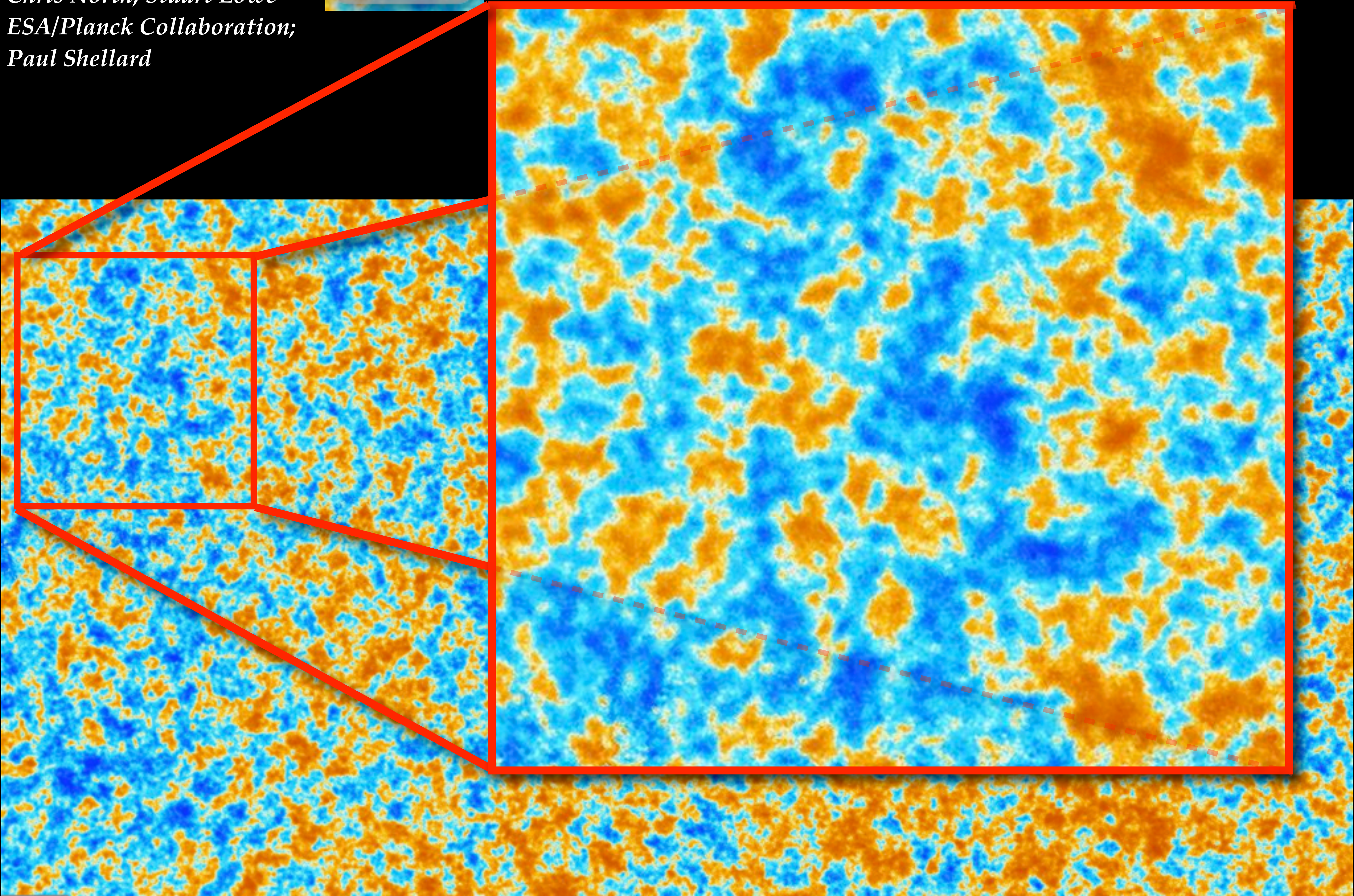

Credit: Planck Chromoscope
http://astrog80.astro.cf.ac.uk/Planck/Chromoscope/
Chris North, Stuart Lowe
ESA/Planck Collaboration;
Paul Shellard

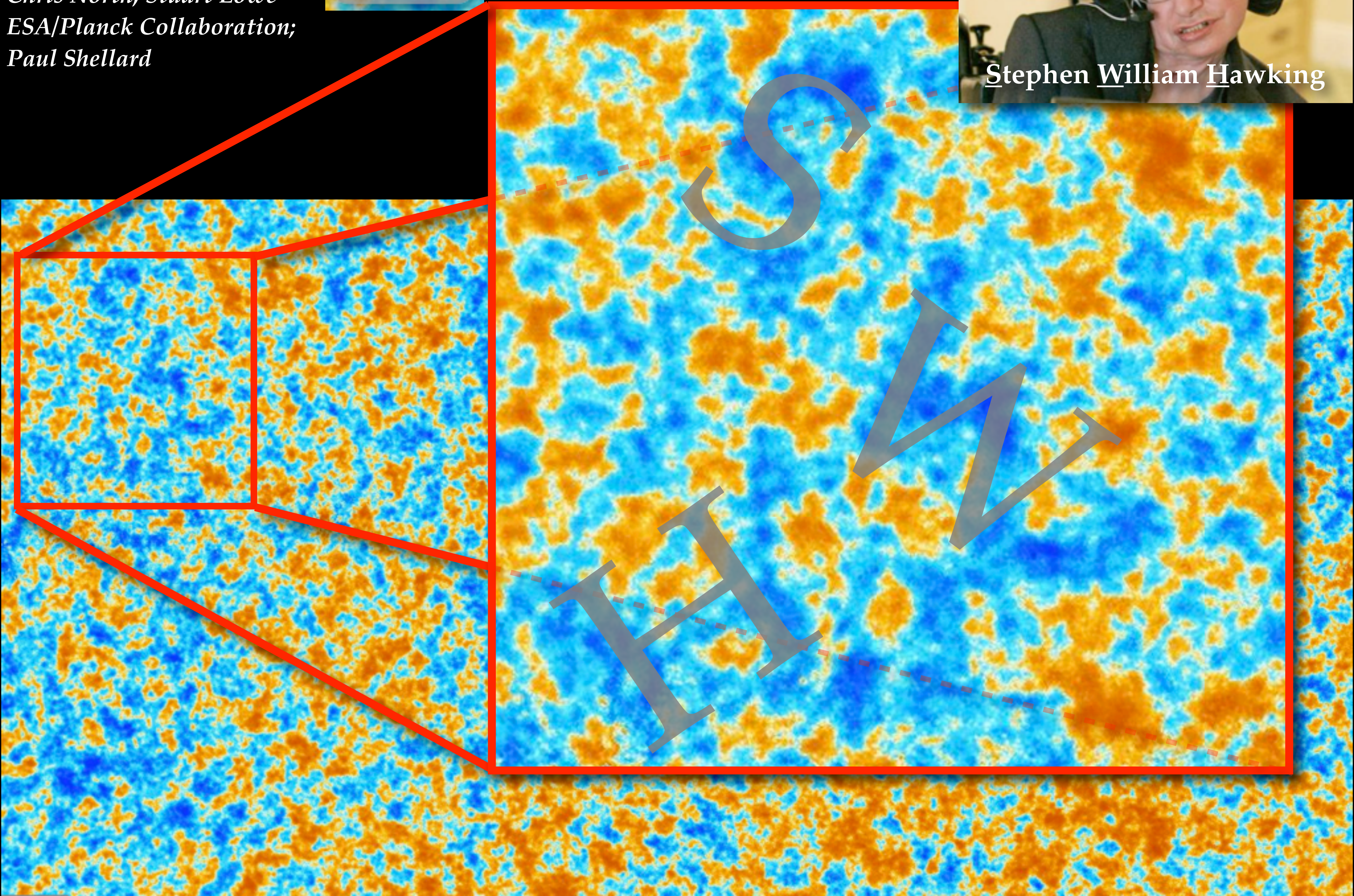

THE COSMIC MICROWAVE BACKGROUND (CMB)
BASICS

- Power spectrum (2-point correlation function in multipole space)

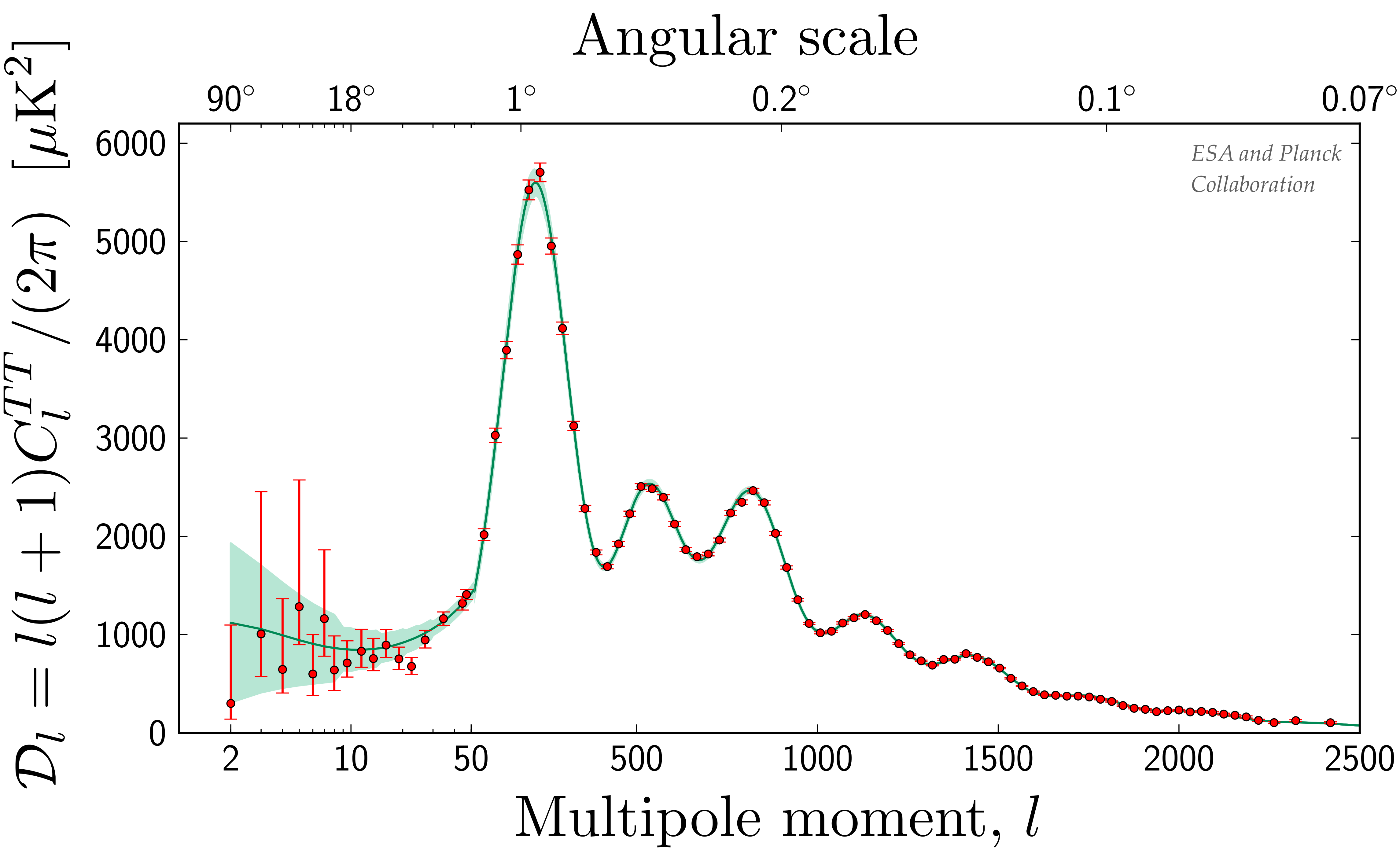

CMB LENSING
BASICS

- CMB photons are deflected by the inhomogeneous distribution of DM along the line of sight:

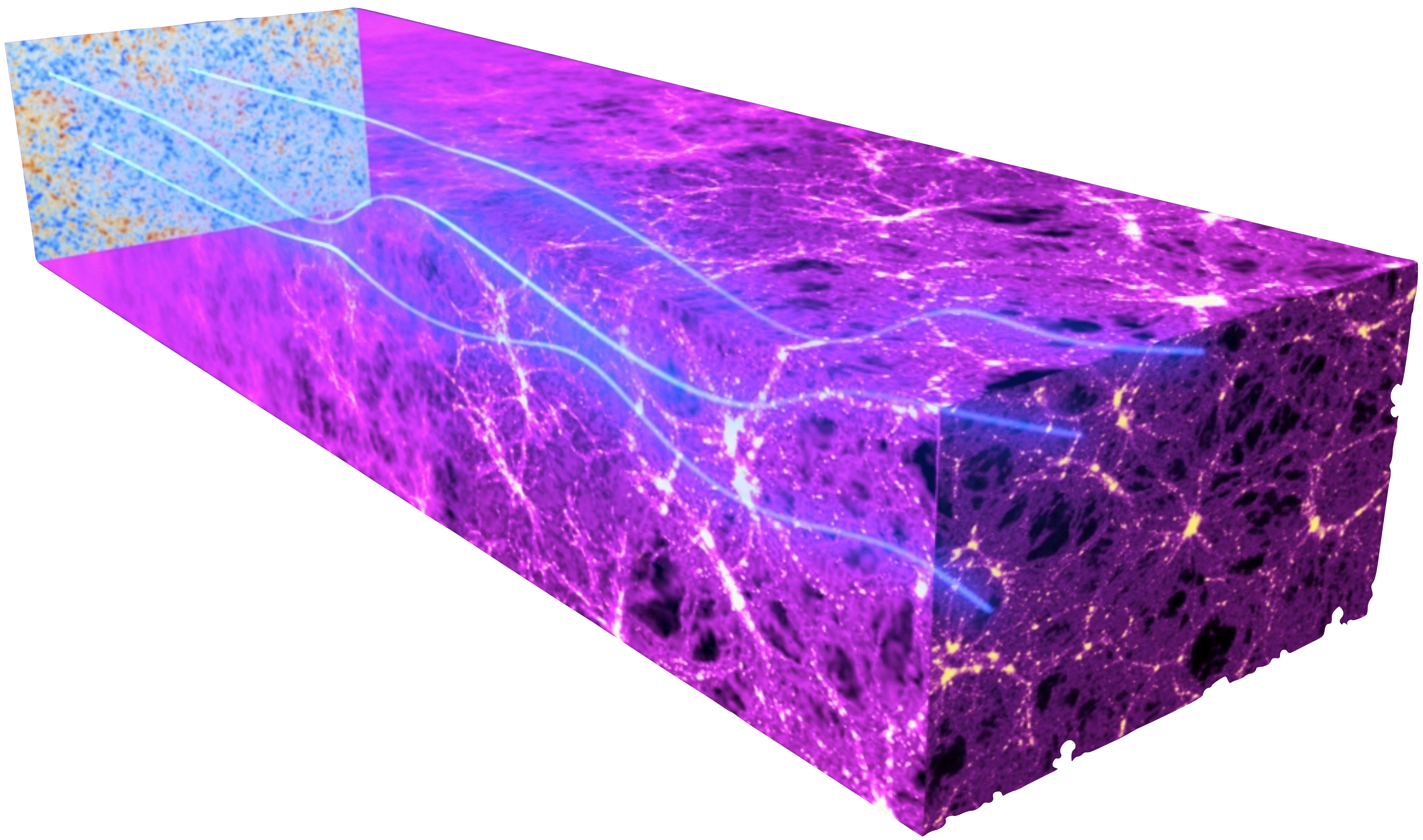

ESA and Planck Collaboration

- Deflection = gradient of **lensing potential ϕ** (integral over matter perturbations along the line of sight)

EFFECTS OF LENSING ON THE CMB

(a) Smoothing CMB 2-point function

Acoustic peaks/troughs are smoothed out by lensing

(since lensed $C^{\tilde{T}\tilde{T}}$ = convolution of unlensed C^{TT} and $C^{\phi\phi}$)

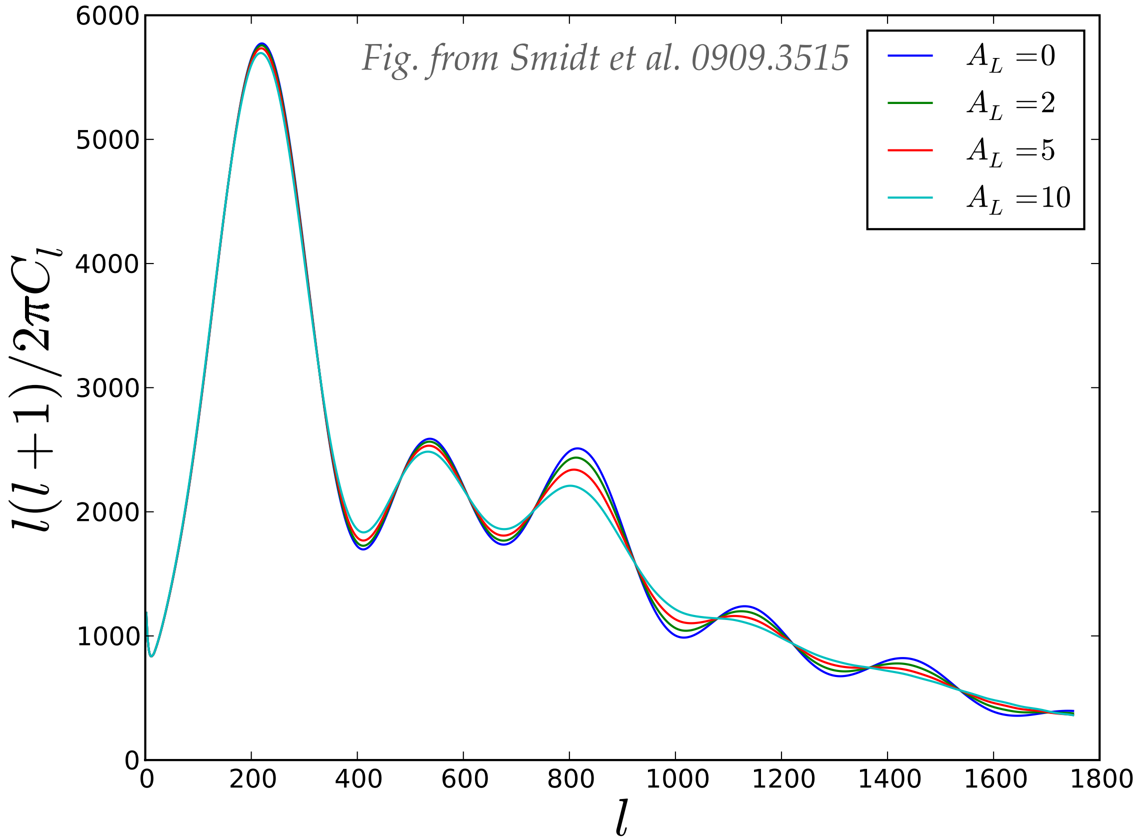

CMB LENSING

EFFECTS OF LENSING ON THE CMB

(a) Smoothing CMB 2-point function

Acoustic peaks / troughs are smoothed out by lensing

(since lensed $C^{\tilde{T}\tilde{T}}$ = convolution of unlensed C^{TT} and $C^{\phi\phi}$)

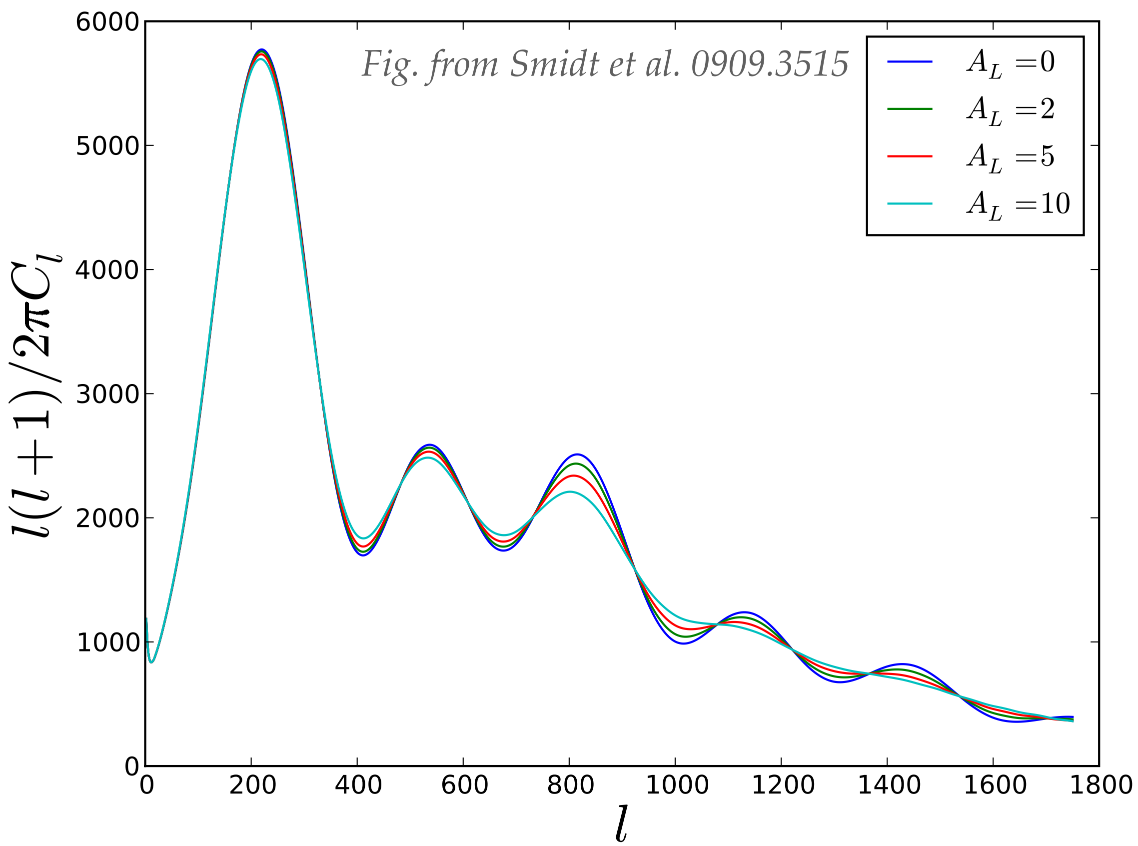

(b) Non-zero CMB 4-point function

For fixed realisation of lenses, the lensed temperature fluctuations are anisotropic

➟ Mode coupling (off-diagonal covariance)

$$\langle \tilde{T}(\mathbf{l}+\mathbf{L})\tilde{T}^*(\mathbf{l})\rangle_{\rm CMB} \propto \phi(\mathbf{L})$$

➟ *Reconstruct* lenses from lensed $\tilde{T}$

$$\hat{\phi}_{\rm rec}(\mathbf{L}) \propto \int_{\mathbf{l}} \tilde{T}(\mathbf{l})\tilde{T}^*(\mathbf{l}-\mathbf{L}) \times \text{weight}$$

➟ Get lensing power from $\tilde{T}$ trispectrum*

$$\hat{C}_L^{\hat{\phi}_{\rm rec}\hat{\phi}_{\rm rec}} \propto \int_{\mathbf{l},\mathbf{l}'} \tilde{T}(\mathbf{l})\tilde{T}^*(\mathbf{l}-\mathbf{L})\tilde{T}(-\mathbf{l}')\tilde{T}^*(\mathbf{L}-\mathbf{l}')$$

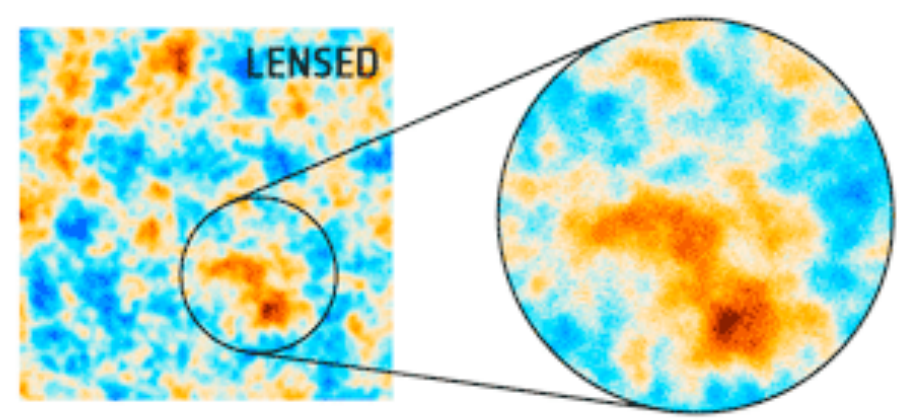

ESA and Planck Collaboration

* All quadrilaterals whose diagonal has length L

CMB LENSING
PLANCK RECONSTRUCTION

- Reconstructed mass map

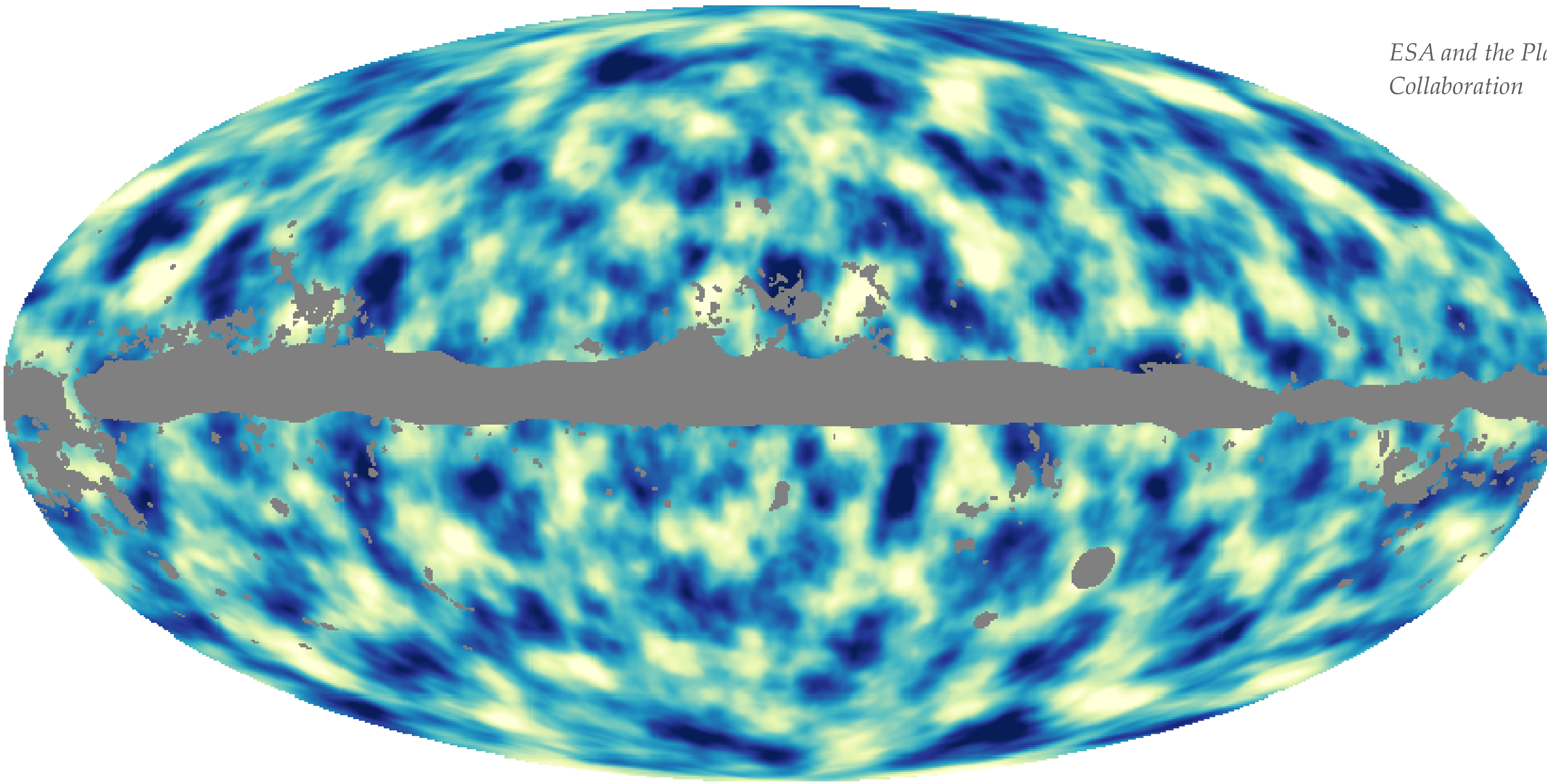

ESA and the Planck Collaboration

CMB LENSING
PLANCK RECONSTRUCTION

- Power spectrum of the deflection field

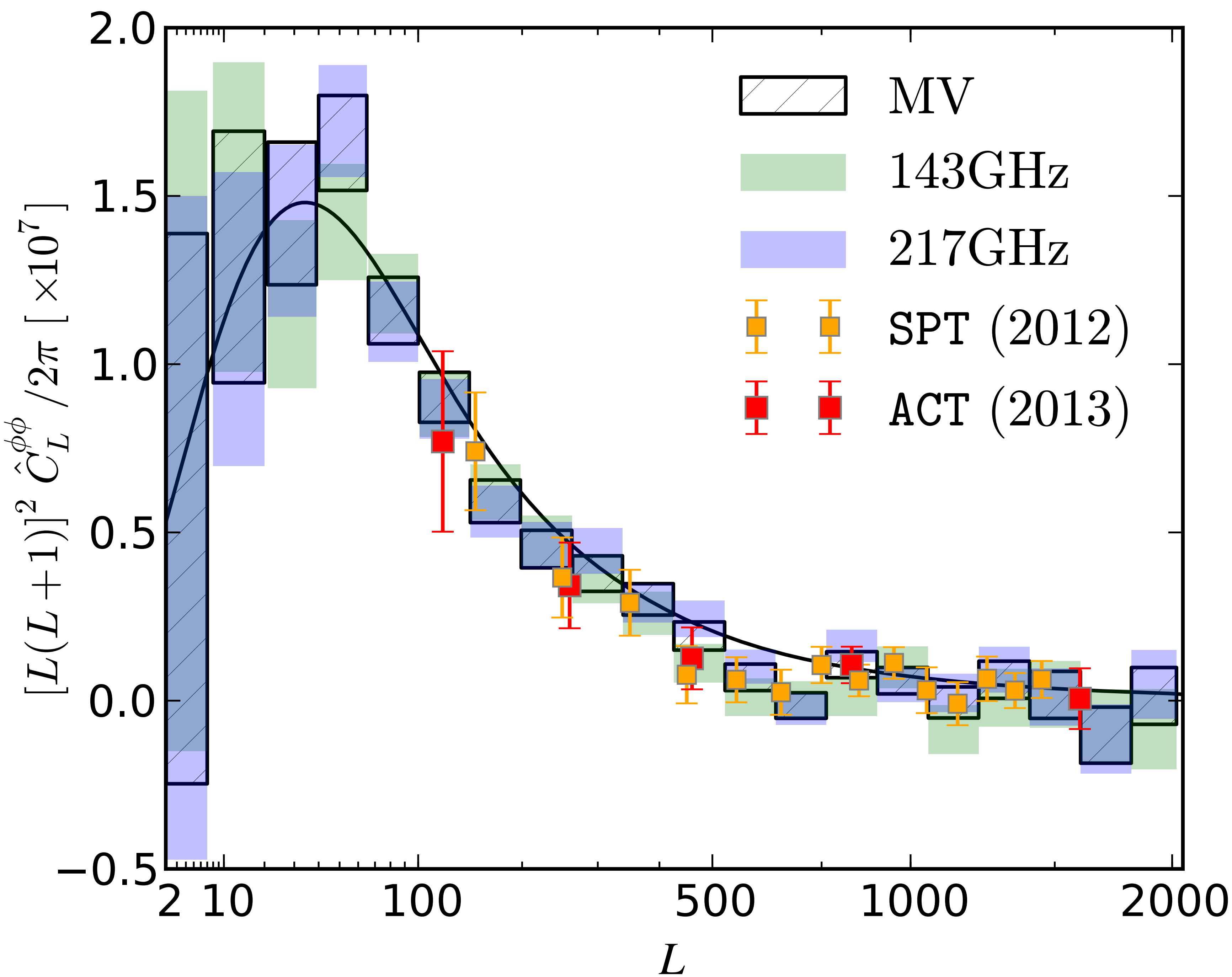

ESA and the Planck Collaboration

CMB LENSING
MOTIVATION

Why do we care?

- Probe late time DM distribution to break degeneracies of primary CMB, or get bias
- Both (a) and (b) detected at many-σ level (ACT, SPT, *Planck*; soon ACTPol, SPTpol)

How do CMB experiments deal with lensing?

(a) Smoothed $C^{\tilde{T}\tilde{T}}$ automatically included by using *lensed* power spectrum

(b) Reconstruction $\hat{\phi}_{\rm rec}$ can be added, e.g. for *Planck*:

- Reduction of errors on Ω_K and Ω_Λ by factor ~2 (evidence for flatness and DE from CMB alone*)
- Constraint on τ without WMAP polarization
- Neutrino masses: curious preference for large m_ν
- Consistency with z~1100 CMB physics seen by *Planck*

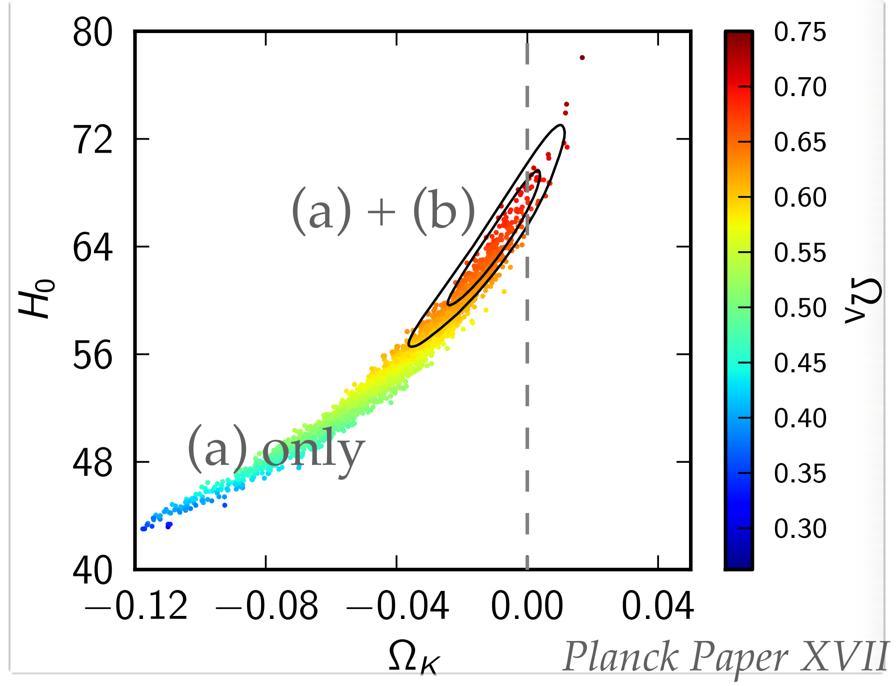

Planck Paper XVII

*First found by Blake Sherwin et al. 2011 (with ACT)

MOTIVATION

Why do we care?

- Probe late time DM distribution to break degeneracies of primary CMB, or get bias
- Both (a) and (b) detected at many-$\boldsymbol{\sigma}$ level (ACT, SPT, *Planck*; soon ACTPol, SPTpol)

How do CMB experiments deal with lensing?

(a) Smoothed $C^{\tilde{T}\tilde{T}}$ automatically included by using *lensed* power spectrum

(b) Reconstruction $\hat{\phi}_{\rm rec}$ can be added, e.g. for *Planck*:

- Reduction of errors on Ω and Ω b
  (evic
- Cons
- Neu
- Cons

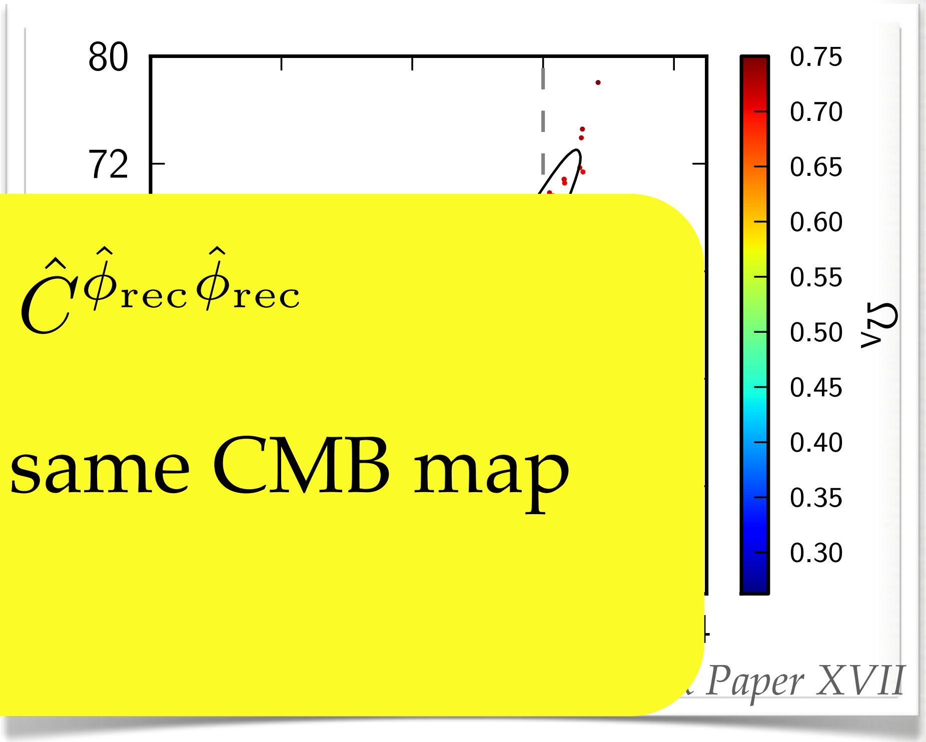

Requires *joint* likelihood for $\hat{C}^{\tilde{T}\tilde{T}}$ and $\hat{C}^{\hat{\phi}_{\rm rec}\hat{\phi}_{\rm rec}}$

➡ Non-trivial because derived from same CMB map

➡ Need $\mathrm{cov}(\hat{C}^{\hat{\phi}_{\rm rec}\hat{\phi}_{\rm rec}}, \hat{C}^{\tilde{T}\tilde{T}})$

*First found by Blake Sherwin et al. 2011 (with ACT)

CMB LENSING RECONSTRUCTION
LIKELIHOOD INGREDIENTS

For likelihood based on reconstruction power spectrum $\hat{C}^{\hat{\phi}_{\rm rec}\hat{\phi}_{\rm rec}} \sim \tilde{T}^4$, need to know:

- **Expectation value** $\langle \hat{C}_L^{\hat{\phi}_{\rm rec}\hat{\phi}_{\rm rec}} \rangle = N_L^{(0)} + C_L^{\phi\phi} + N_L^{(1)}$

disconn. 4-point

connected 4-point

Kesden et al. 0302536; Hanson et al. 1008.4403

MS, Challinor, Hanson, Lewis 2013

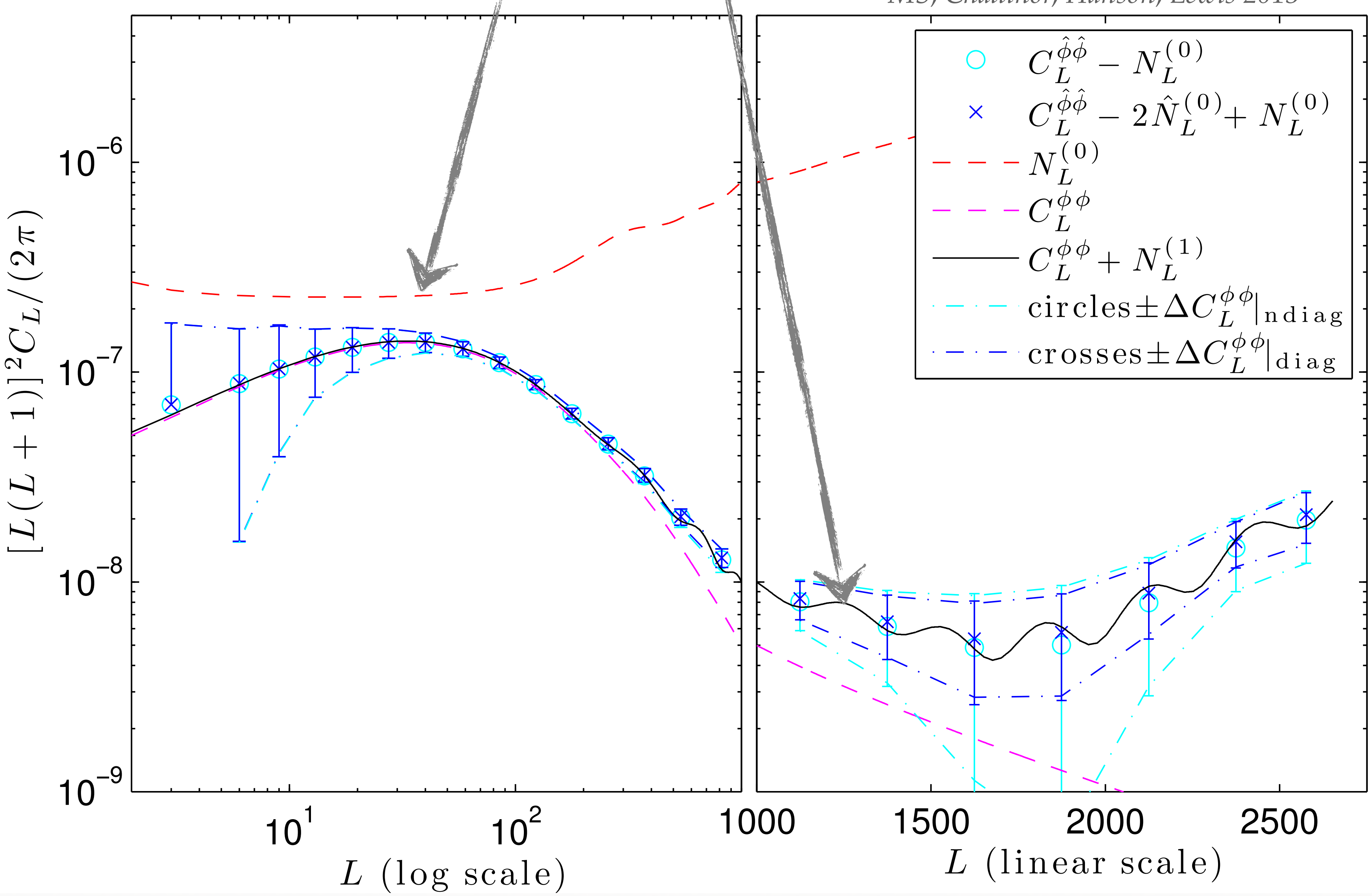

CMB LENSING RECONSTRUCTION
LIKELIHOOD INGREDIENTS

For likelihood based on reconstruction power spectrum $\hat{C}^{\hat{\phi}_{\rm rec}\hat{\phi}_{\rm rec}} \sim \tilde{T}^4$, need to know:

- **Expectation value** $\langle \hat{C}_L^{\hat{\phi}_{\rm rec}\hat{\phi}_{\rm rec}} \rangle = \underbrace{N_L^{(0)}}_{\text{disconn. 4-point}} + \underbrace{C_L^{\phi\phi} + N_L^{(1)}}_{\text{connected 4-point}}$

  Kesden et al. 0302536; Hanson et al. 1008.4403

- **Auto-covariance** $\mathrm{cov}(\hat{C}_L^{\hat{\phi}_{\rm rec}\hat{\phi}_{\rm rec}}, \hat{C}_{L'}^{\hat{\phi}_{\rm rec}\hat{\phi}_{\rm rec}})$
  - ➟ Dominant contributions from disconnected 8-point of $\tilde{T}$, can be diagonalised with realisation-dependent $N^{(0)}$ subtraction

  Hanson et al. 1008.4403; MS, Challinor, Hanson, Lewis 1308.0286

CMB LENSING RECONSTRUCTION
LIKELIHOOD INGREDIENTS

For likelihood based on reconstruction power spectrum $\hat{C}^{\hat\phi_{\rm rec}\hat\phi_{\rm rec}} \sim \tilde{T}^4$, need to know:

- **Expectation value** $\langle \hat{C}_L^{\hat\phi_{\rm rec}\hat\phi_{\rm rec}} \rangle = \underbrace{N_L^{(0)}}_{\text{disconn. 4-point}} + C_L^{\phi\phi} + \underbrace{N_L^{(1)}}_{\text{connected 4-point}}$

Kesden et al. 0302536;
Hanson et al. 1008.4403

- **Auto-covariance** $\mathrm{cov}(\hat{C}_L^{\hat\phi_{\rm rec}\hat\phi_{\rm rec}}, \hat{C}_{L'}^{\hat\phi_{\rm rec}\hat\phi_{\rm rec}})$

  ➟ Dominant contributions from disconnected 8-point of $\tilde{T}$, can be diagonalised with realisation-dependent $N^{(0)}$ subtraction

Hanson et al. 1008.4403;
MS, Challinor, Hanson, Lewis 1308.0286

- **Cross-covariance** $\mathrm{cov}(\hat{C}_L^{\hat\phi_{\rm rec}\hat\phi_{\rm rec}}, \hat{C}_{L'}^{\tilde{T}\tilde{T}})$

  ➟ 6-point:

MS, Challinor, Hanson, Lewis 1308.0286

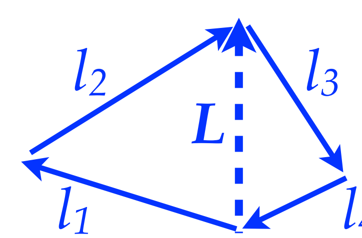

$$\mathrm{cov}(\hat{C}_L^{\hat\phi\hat\phi}, \hat{C}_{L'}^{\tilde{T}\tilde{T}}) \propto \sum_{\underline{l}_1,\underline{l}_2,\underline{l}_3,\underline{l}_4,M,M'} (-1)^{M+M'} \begin{pmatrix} l_1 & l_2 & L \\ m_1 & m_2 & -M \end{pmatrix} \begin{pmatrix} l_3 & l_4 & L \\ m_3 & m_4 & M \end{pmatrix} \overbrace{\tilde{g}_{l_1 l_2}(L)\tilde{g}_{l_3 l_4}(L)}^{\text{weights}}$$

$$\times \left[\langle \tilde{T}_{\underline{l}_1}\tilde{T}_{\underline{l}_2}\tilde{T}_{\underline{l}_3}\tilde{T}_{\underline{l}_4}\tilde{T}_{L'M'}\tilde{T}_{L',-M'} \rangle - \langle \tilde{T}_{\underline{l}_1}\tilde{T}_{\underline{l}_2}\tilde{T}_{\underline{l}_3}\tilde{T}_{\underline{l}_4} \rangle \langle \tilde{T}_{L'M'}\tilde{T}_{L',-M'} \rangle \right].$$

(i) connected 6-point (ii) disconnected (iii) connected 4-point (neglect here)

(i)

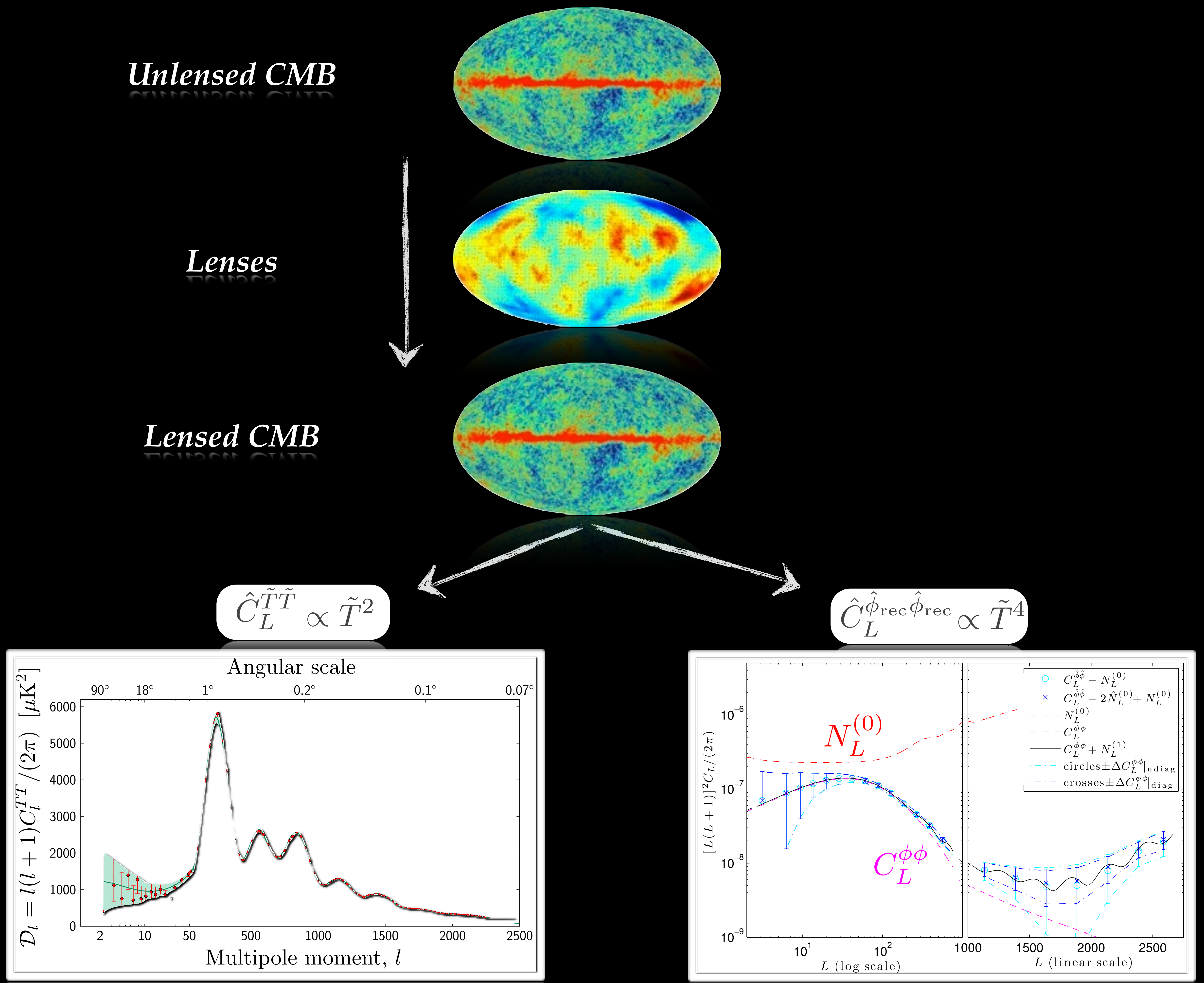

Unlensed CMB
Lenses
Lensed CMB
$\hat{C}_L^{\tilde{T}\tilde{T}} \propto \tilde{T}^2$
$\hat{C}_L^{\hat{\phi}_{\rm rec}\hat{\phi}_{\rm rec}} \propto \tilde{T}^4$
Angular scale
90° 18° 1° 0.2° 0.1° 0.07°
$\mathcal{D}_l = l(l+1)C_l^{TT}/(2\pi)\ [\mu K^2]$
Multipole moment, l
$N_L^{(0)}$
$C_L^{\phi\phi}$
$[L(L+1)]^2 C_L/(2\pi)$
L (log scale)
L (linear scale)
$C_L^{\hat{\phi}\hat{\phi}} - N_L^{(0)}$
$C_L^{\hat{\phi}\hat{\phi}} - 2\hat{N}_L^{(0)} + N_L^{(0)}$
$N_L^{(0)}$
$C_L^{\phi\phi}$
$C_L^{\phi\phi} + N_L^{(1)}$
circles$\pm\Delta C_L^{\phi\phi}|_{\rm ndiag}$
crosses$\pm\Delta C_L^{\phi\phi}|_{\rm diag}$

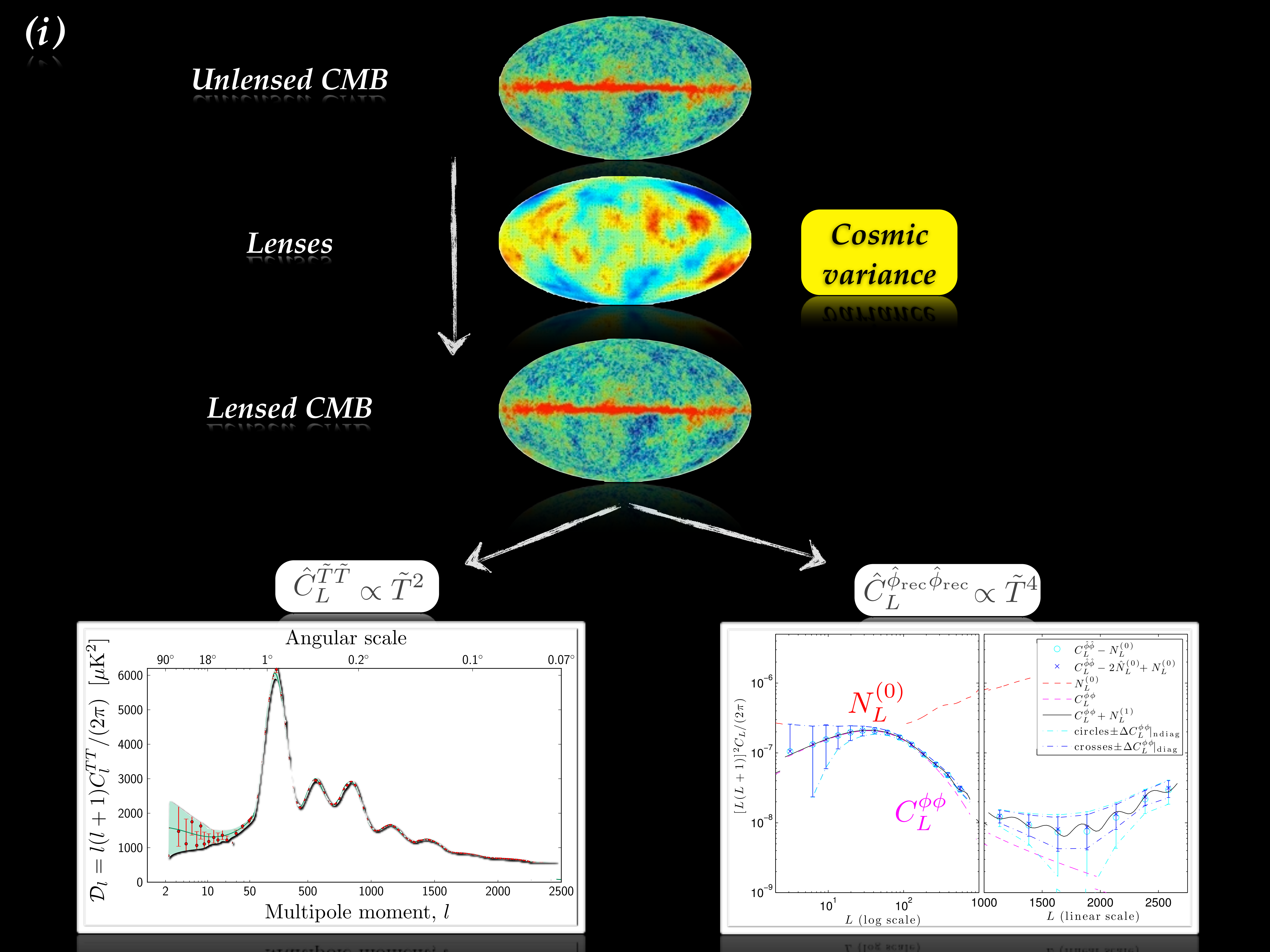

(i)
Unlensed CMB
Lenses
Cosmic variance
Lensed CMB
$\hat{C}_L^{\tilde{T}\tilde{T}} \propto \tilde{T}^2$
$\hat{C}_L^{\hat{\phi}_{\rm rec}\hat{\phi}_{\rm rec}} \propto \tilde{T}^4$
Angular scale
90° 18° 1° 0.2° 0.1° 0.07°
$\mathcal{D}_l = l(l+1)C_l^{TT}/(2\pi)$ [μK^2]
6000 5000 4000 3000 2000 1000 0
2 10 50 500 1000 1500 2000 2500
Multipole moment, l
$[L(L+1)]^2 C_L/(2\pi)$
10^{-6} 10^{-7} 10^{-8} 10^{-9}
$N_L^{(0)}$
$C_L^{\phi\phi}$
10^1 10^2
L (log scale)
1000 1500 2000 2500
L (linear scale)
$C_L^{\hat{\phi}\hat{\phi}} - N_L^{(0)}$
$C_L^{\hat{\phi}\hat{\phi}} - 2\hat{N}_L^{(0)} + N_L^{(0)}$
$N_L^{(0)}$
$C_L^{\phi\phi}$
$C_L^{\phi\phi} + N_L^{(1)}$
circles$\pm\Delta C_L^{\phi\phi}|_{\rm ndiag}$
crosses$\pm\Delta C_L^{\phi\phi}|_{\rm diag}$

LIKELIHOOD INGREDIENTS
TEMPERATURE-LENSING POWER-COVARIANCE

MS, Challinor, Hanson, Lewis ***1308.0286***

(i) If lensing field fluctuates high, CMB power is smoother and reconstruction is high

➟ Derives from connected CMB 6-point at $\mathcal{O}(\phi^4)$

$$\mathrm{cov}\left(\hat{C}^{\hat{\phi}_{\mathrm{rec}}\hat{\phi}_{\mathrm{rec}}}_{L_\phi}, \hat{C}^{\tilde{T}\tilde{T}}_{L_T,\mathrm{expt}}\right)^{\mathcal{O}(\phi^4)}_{\mathrm{conn.6pt.}} = \frac{2}{2L_\phi+1}\left(C^{\phi\phi}_{L_\phi}\right)^2 \frac{\partial C^{\tilde{T}\tilde{T}}_{L_T}}{\partial C^{\phi\phi}_{L_\phi}}$$

Correlation of *unbinned* power spectra is up to ~0.04% (at low L_ϕ!):

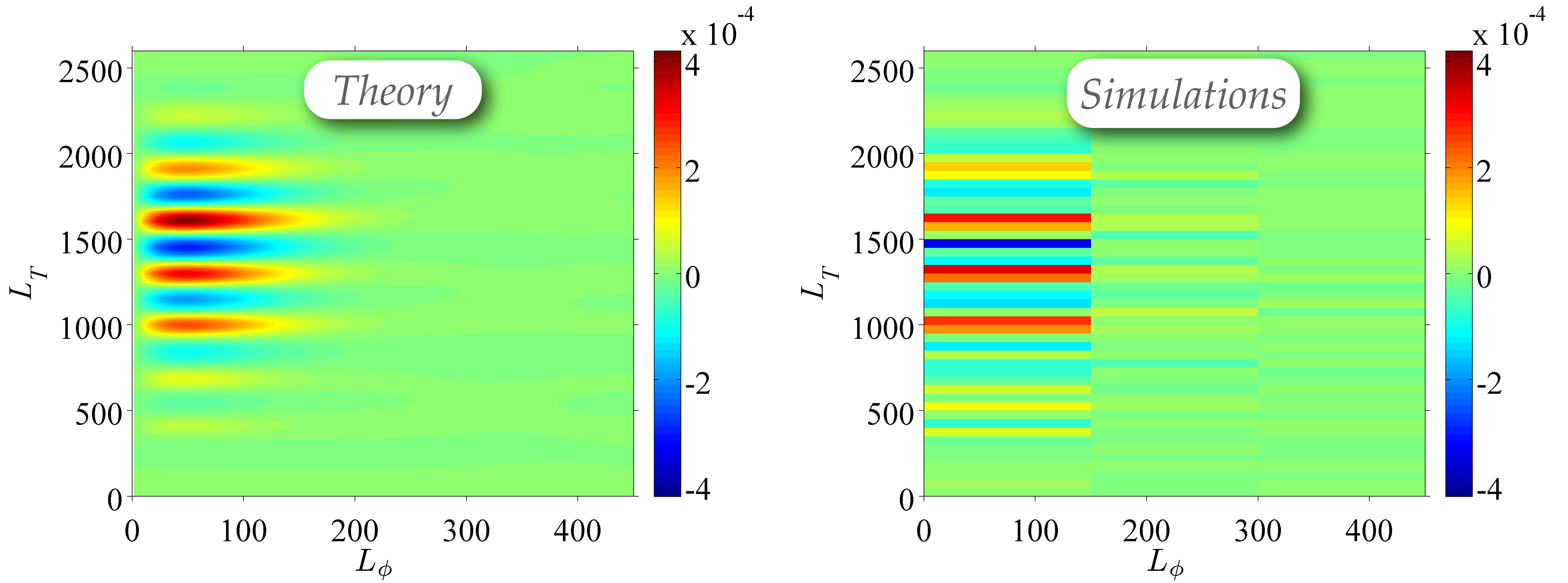

Minima at acoustic peaks of temperature power which are decreased by larger lensing power; maxima at acoustic troughs

(ii)

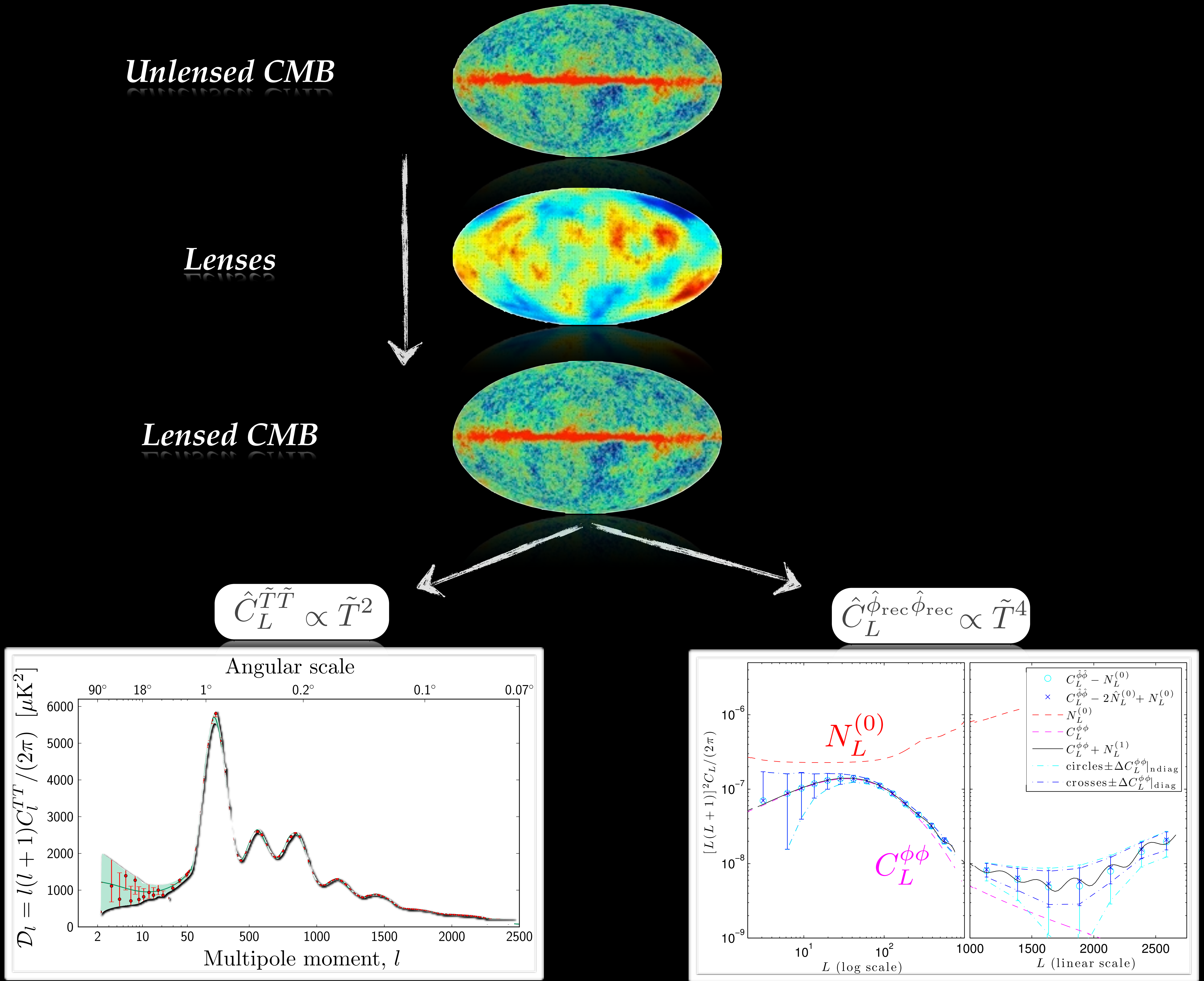

Unlensed CMB
Lenses
Lensed CMB
$\hat{C}_L^{\tilde{T}\tilde{T}} \propto \tilde{T}^2$
$\hat{C}_L^{\hat{\phi}_{\rm rec}\hat{\phi}_{\rm rec}} \propto \tilde{T}^4$
Angular scale
90° 18° 1° 0.2° 0.1° 0.07°
$\mathcal{D}_l = l(l+1)C_l^{TT}/(2\pi)\ [\mu K^2]$
6000 5000 4000 3000 2000 1000 0
2 10 50 500 1000 1500 2000 2500
Multipole moment, l
$[L(L+1)]^2 C_L/(2\pi)$
10^{-6} 10^{-7} 10^{-8} 10^{-9}
$N_L^{(0)}$
$C_L^{\phi\phi}$
10^1 10^2
L (log scale)
1000 1500 2000 2500
L (linear scale)
$C_L^{\hat{\phi}\hat{\phi}} - N_L^{(0)}$
$C_L^{\hat{\phi}\hat{\phi}} - 2\hat{N}_L^{(0)} + N_L^{(0)}$
$N_L^{(0)}$
$C_L^{\phi\phi}$
$C_L^{\phi\phi} + N_L^{(1)}$
circles$\pm\Delta C_L^{\phi\phi}|_{\rm ndiag}$
crosses$\pm\Delta C_L^{\phi\phi}|_{\rm diag}$

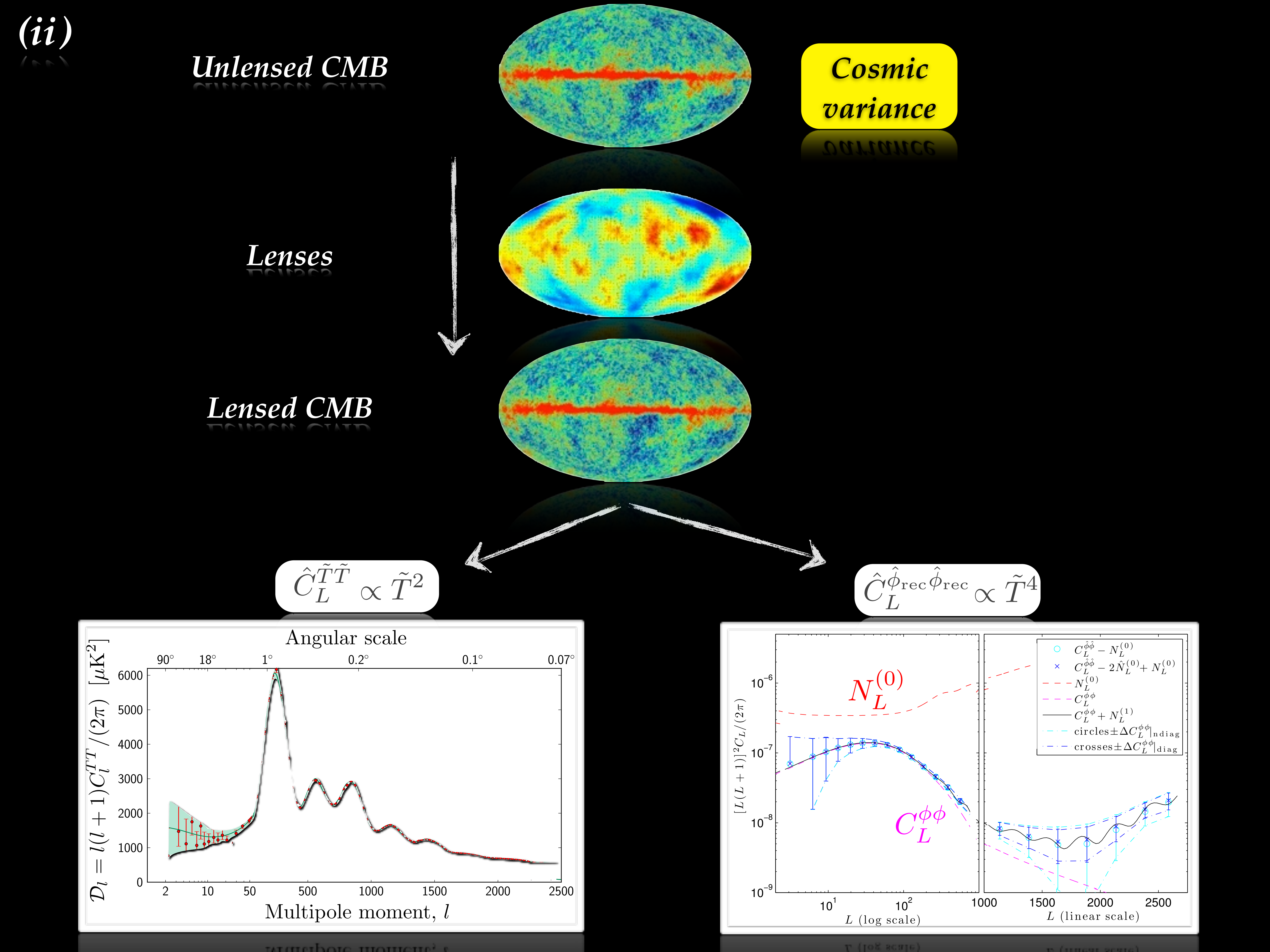
(ii)
Unlensed CMB
Cosmic variance
Lenses
Lensed CMB
$\hat{C}_L^{\tilde{T}\tilde{T}} \propto \tilde{T}^2$
$\hat{C}_L^{\hat{\phi}_{\rm rec}\hat{\phi}_{\rm rec}} \propto \tilde{T}^4$
Angular scale
90° 18° 1° 0.2° 0.1° 0.07°
$\mathcal{D}_l = l(l+1)C_l^{TT}/(2\pi)$ [μK^2]
Multipole moment, l
$N_L^{(0)}$
$C_L^{\phi\phi}$
$C_L^{\hat{\phi}\hat{\phi}} - N_L^{(0)}$
$C_L^{\hat{\phi}\hat{\phi}} - 2\hat{N}_L^{(0)} + N_L^{(0)}$
$N_L^{(0)}$
$C_L^{\phi\phi}$
$C_L^{\phi\phi} + N_L^{(1)}$
circles$\pm\Delta C_L^{\phi\phi}|_{\rm ndiag}$
crosses$\pm\Delta C_L^{\phi\phi}|_{\rm diag}$
$[L(L+1)]^2 C_L/(2\pi)$
L (log scale)
L (linear scale)

LIKELIHOOD INGREDIENTS

TEMPERATURE-LENSING POWER-COVARIANCE

MS, Challinor, Hanson, Lewis ***1308.0286***

(ii) If unlensed CMB fluctuates high, CMB power and Gaussian rec. noise $N^{(0)}$ are high

➟ Derives from disconnected CMB 6-point

$$\mathrm{cov}\left(\hat{C}_{L_\phi}^{\hat{\phi}_{\rm rec}\hat{\phi}_{\rm rec}}, \hat{C}_{L_T,\rm expt}^{\tilde{T}\tilde{T}}\right)_{\rm disc.}^{\mathcal{O}(\phi^0)} = \frac{\partial(2\hat{N}_{L_\phi}^{(0)})}{\partial \hat{C}_{L_T,\rm expt}^{\tilde{T}\tilde{T}}} \frac{2}{2L_T+1}\left(C_{L_T,\rm expt}^{\tilde{T}\tilde{T}}\right)^2$$

Correlation of *unbinned* power spectra is up to ~0.5% (at very high L_ϕ):

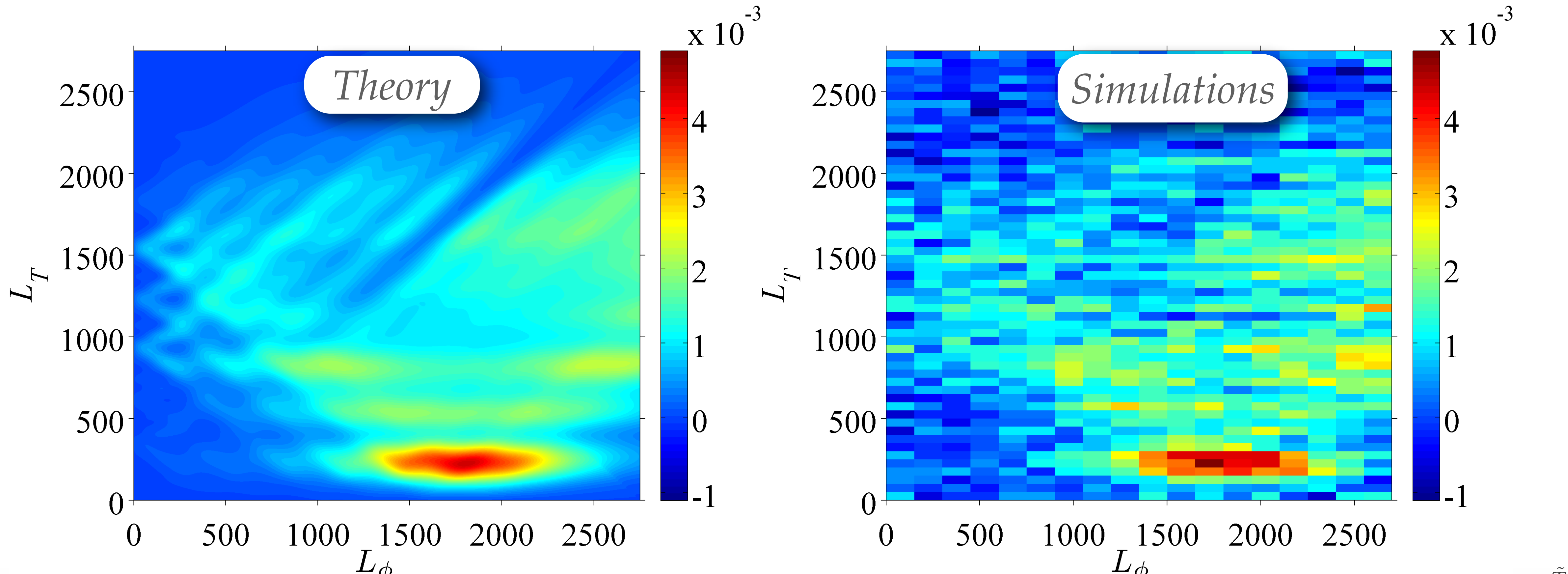

Peak at $L_\phi \sim 1800$ = minimum of beam-deconvolved noisy temperature power $C_{\rm expt}^{\tilde{T}\tilde{T}}$

TEMPERATURE-LENSING POWER-COVARIANCE

MS, Challinor, Hanson, Lewis ***1308.0286***

- **Decorrelating** power spectra
  - ➟ Can remove noise contribution (ii) with realisation-dependent bias correction

$$\hat{C}_L^{\hat{\phi}\hat{\phi}} - 2\hat{N}_L^{(0)} = \hat{C}_L^{\hat{\phi}\hat{\phi}} - \sum_{L'} \frac{\partial(2\hat{N}_L^{(0)})}{\partial \hat{C}_{L',\mathrm{expt}}^{\tilde{T}\tilde{T}}} \hat{C}_{L',\mathrm{expt}}^{\tilde{T}\tilde{T}}$$

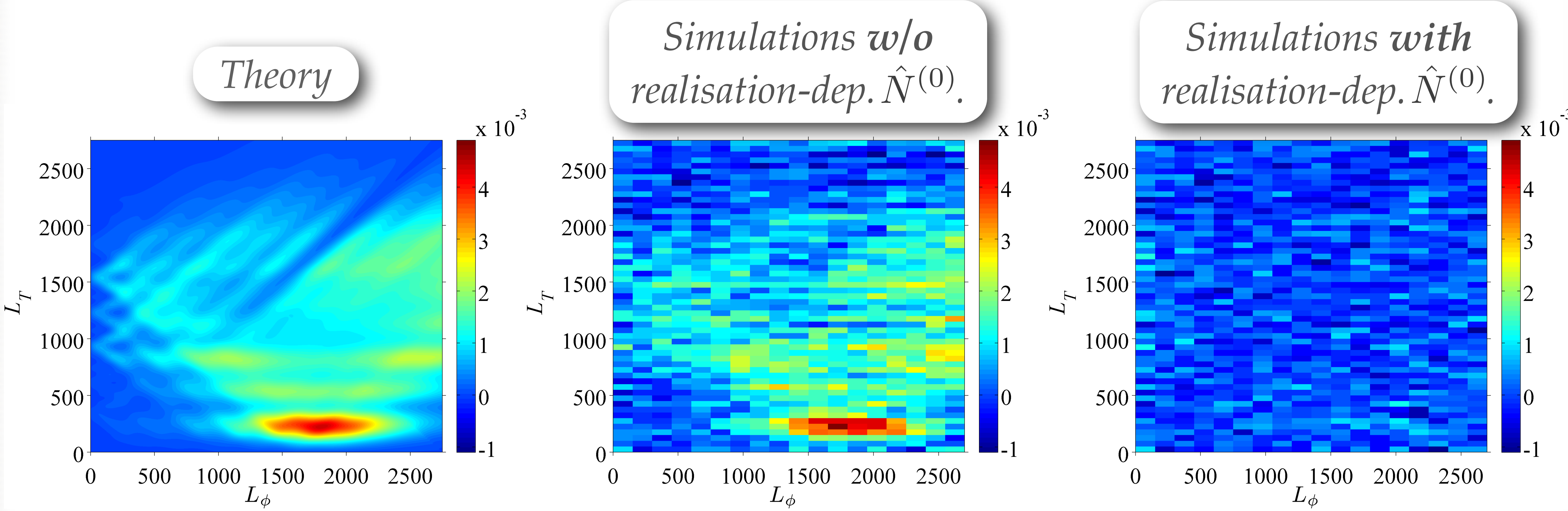

  - ➟ This also mitigates the off-diagonal reconstruction power *auto*-covariance (for the same reason); can be understood from optimal trispectrum estimation

OPTIMAL TRISPECTRUM ESTIMATION

Obtain realisation-dependent $\hat{N}^{(0)}$ bias mitigation also from optimal trispectrum estimator using Edgeworth-expansion of lensed temperature around Gaussian:

reconstruction power *realisation-dep.* *realisation-**in**dep.*

$$\hat{C}^{\hat{\phi}_{\mathrm{rec}}\hat{\phi}_{\mathrm{rec}}} \quad - \quad 2\hat{N}^{(0)} \quad + \quad N^{(0)}$$

$$P(T) = \left\{ 1 + \frac{1}{24} \underbrace{\langle T_i T_j T_k T_l \rangle_c}_{\text{lensing trispectrum}} \left[\bar{T}_i \bar{T}_j \bar{T}_k \bar{T}_l - \left(C_{ij}^{-1} \bar{T}_k \bar{T}_l + 5 \text{ perms} \right) + \left(C_{ij}^{-1} C_{kl}^{-1} + 2 \text{ perms} \right) \right] \right\} \times \frac{e^{-T_i C_{ij}^{-1} T_j / 2}}{\sqrt{\det(2\pi C)}}$$

T_i = lensed temperature

$C_{ij} = \langle T_i T_j \rangle$

$\bar{T}_i = C_{ij}^{-1} T_j$

IMPACT OF $\mathrm{cov}(\hat{C}_L^{\hat{\phi}_{\mathrm{rec}}\hat{\phi}_{\mathrm{rec}}}, \hat{C}_{L'}^{\tilde{T}\tilde{T}})$ ON LENSING AMPLITUDE

MS, Challinor, Hanson, Lewis ***1308.0286***

Impact of temperature-lensing power covariance on **lensing amplitude *A***:

- Rescale lensing power spectrum $\boxed{C_L^{\phi\phi} \rightarrow AC_L^{\phi\phi}}$
- Estimate from reconstruction power spectrum, $\hat{A}[\hat{C}^{\hat{\phi}\hat{\phi}}]$
- and from smoothing of temperature power spectrum, $\hat{A}'[\hat{C}^{\tilde{T}\tilde{T}}_{\mathrm{expt}}]$

➟ $\mathrm{cov}(\hat{A}, \hat{A}')$ is linearly related to $\mathrm{cov}(\hat{C}_L^{\hat{\phi}_{\mathrm{rec}}\hat{\phi}_{\mathrm{rec}}}, \hat{C}_{L'}^{\tilde{T}\tilde{T}})$

IMPACT OF $\mathrm{cov}(\hat{C}_L^{\hat{\phi}_{\mathrm{rec}}\hat{\phi}_{\mathrm{rec}}}, \hat{C}_{L'}^{\tilde{T}\tilde{T}})$: LENSING AMPLITUDE

MS, Challinor, Hanson, Lewis ***1308.0286***

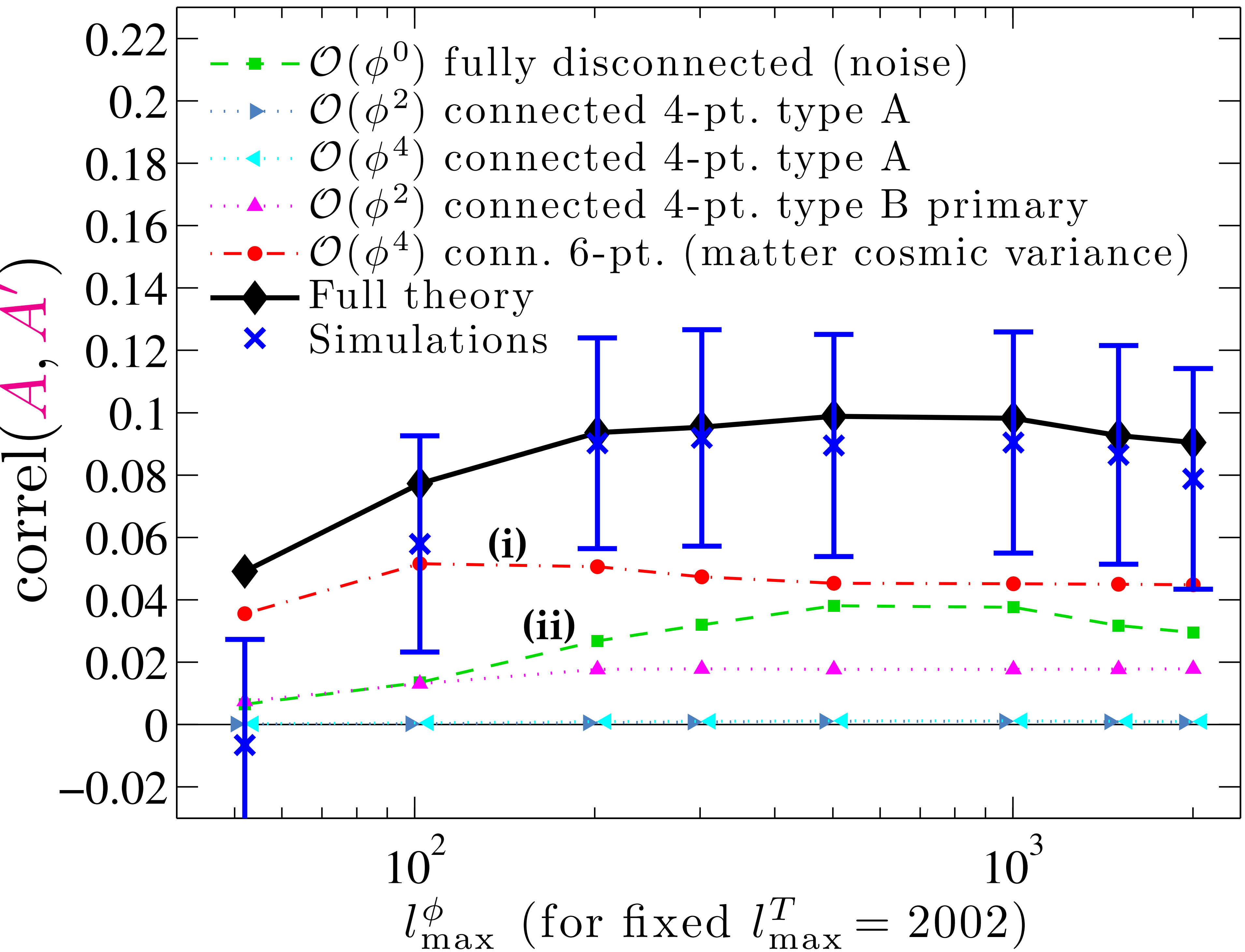

IMPACT OF $\mathrm{cov}(\hat{C}_L^{\hat{\phi}_{\mathrm{rec}}\hat{\phi}_{\mathrm{rec}}}, \hat{C}_{L'}^{\tilde{T}\tilde{T}})$: LENSING AMPLITUDE

MS, Challinor, Hanson, Lewis ***1308.0286***

***With** realisation-dependent* $\hat{N}^{(0)}$.

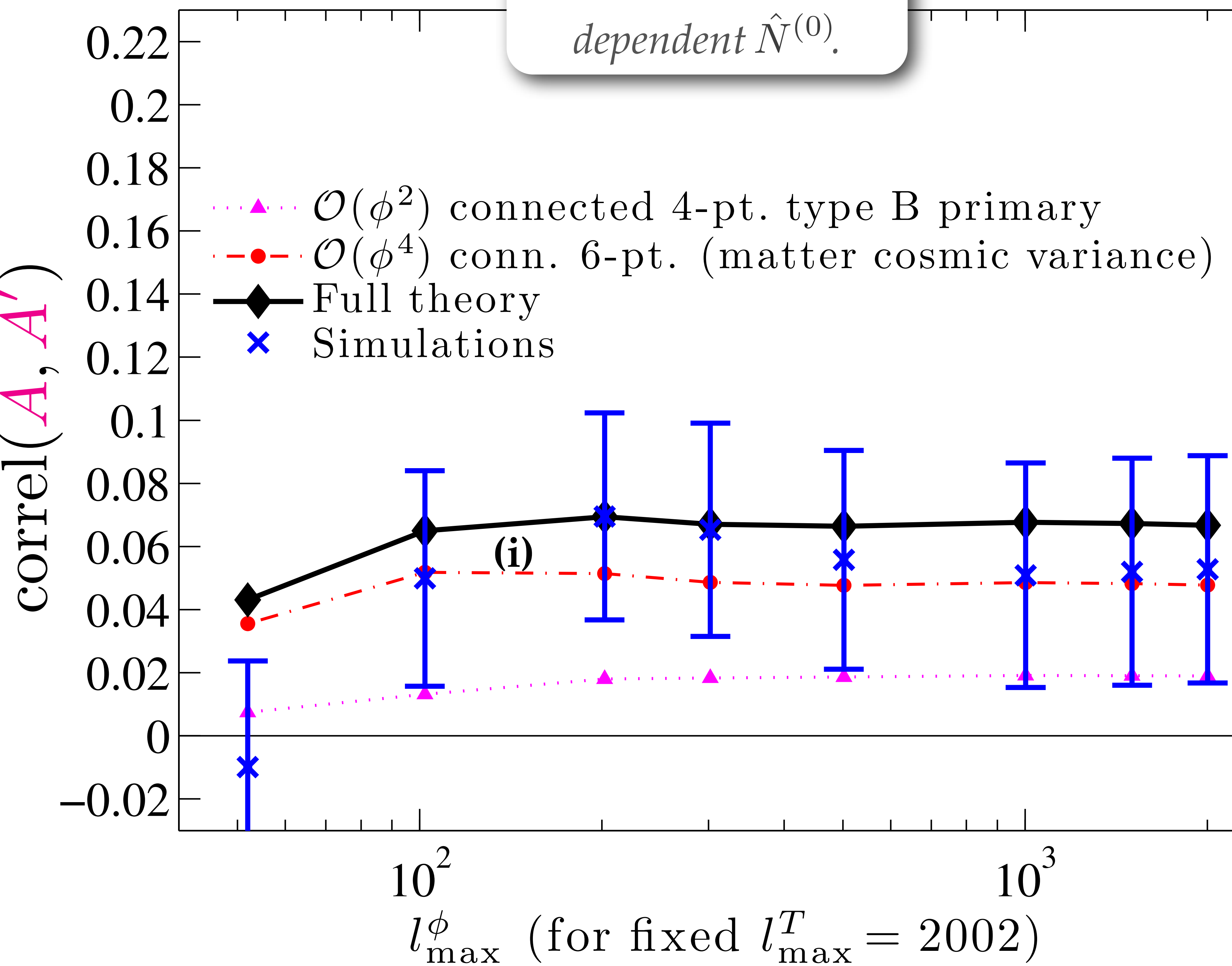

IMPACT OF $\mathrm{cov}(\hat{C}_L^{\hat{\phi}_{\rm rec}\hat{\phi}_{\rm rec}}, \hat{C}_{L'}^{\tilde{T}\tilde{T}})$ ON LENSING AMPLITUDE

MS, Challinor, Hanson, Lewis ***1308.0286***

➟ Neglecting $\mathrm{cov}(\hat{C}_L^{\hat{\phi}_{\rm rec}\hat{\phi}_{\rm rec}}, \hat{C}_{L'}^{\tilde{T}\tilde{T}})$ underestimates error of joint amplitude estimate by

$$\Delta\sigma_{A_{\rm joint}} \sim \mathrm{correl}(\hat{A}, \hat{A}')/2 \sim 3.5\%$$

(with realisation-dependent $\hat{N}^{(0)}$, otherwise ~ 5%)

➟ ***Temperature-lensing power-covariance is negligible for combined amplitude estimate (and for cosmological parameters)***

IMPACT OF $\mathrm{cov}(\hat{C}_L^{\hat{\phi}_{\mathrm{rec}}\hat{\phi}_{\mathrm{rec}}}, \hat{C}_{L'}^{\tilde{T}\tilde{T}})$ LENSING AMPLITUDE

MS, Challinor, Hanson, Lewis ***1308.0286***

Physical reasons for smallness of amplitude correlation

(i) Lens cosmic variance

- cov(A,A') is limited by the small number of $C^{\phi\phi}$ modes affecting acoustic region of $C^{\tilde{T}\tilde{T}}$ (including more lensing modes in $A[C^{\phi\phi}]$ reduces cov(A,A') because there are increasingly more lensing modes in $A[C^{\phi\phi}]$ whose fluctuations don't enter $A'[C^{\tilde{T}\tilde{T}}]$).
- correl(A,A') due to cosmic variance of these modes is diluted by CMB cosmic variance and instrumental noise (because A and A' are not limited by cosmic variance of the lenses)

IMPACT OF $\mathrm{cov}(\hat{C}_L^{\hat{\phi}_{\rm rec}\hat{\phi}_{\rm rec}}, \hat{C}_{L'}^{\tilde{T}\tilde{T}})$: LENSING AMPLITUDE

MS, Challinor, Hanson, Lewis ***1308.0286***

Physical reasons for smallness of amplitude correlation

(i) Lens cosmic variance

- cov(A,A') is limited by the small number of $C^{\phi\phi}$ modes affecting acoustic region of $C^{\tilde{T}\tilde{T}}$ (including more lensing modes in $A[C^{\phi\phi}]$ reduces cov(A,A') because there are increasingly more lensing modes in $A[C^{\phi\phi}]$ whose fluctuations don't enter $A'[C^{\tilde{T}\tilde{T}}]$).
- correl(A,A') due to cosmic variance of these modes is diluted by CMB cosmic variance and instrumental noise (because A and A' are not limited by cosmic variance of the lenses)

(ii) CMB cosmic variance

Roughly disjoint (independently fluctuating) scales in the CMB contribute to amplitude determination from peak-smearing and to lens reconstruction

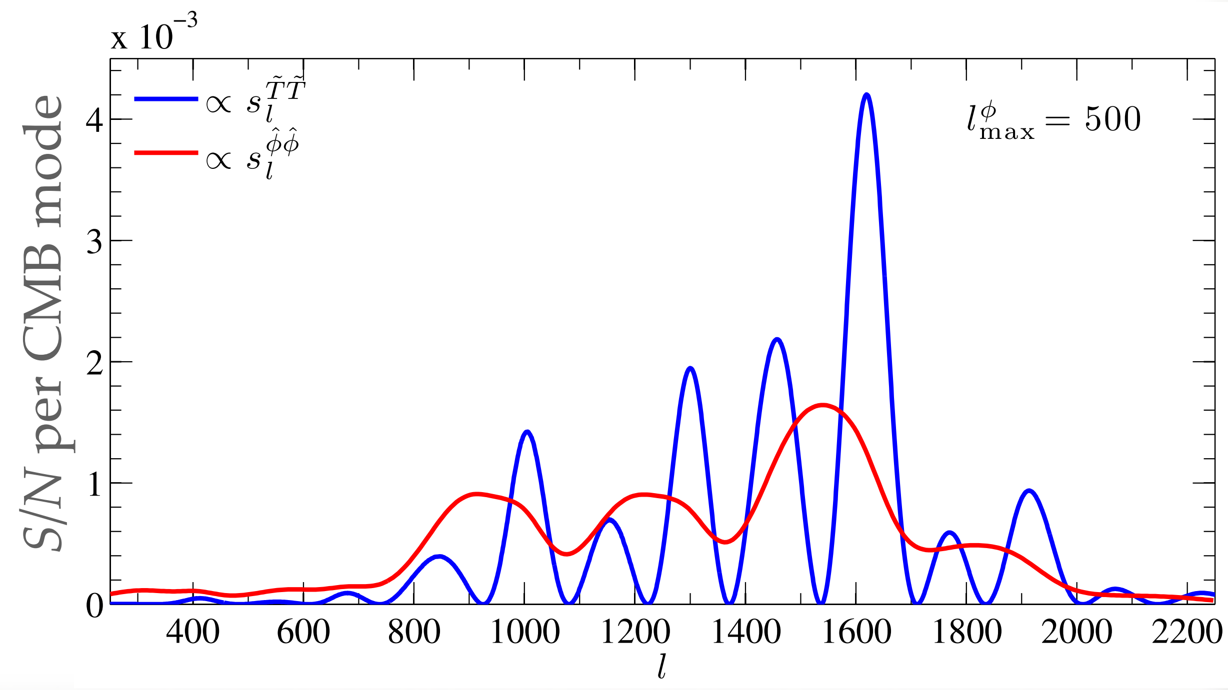

IMPACT OF $\mathrm{cov}(\hat{C}_L^{\hat{\phi}_{\rm rec}\hat{\phi}_{\rm rec}}, \hat{C}_{L'}^{\tilde{T}\tilde{T}})$ ON PHYSICAL PARAMETERS

MS, Challinor, Hanson, Lewis ***1308.0286***

Impact of $\mathrm{cov}(\hat{C}_L^{\hat{\phi}_{\rm rec}\hat{\phi}_{\rm rec}}, \hat{C}_{L'}^{\tilde{T}\tilde{T}})$ on **phys. params.** $\mathbf{p} = (\Omega_b h^2, \Omega_c h^2, h, \tau, A_s, n_s, \Omega_\nu h^2, \Omega_K)$

- Joint data vector: $\underline{\hat{C}} = (\hat{C}^{\tilde{T}\tilde{T}}_{\rm expt}, \hat{C}^{\hat{\phi}\hat{\phi}} - 2\hat{N}^{(0)} + N^{(0)})$
- Joint covariance

$$\mathrm{cov}_{LL',\,\mathrm{joint}} \equiv \mathrm{cov}(\underline{\hat{C}}_L, \underline{\hat{C}}_{L'}) = \begin{pmatrix} \delta_{LL'}\mathrm{var}_G(C^{\tilde{T}\tilde{T}}_{L,\rm expt}) & \mathrm{cov}(\hat{C}_L^{\tilde{T}\tilde{T}}, \hat{C}_{L'}^{\hat{\phi}_{\rm rec}\hat{\phi}_{\rm rec}}) \\ \mathrm{cov}(\hat{C}_L^{\hat{\phi}_{\rm rec}\hat{\phi}_{\rm rec}}, \hat{C}_{L'}^{\tilde{T}\tilde{T}}) & \delta_{LL'}\mathrm{var}_G(\langle \hat{C}_L^{\hat{\phi}\hat{\phi}}\rangle) \end{pmatrix}$$

- Fisher matrix: $F_{ij} = \sum_{LL'} \frac{\partial \underline{C}_L}{\partial p_i} (\mathrm{cov}^{-1}_{\rm joint})_{LL'} \frac{\partial \underline{C}_{L'}}{\partial p_j}$

➟ Fisher errors increase by **at most 0.7%** if $\mathrm{cov}(\hat{C}_L^{\hat{\phi}_{\rm rec}\hat{\phi}_{\rm rec}}, \hat{C}_{L'}^{\tilde{T}\tilde{T}})$ is included

➟ *Temperature-lensing power-covariance negligible for physical parameter errors*

CMB LENSING RECONSTRUCTION
LIKELIHOOD FORM

MS, Challinor, Hanson, Lewis ***1308.0286***

So far assumed likelihood based on reconstruction *power* $\hat{C}^{\hat{\phi}_{\rm rec}\hat{\phi}_{\rm rec}}$ instead of $\hat{\phi}_{\rm rec}$ *map*

- Well established for temperature, but unclear for (non-Gaussian) reconstruction
- Compare two lensing-likelihood models:

1. Gaussian in $\hat{\phi}_{\rm rec}$:

$$-2\ln\mathcal{L}_1(\hat{\phi}|A) \propto \sum_l (2l+1)\left(\frac{\hat{C}_l^{\hat{\phi}\hat{\phi}}}{AC_l^{\phi\phi}+N_l} + \ln\left|AC_l^{\phi\phi}+N_l\right|\right)$$

2. Gaussian in $\hat{C}^{\hat{\phi}_{\rm rec}\hat{\phi}_{\rm rec}}$ (with parameter-independent covariance):

$$-2\ln\mathcal{L}_2(\hat{C}^{\hat{\phi}\hat{\phi}}|A) \propto \sum_{l,l'}\left[\hat{C}_l^{\hat{\phi}\hat{\phi}} - (AC_l^{\phi\phi}+N_l)\right](\mathrm{cov}^{-1}_{\phi\phi})_{ll'}\left[\hat{C}_{l'}^{\hat{\phi}\hat{\phi}} - (AC_{l'}^{\phi\phi}+N_{l'})\right]$$

- Estimate lensing amplitude (and tilt) from both likelihoods, compare scatter of best-fit parameter vs. likelihood width

CMB LENSING RECONSTRUCTION
LIKELIHOOD FORM

MS, Challinor, Hanson, Lewis ***1308.0286***

So far assumed likelihood based on reconstruction *power* $\hat{C}^{\hat{\phi}_{\rm rec}\hat{\phi}_{\rm rec}}$ instead of $\hat{\phi}_{\rm rec}$ *map*

- Well established for temperature, but unclear for (non-Gaussian) reconstruction
- Compare two lensing-likelihood models:

1. Gaussian in $\hat{\phi}_{\rm rec}$:

$$-2\ln\mathcal{L}_1(\hat{\phi}|A) \propto \sum_l (2l+1)\left(\frac{\hat{C}_l^{\hat{\phi}\hat{\phi}}}{AC_l^{\phi\phi}+N_l} + \ln\left|AC_l^{\phi\phi}+N_l\right|\right)$$

2. Gaussian in $\hat{C}^{\hat{\phi}_{\rm rec}\hat{\phi}_{\rm rec}}$ (with parameter-independent covariance):

$$-2\ln\mathcal{L}_2(\hat{C}^{\hat{\phi}\hat{\phi}}|A) \propto \sum_{l,l'}\left[\hat{C}_l^{\hat{\phi}\hat{\phi}} - (AC_l^{\phi\phi}+N_l)\right](\mathrm{cov}^{-1}_{\phi\phi})_{ll'}\left[\hat{C}_{l'}^{\hat{\phi}\hat{\phi}} - (AC_{l'}^{\phi\phi}+N_{l'})\right]$$

- Estimate lensing amplitude (and tilt) from both likelihoods, compare scatter of best-fit parameter vs. likelihood width
  - 2. performs better than 1. (see paper)

CMB LENSING RECONSTRUCTION
LIKELIHOOD TESTS

MS, Challinor, Hanson, Lewis ***1308.0286***

Scatter of best-fit lensing amplitude *A* vs. likelihood width in single realisations

Gaussian in $\hat{\phi}_{\mathrm{rec}}$

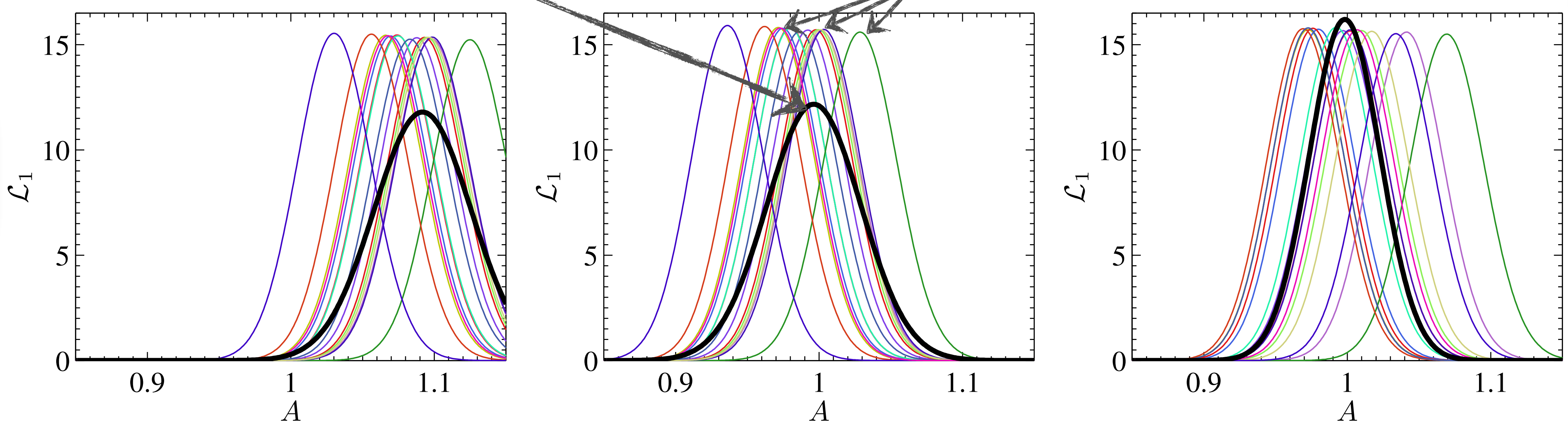

(a) $\mathcal{L}_1$ without $N^{(1)}$: biased

(b) $\mathcal{L}_1$ with $N^{(1)}$: unbiased but underestimates variance

(c) $\mathcal{L}_1$ for Gaussian mock $\hat{\phi}_{\mathrm{G}}$ with power $C^{\phi\phi} + N^{(0)} + N^{(1)}$: good

CMB LENSING RECONSTRUCTION
LIKELIHOOD TESTS

MS, Challinor, Hanson, Lewis ***1308.0286***

Scatter of best-fit lensing amplitude A vs. likelihood width in single realisations

Gaussian in $\hat{\phi}_{\mathrm{rec}}$

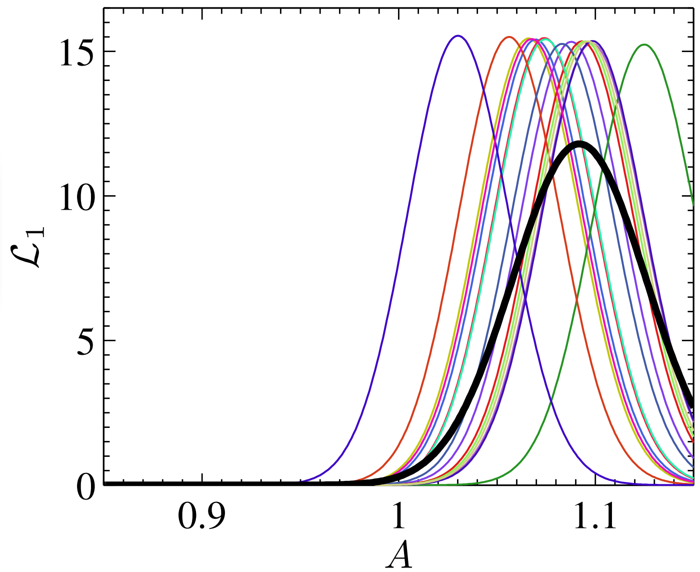

(a) $\mathcal{L}_1$ without $N^{(1)}$: biased

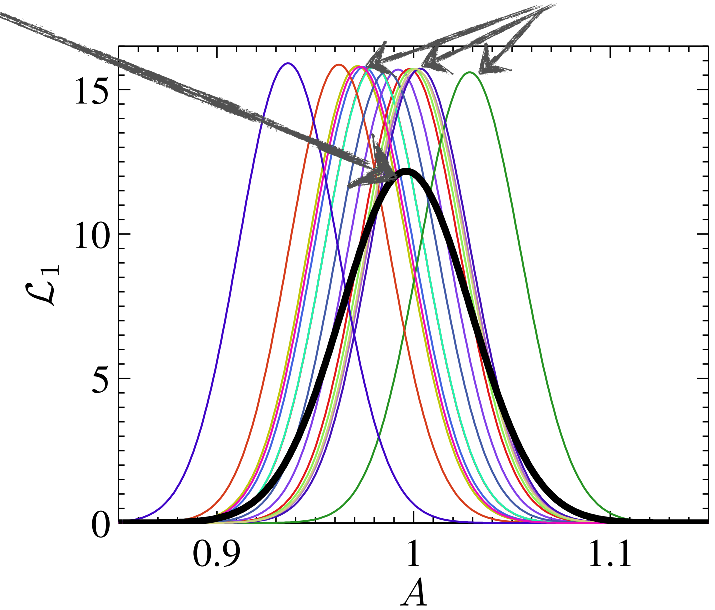

(b) $\mathcal{L}_1$ with $N^{(1)}$: unbiased but underestimates variance

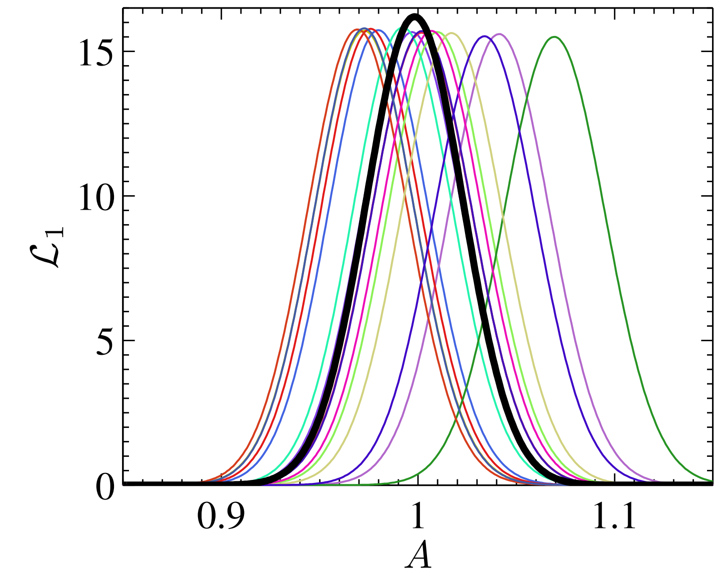

(c) $\mathcal{L}_1$ for Gaussian mock $\hat{\phi}_{\mathrm{G}}$ with power $C^{\phi\phi} + N^{(0)} + N^{(1)}$: good

Gaussian in $\hat{C}^{\hat{\phi}_{\mathrm{rec}}\hat{\phi}_{\mathrm{rec}}}$

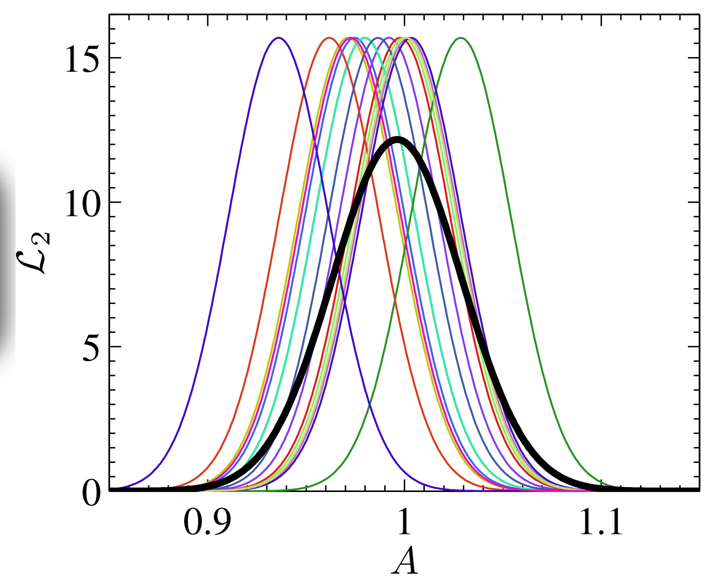

(d) $\mathcal{L}_2$ with diagonal covariance: underestimates variance

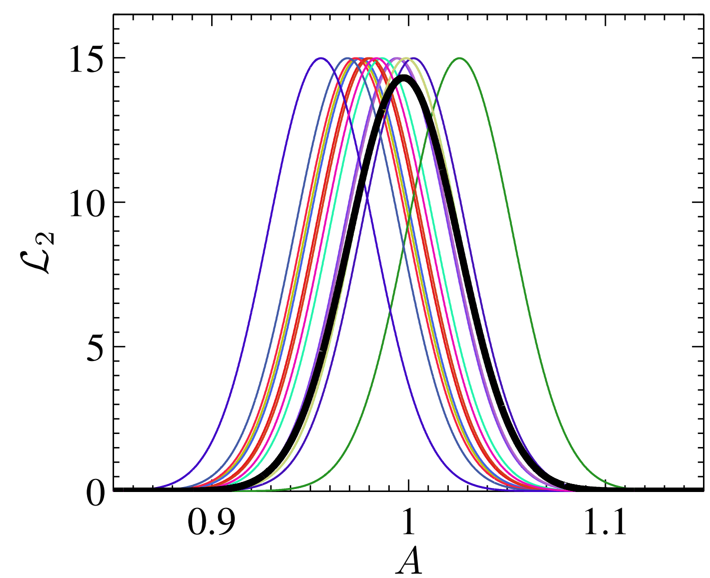

(e) $\mathcal{L}_2$ with non-diagonal, non-Gaussian covariance: good

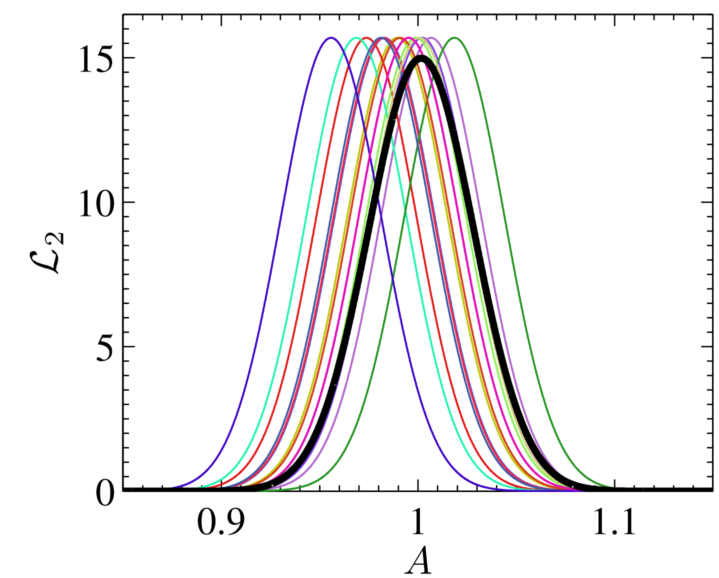

(f) $\mathcal{L}_2$ with empirical $\hat{N}^{(0)}$ subtraction and diagonal covariance: good

CMB LENSING RECONSTRUCTION
LIKELIHOOD TESTS

MS, Challinor, Hanson, Lewis ***1308.0286***

Scatter of best-fit lensing amplitude *A* vs. likelihood width in single realisations

Gaussian in $\hat{\phi}_{\mathrm{rec}}$

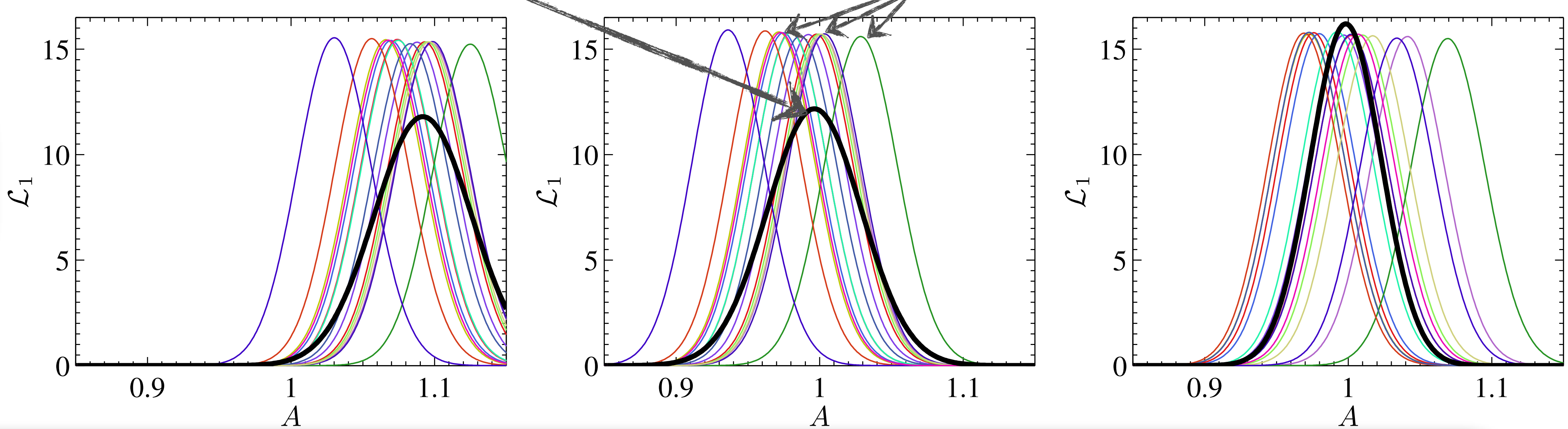

with
ood

➟ *Including non-Gaussianity of reconstruction is important to get correct error bar*

Gaussian in $\hat{C}^{\hat{\phi}_{\mathrm{rec}}\hat{\phi}_{\mathrm{rec}}}$

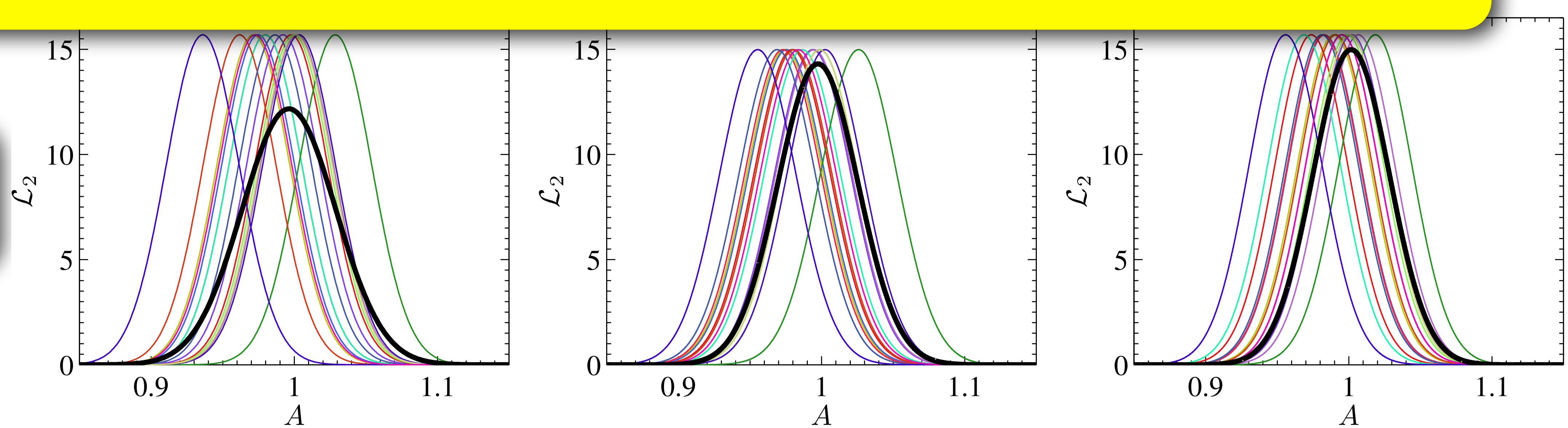

(d) $\mathcal{L}_2$ with diagonal covariance: underestimates variance

(e) $\mathcal{L}_2$ with non-diagonal, non-Gaussian covariance: good

(f) $\mathcal{L}_2$ with empirical $\hat{N}^{(0)}$ subtraction and diagonal covariance: good

CMB LENSING RECONSTRUCTION
LIKELIHOOD TESTS

MS, Challinor, Hanson, Lewis ***1308.0286***

For $\mathcal{L}_2$, we do not test the likelihood but rather the reconstruction power covariance (because $\hat{A} \propto \hat{C}^{\hat{\phi}\hat{\phi}}$)

➟ Additionally vary **lensing tilt *n*** to test $\mathcal{L}_2$: $C_l^{\phi\phi} \to A \left(\frac{l}{l_*}\right)^n C_l^{\phi\phi}, \qquad l_* = 124$

$\mathcal{L}_2$ with *diagonal* $\mathrm{cov}(\hat{C}_L^{\hat{\phi}\hat{\phi}}, \hat{C}_{L'}^{\hat{\phi}\hat{\phi}})$

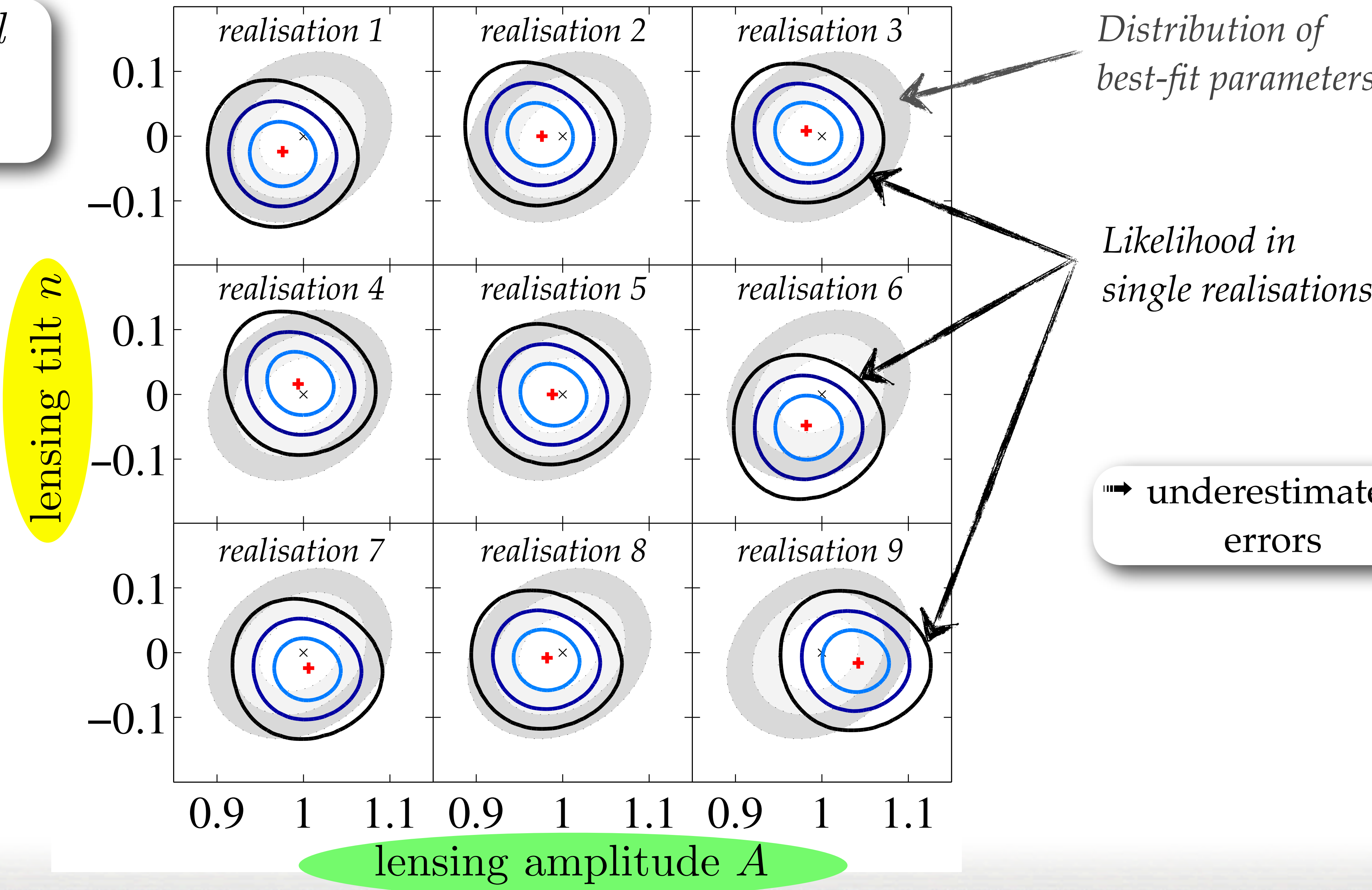

➟ underestimates errors

CMB LENSING RECONSTRUCTION
LIKELIHOOD TESTS

MS, Challinor, Hanson, Lewis ***1308.0286***

For $\mathcal{L}_2$, we do not test the likelihood but rather the reconstruction power covariance (because $\hat{A} \propto \hat{C}^{\hat{\phi}\hat{\phi}}$)

➟ Additionally vary **lensing tilt *n*** to test $\mathcal{L}_2$: $C_l^{\phi\phi} \rightarrow A \left(\frac{l}{l_*}\right)^n C_l^{\phi\phi}$, $\quad l_* = 124$

$\mathcal{L}_2$ with *non*-diagonal $\mathrm{cov}(\hat{C}_L^{\hat{\phi}\hat{\phi}}, \hat{C}_{L'}^{\hat{\phi}\hat{\phi}})$

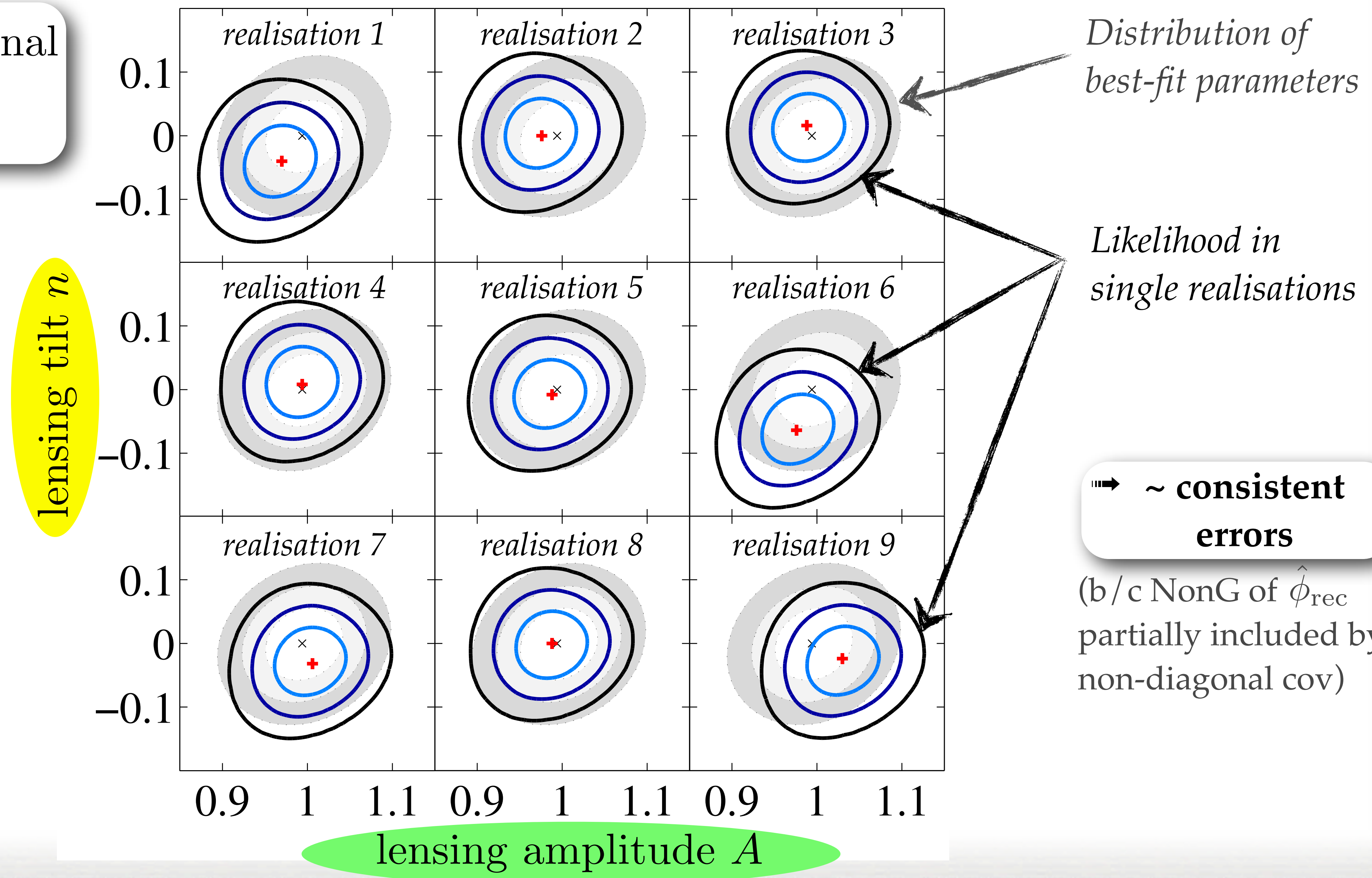

➟ **~ consistent errors**

(b/c NonG of $\hat{\phi}_{\mathrm{rec}}$ partially included by non-diagonal cov)

CMB LENSING RECONSTRUCTION
LIKELIHOOD TESTS: QUANTITATIVELY

$\mathcal{L}_2$ with *diagonal* $\mathrm{cov}(\hat{C}_L^{\hat{\phi}\hat{\phi}}, \hat{C}_{L'}^{\hat{\phi}\hat{\phi}})$	$\mathcal{L}_2$ with *non*-diagonal $\mathrm{cov}(\hat{C}_L^{\hat{\phi}\hat{\phi}}, \hat{C}_{L'}^{\hat{\phi}\hat{\phi}})$	$\mathcal{L}_2$ with *diagonal* $\mathrm{cov}(\hat{C}_L^{\hat{\phi}\hat{\phi}}, \hat{C}_{L'}^{\hat{\phi}\hat{\phi}})$ and realisation-dep. $\hat{N}^{(0)}$

Deviation of areas of confidence ellipses

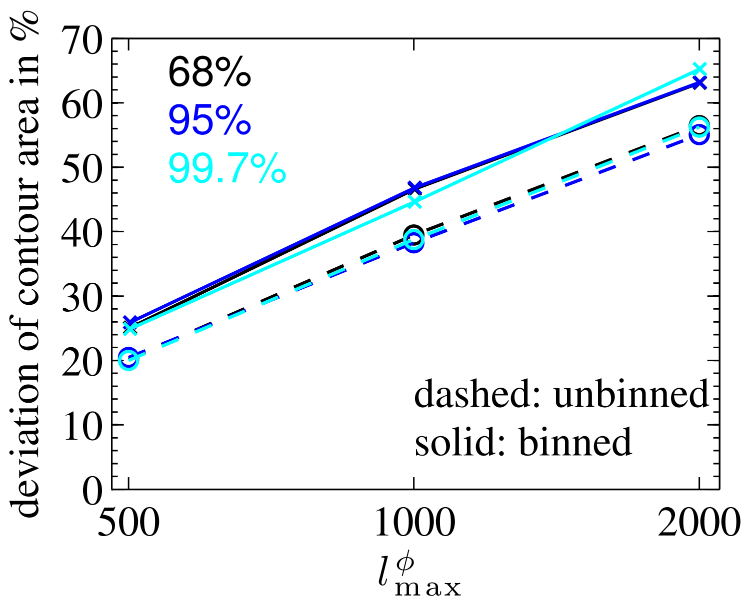

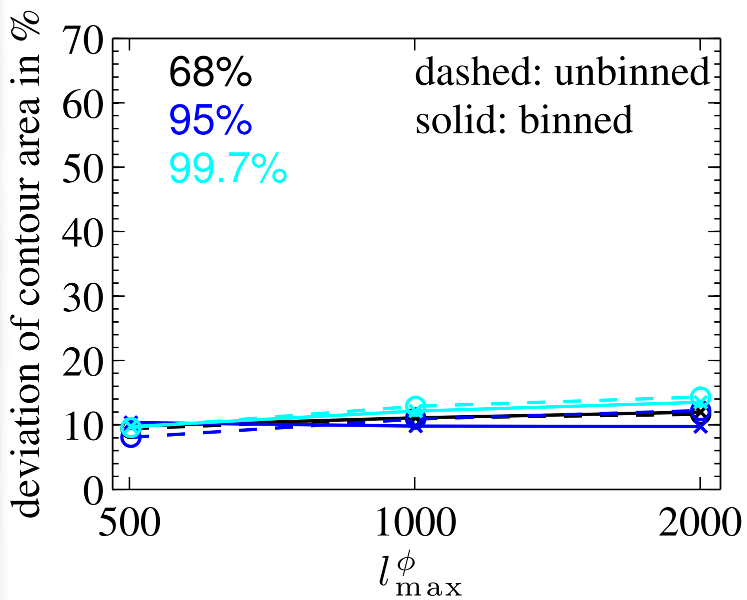

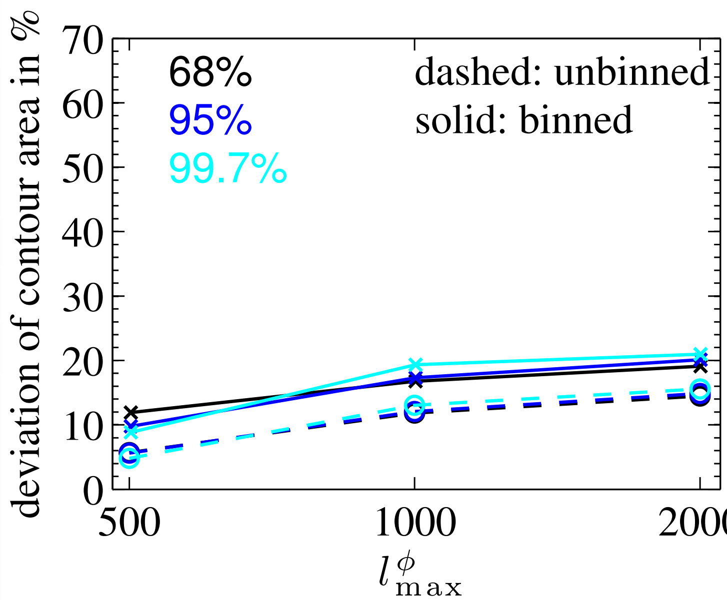

Fractional error of marginalised error bars of A or n: ~ (area dev.)/2

~ 34%	~ 8%	~ 11%

➠ *$\mathcal{L}_2$ is accurate likelihood approximation if non-diagonal $\mathrm{cov}(\hat{C}_L^{\hat{\phi}\hat{\phi}}, \hat{C}_{L'}^{\hat{\phi}\hat{\phi}})$ or $\hat{N}^{(0)}$ is used*

CONCLUSIONS

MS, Challinor, Hanson, Lewis ***1308.0286***

- Understand non-Gaussianity of $\phi_{\rm rec}$ and correlation with temperature analytically

$$\mathrm{cov}(\hat{C}^{\hat{\phi}_{\rm rec}\hat{\phi}_{\rm rec}}_{L_\phi}, \hat{C}^{\tilde{T}\tilde{T}}_{L_T,\rm expt}) = \frac{\partial(2\hat{N}^{(0)}_{L_\phi})}{\partial\hat{C}^{\tilde{T}\tilde{T}}_{L_T,\rm expt}} \frac{2}{2L_T+1}\left(C^{\tilde{T}\tilde{T}}_{L_T,\rm expt}\right)^2 \left[1+2\frac{C^{\phi\phi}_{L_\phi}}{A_{L_\phi}}\right] + \frac{2}{2L_\phi+1}\left(C^{\phi\phi}_{L_\phi}\right)^2 \frac{\partial C^{\tilde{T}\tilde{T}}_{L_T}}{\partial C^{\phi\phi}_{L_\phi}}$$

noise contribution (disconnected 6-point)

connected 4-point

matter cosmic variance (connected 6-point)

- Found methods to treat/mitigate both

- This has significantly simplified joint analysis of $C^{\tilde{T}\tilde{T}}$ and $\phi_{\rm rec}$ for Planck:

no cross-term!

  ➟ Likelihoods can be modeled separately, $\boxed{\ln\mathcal{L}(C^{\tilde{T}\tilde{T}}, \phi_{\rm rec}) = \ln\mathcal{L}(C^{\tilde{T}\tilde{T}}) + \ln\mathcal{L}_2(\phi_{\rm rec})}$

  ➟ Non-Gaussianity of $\phi_{\rm rec}$ modeled by likelihood that's Gaussian in $\hat{C}^{\hat{\phi}_{\rm rec}\hat{\phi}_{\rm rec}}$

Thanks